UNIVERSITY OF NATURAL RESOUCES AND
LIFE SCIENCES, VIENNA
Department of Biotechnology

VIRAL ENGINEERING FOR AN IMPROVED INSECT CELL-BASED PRODUCTION PLATFORM

Dissertation

for obtaining the Doctor of Philosophy degree
at the University of Natural Resources and Life Sciences, Vienna

Submitted by **Krisztina Koczka MSc**

Supervisors: **Dr. Reingard Grabherr**

Dr. Wolfgang Ernst

Vienna, February 2019

BioToP Biomolecular Technology of Proteins
VIBT Vienna Institute of BioTechnology
FWF Der Wissenschaftsfonds.
acib

ACKNOWLEDGEMENTS

I would like to express my deep gratitude to Reingard and Wolfgang, my research supervisors, for giving me the chance to do my PhD as part of the Baculo group. I am truly grateful for all the kind support and guidance I received, which always helped me to overcome the various challenges I faced through the past few years. Their willingness for giving useful critiques and valuable input to my research in the form of countless hours of discussions was indispensable for this dissertation.

I would like to offer my sincere thanks to Didi, from whom I have learned a lot during my PhD, as he showed me all the tricks of molecular biology. I am thankful for the constructive suggestions and ideas he had, even after he was only unofficially part of our research group. My special thanks goes to Lisa as well, with whom we shared all the ups and downs of our PhD journeys and who always provided help when I was in need. I am also very thankful that I could be part of the BioToP community and here I would like to thank Christa Jakopitsch in particular, for organizing everything and bringing us together.

I would also like to extend my thanks to every member of the Baculo group, who in some way all contributed to this work: Shirin, the two Stefans, Miriam, Christopher and Kristina.

I would like to express my very great appreciation to Professor Amine Kamen for the opportunity to do my research stay in his lab in Canada. Very special thanks should be given to Alina, Aline, Sascha, David, Xavier, Pranav and Jean-Francois for immediately welcoming me in the group and for making my time at McGill a great professional and personal experience.

Finally, I wish to thank my parents Emília and Béla and my brother Béci for their endless support and loving encouragement throughout my life and studies. All this would have not been possible without you. Thank you Emanuel for making Vienna my second home and for standing by my side throughout this journey.

ABSTRACT

The baculovirus-insect cell expression system is a popular tool for the production of recombinant proteins. However, it holds a special place among the established eukaryotic manufacturing platforms, as heterologous protein expression is coupled to a lytic infection with engineered baculoviruses. This introduces certain limitations to the system such as obstacles by the setup of continuous bioprocesses, the induction of stress and the unfolded protein response in the insect host upon recombinant protein production and the concurrent formation of contaminating baculovirus particles during product manufacturing. In order to circumvent their negative consequences, e.g. low soluble product yields and laborious downstream processing, these weaknesses need to be addressed.

The first part of the thesis focuses on the elucidation of secretory and metabolic bottlenecks in insect cells leading to protein aggregates upon infection with recombinant baculoviruses encoding a soluble protein. By conducting a comparative transcriptome analysis in a *Trichoplusia ni* derivative cell line, key processing and folding enzymes, chaperones involved in the stress response induced by the infection itself and the parallel high-level protein formation were identified. These specifically regulated genes could serve as interesting targets for upcoming cell line and viral engineering attempts.

The second part of the thesis aims at the development of an inducible knockdown system for the effective downregulation of host or viral proteins during an infection process. The established system exploits the natural RNA interference mechanism in insect cells in combination with the prokaryotic T7 transcription machinery. Through the example of downregulating a model fluorescent protein, the dual-vector system was proven functional and suitable for future experiments targeting genes essential for baculovirus budding in order to reduce the viral titers in the supernatant.

KURZFASSUNG

Das Baculovirus-Insektenzellen-Expressionssystem wird oft zur Produktion rekombinanter Proteine verwendet. Jedoch ist es unter den etablierten eukaryotischen Produktionsplattformen ein besonderes System, da die rekombinante Proteinexpression an eine lytische Infektion mit Baculoviren gekoppelt ist. Dies bringt bestimmte Einschränkungen mit sich, wie z. B. Hindernisse beim Aufbau kontinuierlicher Bioprozesse, die Induktion von Stress und den Unfolded Protein Response im Insektenwirt bei der Produktion rekombinanter Proteine sowie die gleichzeitigen Bildung kontaminierender Baculovirus-Partikel während der Produktherstellung. Diesen Schwächen, z. B. der geringen Ausbeute an löslichem Produkt und der mühsamen Weiterverarbeitung muss entsprechend begegnet werden, um diese negativen Folgen zu umgehen.

Der erste Teil der Arbeit konzentriert sich auf die Aufklärung sekretorischer und metabolischer Engpässe in Insektenzellen, die zur Bildung von Proteinaggregaten führen, ausgelöst durch Infektion mit Baculoviren, die ein heterologes lösliches Protein kodieren. Nicht nur wichtige Prozessierungs- und Faltungsenzyme, auch Chaperone, die durch die direkte Stressantwort und die parallel dazu stattfindende hohe Fremdproteinbildung induziert werden, wurden durch eine vergleichende Transkriptomanalyse in einer *Trichoplusia ni* Zelllinie identifiziert. Diese spezifisch regulierten Gene stellen interessante Ziele für zukünftige Zelllinienentwicklung und virale Vektorentwicklung dar.

Der zweite Teil der Arbeit beschäftigt sich mit der Entwicklung eines induzierbaren Gen-Knockdown Systems zur effektiven Stilllegung von Insekten- oder Virusgenen während eines Infektionsprozesses. Das etablierte System nutzt den natürlichen RNA-Interferenz Mechanismus in Insektenzellen in Kombination mit der prokaryotischen T7-Transkription Maschinerie. Am Beispiel der Herunterregulierung eines Modellfluoreszenzproteins erwies sich das Doppelvektorsystem als funktional und geeignet für zukünftige Experimente an essentiellen Genen für die Baculovirus-Entstehung, zur Reduktion der Virusmenge im Überstand.

TABLE OF CONTENTS

1 INTRODUCTION

Since its introduction to the scientific community in 1983 (Smith et al., 1983), the baculovirus-insect cell expression system has become a powerful tool for the manufacturing of recombinant proteins. A first report describing the expression of human interferon-beta by infecting *Spodoptera frugiperda Sf*21 insect cells with an engineered *Autographa californica* multiple nucleopolyhedrovirus (*Ac*MNPV) has provided the basis for the establishment of a new and promising eukaryotic production platform. Over the years, the use of *Ac*MNPV as recombinant gene delivery vector for protein production in insect cells has become greatly facilitated thanks to the numerous studies aiming to understand and improve this binary system (van Oers et al., 2015). Insect cells are feasible for large-scale manufacturing of various intracellular as well as secreted proteins using serum-free media in suspension cultures. Moreover, high titer production (Thompson et al., 2015) is combined with safe handling, lower production costs as compared to mammalian cell systems, and extensive eukaryotic post-translational modifications (Summers, 2006). Among others, enzymes (Morais et al., 2001), viral proteins (Cruz et al., 1998), virus-like particles (VLPs) (Fernandes et al., 2013) and viral vectors (Aucoin et al., 2007) have been successfully expressed in the past, using *Spodoptera frugiperda* (e.g. *Sf*9 or *Sf*21 clones) and *Trichoplusia ni* (e.g. High Five clone) cells. Additionally, over the years the baculovirus-insect cell-based production platform has become the preferred choice for the industrial manufacturing of various complex products of biopharmaceutical interest such as vaccines (Mena and Kamen, 2011) and gene therapy vectors (Meghrous et al., 2005). The market entry of the VLP-based vaccine Cervarix in 2009 against cervical cancer (Harper, 2008), the prostate cancer vaccine Provenge in 2010 (Kantoff et al., 2010) and the recombinant hemagglutinin-based trivalent influenza vaccine FluBlok (Treanor et al., 2011) in 2013 has further confirmed the relevance of this production platform.

1.1 THE BACULOVIRUS-INSECT CELL EXPRESSION SYSTEM

1.1.1 Baculovirus biology

Baculoviridae is a diverse family of insect-specific viruses that mainly infect insect larvae of the Lepidopteran order. Baculoviruses are enveloped viruses with a particle size of 30-60 nm in diameter and 250-300 nm in length (Clem and Passarelli, 2013). The rod-shaped

nucleocapsid of these viruses harbors the circular, double-stranded DNA genome of 80-180 kilobase pairs (kbp). Due to the open structure of the capsid, the DNA packaging capacity can be increased up to 38 kb (Cheshenko et al., 2001), which allows for the simultaneous expression of multiple heterologous proteins (Kost et al., 2005). Originally isolated from the alfalfa looper, the *Ac*MNPV of the *Alphabaculovirus* genus is considered the most studied representative of *Baculoviridae* that was also used to create the first recombinant baculovirus vector (Pennock et al., 1984; Smith et al., 1983). Thanks to its relatively broad host range of around 25 lepidopteran insects and its complete genomic sequence available (Ayres et al., 1994), engineered versions of *Ac*MNPV still remain one of the most widely used baculoviral backbones for the production of recombinant proteins in insect cells.

Due to the biphasic nature of their life cycle, two different viral phenotypes (Fig 1) are observed in *Ac*MNPVs: the occlusion derived viruses (ODVs) and the budded viruses (BVs). ODVs are responsible for the primary infection of the host, while BVs take part in the secondary infection that spreads the disease within the host (Jarvis, 2009).

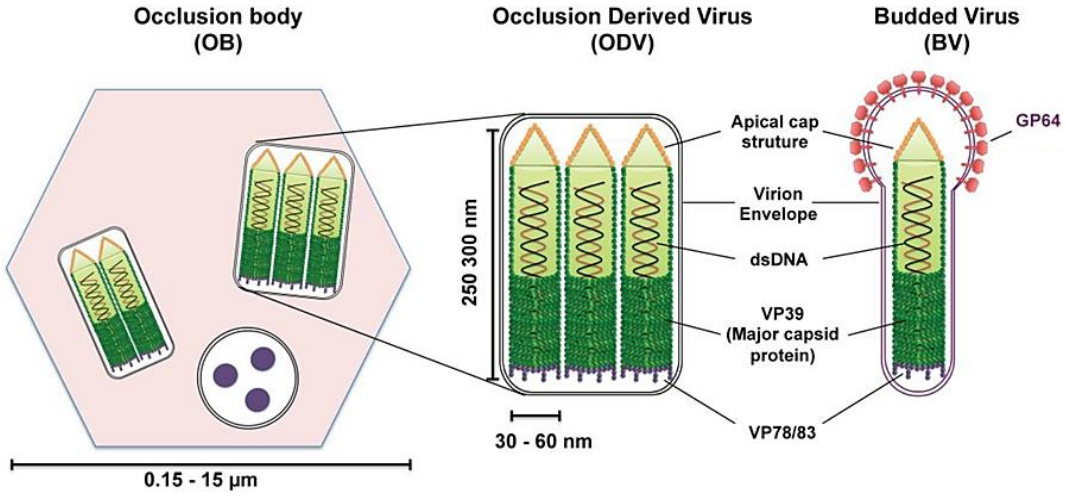

Fig 1. Schematic structure of baculovirus phenotypes. Occlusion bodies (OBs) are polyhedral-shaped crystalline matrices built up of the viral polyhedrin protein to surround and protect multiple nucleocapsids outside the host. OBs contain the occlusion derived viruses (ODVs) that establish the primary infection by targeting the host`s midgut cells upon ingestion by an insect larva. After the establishment of the infection within the host, the nucleocapsids obtain a host cell-derived envelope via budding that is enriched in the membrane fusion protein gp64. Thus, budded viruses (BVs) are formed that spread the infection from cell to cell within the host. The two viral phenotypes share the same nucleocapsid core consisting mainly of the major capsid protein vp39 that encapsulates the circular double-stranded DNA genome. Figure modified from (Au et al., 2013).

Although the two viral phenotypes share an identical DNA content and nucleocapsid structure, they differ in the envelope composition and their comparative infectivity (Volkman

and Summers, 1977). ODVs mainly infect the midgut cells in insect larvae, whereas BVs spread the infection from cell to cell within the host. For the generation of BVs, a single nucleocapsid comprising mainly of the major capsid protein vp39 embeds the circular, supercoiled DNA genome of 134 kbp. Upon budding, the nucleocapsid obtains the host's cell membrane, enriched in the BV encoded membrane fusion protein gp64 that is essential for the spread of systemic infection.

ODVs appear at the latest stage of the infection in the nucleus where polyhedral-shaped occlusion bodies (OBs) are formed. OBs are crystalline protein matrices consisting of the viral polyhedrin protein that is produced to protect the nucleocapsids in a suboptimal environment outside the host (Slack and Arif, 2006).

The *Ac*MNPV infection cycle and gene expression can be divided into three, temporally sequential phases: the early, the late and the very late phases (Miller, 1988). The early phase of gene expression (0-6 hours post-infection) can be further categorized to the formation of immediate- and delayed-early genes. During the immediate-early phase, the expression of early viral genes and transregulators takes place that are under the control of mostly weak, host-like viral promoters. Thus, their transcription is independent of the presence of other viral genes or regulators. In contrast, the transcription of delayed-early genes require the presence of viral proteins of the immediate-early phase, which are therefore, a prerequisite for the progression of the viral cycle. The delayed-early genes take part in the viral replication process and the manipulation of the host cell. The end of the early phase is followed by a transition phase that is associated with the shutdown of host cell replication and its protein synthesis machinery. This marks the beginning of the late phase of the infection.

The late phase (6-24 hours post-infection) includes the formation of nucleocapsids (vp39), the major viral structural proteins (e.g. gp64) and the BVs that spread the infection within the host. In the very late phase (18-24 to 72 hours post-infection), ODVs are generated with the concurrent formation of the two major very late proteins, the p10 and the polyhedrin. Subsequently, through the lysis of the host cell, ODVs are released from the nuclei and can be taken up by new hosts to spread the infection horizontally (Contreras-Gomez et al., 2014). One of the fundamental observations that made recombinant protein production feasible with baculovirus vectors was the fact that the p10 and polyhedrin viral proteins are produced in extremely large quantities during the last stage of the infectious cycle; however, they are

not essential for the viral replication (van Oers, 2011). Therefore, in order to achieve high product titers during recombinant protein production, the transgene is usually inserted in place of their gene sequences.

Initially, recombinant baculovirus production was achieved through the linearization of viral DNA (in e.g. the *polh* or *p10* loci), its co-transfection and subsequent recombination with a transfer vector in insect cells. Compared to this early system, a greatly improved and simplified strategy was introduced in 1993, based on site-specific recombination of *Ac*MNPV genomes (bacmids) harbored by *Escherichia coli* cells. Although, this setup facilitates the modification of the viral genome, due to the presence of bacterial sequences and the necessary antibiotic selection, the system is not suitable for the manufacturing of human therapeutics. One of the most popular baculovirus systems circumventing this limitation is the *flash*Bac that is based on homologous recombination. Another highly common setup is the MultiBac technology, which is compatible with the OmniBac transfer vector. Thus, it allows for recombinant virus and protein production using either linearized viral genomes (homologous recombination) or the bacmid system in *E. coli*. Additionally, in order to impede liquefaction of the host and the proteolytic lysis of the recombinant protein, the viral backbone of the MultiBac system lacks the *v-cath* and *chiA* genes encoding a cathepsin L-like cysteine protease and a chitinase, respectively.

1.1.2 Insect cell lines

Recombinant protein production with the baculovirus-insect cell expression system relies on two main components: engineered baculoviruses serving as gene delivery vectors and insect production hosts. Since 1962, when the *in vitro* culture of insect cells first became possible (Grace, 1962), more than hundreds of different insect cell lines have been isolated, predominantly from the Lepidopteran and Dipteran orders (Lynn, 2001). Although several insects are highly susceptible to *Ac*MNPV infection, the recombinant baculovirus vectors are mostly used in combination with three lepidopteran cell lines in industrial production processes (Fig 2). The *Sf*21 and *Sf*9 cell lines are a derivative of the pupal ovarian tissue of the fall armyworm *Spodoptera frugiperda* (Vaughn et al., 1977), whereas the High Five cell line originates from the adult ovarian tissue of the cabbage looper *Trichoplusia ni* (Drugmand et al., 2012).

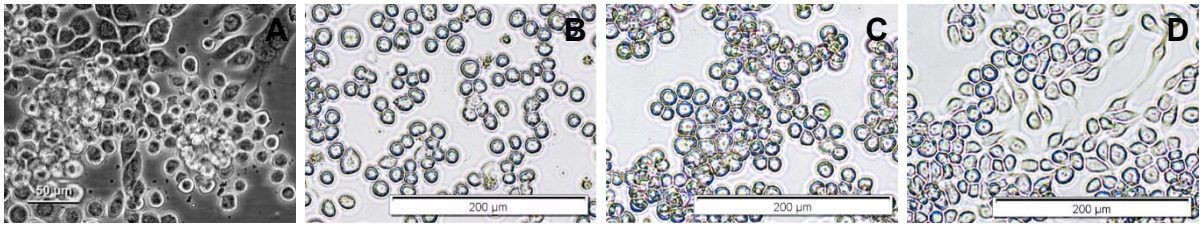

Fig 2. Insect cell lines. Cultured insect cells show either spherical or fibroblast-like morphology within a size range of 10-20 µm in diameter. The most widely used cell lines for recombinant protein production are the *S. frugiperda* derivative *Sf*21 (Lynn, 2002)(A) and *Sf*9 (B) cells and the *T. ni* derivative High Five (C) cell line. Recently a new cell line, the alphanodavirus-free *T. ni* derivative *Tnms*42 (D) was generated (Granados et al., 2016).

Occasionally other, less typical cell lines are also used for heterologous protein expression; these include the *Bombyx mori* derivative *Bm*5 (Grace, 1967) or the *Trichoplusia ni* derivative *Tn*368 (Hink, 1970) cell lines. However, with the discovery of the latent alphanodavirus infection of High Five cells (Li et al., 2007) and rhabdovirus infection of *Sf*9 cells (Ma et al., 2014), certain concerns have been raised with regard to the safety of the related production platforms. Despite the fact that these insect-specific viruses are not capable of infecting vertebrates and are therefore harmless for humans, a strong demand for virus-free cell lines has aroused in the recent years. This led to the development of the novel *T. ni* derivative *Tnms*42 cell line (Fig 2), which was proven to be free of latent viral infections (Granados et al., 2016).

A key feature that has led to the widespread application of these lepidopteran cell lines (*Sf*21, *Sf*9, High Five) is that they can be cultivated in adherent, as well as suspension cultures, also in serum-free medium. For the amplification of baculoviruses, normally the *S. frugiperda* derivative *Sf*9 cell line is preferred over the parental *Sf*21 or *T. ni* lines, as it is capable of achieving higher viral titers (Wang et al., 1992; Wilde et al., 2014). Furthermore, *Sf*9 cells show higher growth rates and greater tolerance to shear, osmotic and pH stress than *Sf*21 cells (Drugmand et al., 2012). In contrast, High Five cells are favored generally for protein production processes, as they are capable of achieving considerably higher product titers on a per cell basis than their *S. frugiperda* counterparts (Saarinen et al., 1999; Wilde et al., 2014), in combination with a greater shear and osmotic stress tolerance (Kioukia et al., 1995). Although, due to its increased growth rate compared to High Five, greater volumetric productivities can be achieved with the *Sf*9 cell line (Aucoin et al., 2010).

1.2 LIMITATIONS OF THE BACULOVIRUS-INSECT CELL SYSTEM

1.2.1 Insect cell bioprocesses

Besides the various advantageous characteristics of the system, the baculovirus-insect cell-based protein production platform possesses certain weaknesses as well. One major drawback of the system arises from the lytic nature of the baculovirus infection cycle that is coupled to the heterologous protein expression in insect cells. Thus, for large scale industrial recombinant protein production, mostly the batch or fed-batch modes of operation are preferred (Bedard et al., 1994; Elias et al., 2000). These include the scale-up of insect cell cultures to the desired cell density and the subsequent infection of cells with recombinant baculovirus vectors carrying the gene of interest. Such simple and flexible processes have shown to suit this binary expression system well, especially fed-batch cultures that can be operated at higher cell densities as compared to batch mode, where nutrient depletion and by-product accumulation in the culture medium usually lead to reduced cell-specific productivity. Alternatively, with the continuous renewal of spent medium in perfusion cultures, an even higher cell density and product yield can be obtained, but the scalability of such a system can be expensive and problematic (Caron et al., 1994). Ideally, continuous production processes should be established. However, as protein expression in insect cells has a transient nature that is separated into cell growth and infection phases, a continuous mode of operation is not easy to implement. The current setups are based on e.g. the operation of cascade bioreactors, where fresh cells are cultivated separately and fed into the infection vessel (van Lier et al., 1990). Besides, continuous processes completely bypassing the baculovirus infections have been established, using stably transfected insect cell lines for the production of recombinant proteins (Harrison and Jarvis, 2007). However, due to the observed drop in product yields, none of these strategies has been taken over by the industry.

1.2.2 Glycosylation

The performance of mammalian-like protein folding and glycosylation is one of the great advantages insect cells offer over microbial and yeast production systems. However, despite the fact that insects belong to eukaryotes, their portfolio of feasible post-translational modifications may not always be identical to those found in higher eukaryotes. In comparison to the complex, terminally sialylated glycoforms observed in mammalian cells, insect cells produce more uniform, but simpler N-glycans with terminal mannose residues (Harrison and

Jarvis, 2006). Due to the fact that therapeutics with non-mammalian-like glycoforms are highly immunogenic in humans (Altmann, 2007), the lack of ability to perform complex, terminally sialylated N-glycosylation in insects may reduce the value and limit the utility of this production platform. Additionally, the presence and structure of N-glycans influence the product functionality and stability, as it can provide protection against proteolysis (Imperiali and O'Connor, 1999; Lis and Sharon, 1993). Furthermore, several product-related cellular mechanisms may be also affected by the glycoforms, such as folding and quality control of the recombinant protein, which ultimately may also have an effect on the product yield.

Thus, it is not surprising that extensive research has been dedicated to the engineering of the insect glycosylation pathway, in order to overcome the limitations of the system. One approach is the remodeling of the host N-glycan biosynthetic pathway by creating stably transformed insect cell lines that express various glycosyltransferases and glycan processing enzymes of higher eukaryotes to achieve a more humanized glycan structure (Breitbach and Jarvis, 2001; Hollister et al., 1998; Mabashi-Asazuma et al., 2013; Okada et al., 2010). Besides, independent of the preferred production cell line, baculovirus vectors can be also engineered to either simultaneously or sequentially co-express mammalian glycosyltransferases and a heterologous protein (Jarvis and Finn, 1996; Palmberger et al., 2012).

1.2.3 Unfolded protein response and the bottleneck protein secretion: strategies to improve secretion of complex proteins

The achievable product titers with the baculovirus-insect cell system depend strongly on the nature of the recombinant product. Secreted proteins such as glycoproteins and complex membrane-bound proteins, especially those crossing the membrane more than once, usually cannot be expressed in quantities comparable to that of non-secreted products remaining in the cytoplasm (van Oers, 2011). The insect cell-based production platform holds a special place among other eukaryotic systems, as recombinant protein production with lepidopteran cells is linked to a viral infection that completely reprograms the host. Additionally, with the use of the strong, very late polyhedrin and p10 baculoviral promoters to drive the heterologous gene expression, the generation of extremely large amounts of often complex, glycosylated foreign proteins is demanded from the deteriorating host. As most of the cellular pathways shut down due to the infection itself (Chen et al., 2014), the protein folding and processing machinery is unable to keep up with this demand, which leads to the accumulation

of unfolded or misfolded proteins and not properly glycosylated products in the endoplasmic reticulum (ER) lumen. Eventually, this leads to ER stress and the induction of the unfolded protein response (UPR) in order to assist the protein processing and to reduce the protein folding load on the ER (Fig 3) (Hetz, 2012).

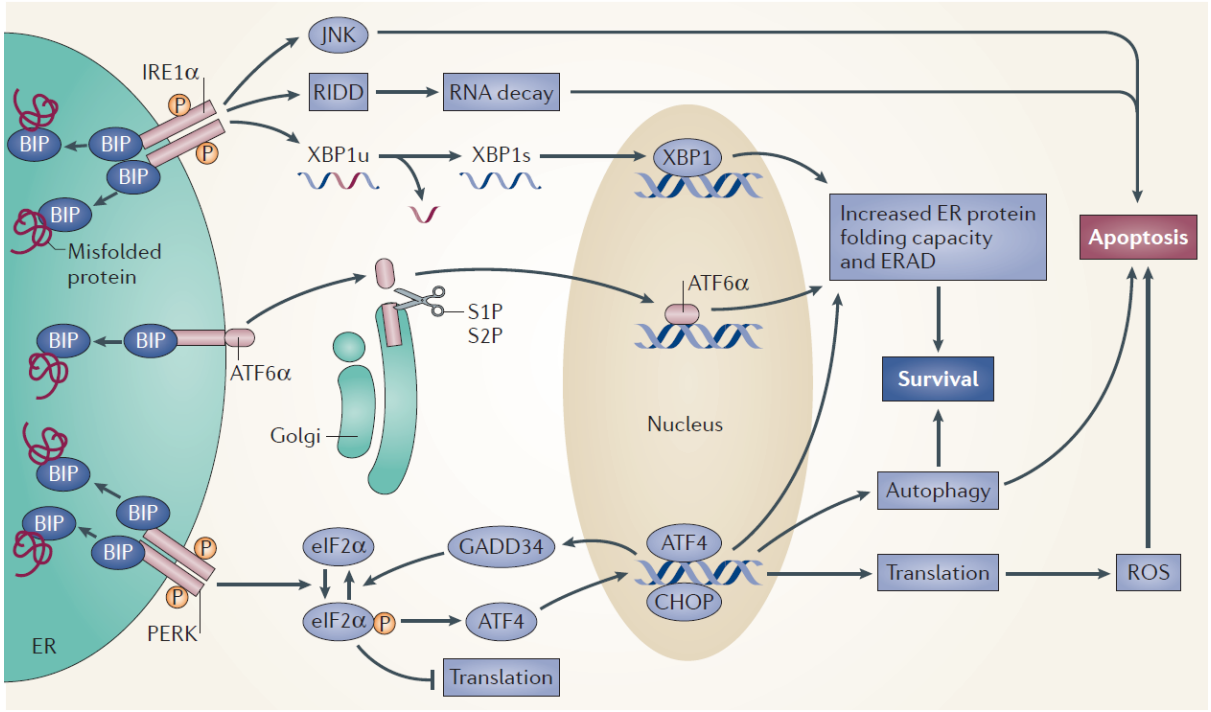

Fig 3. The unfolded protein response. In a homeostatic state, the binding of the chaperone BiP keeps the three UPR branches (IRE1α, PERK, and ATF6α) inactivated. However, upon elevated levels of unfolded or misfolded proteins in the ER, the level of free BiP decreases. With the reduced levels of the free chaperone, the UPR is activated, which encompasses the signaling pathways that induce the expression of e.g. BiP, protein disulfide isomerase (PDI), GRP94 (glucose regulated protein 94, chaperone of the Hsp90 family) and other chaperones and folding enzymes (Kozutsumi et al., 1988). As a result of the UPR, general translational attenuation occurs, the capacity for protein folding, processing and trafficking through the ER is increased, but also protein degradative pathways are upregulated. Eventually, when all these measures fail to reduce ER stress, the cells enter apoptosis (Hetz, 2012). Figure obtained from (Wang and Kaufman, 2014).

The UPR comprises of three major stress sensors that function concurrently: IRE1α (Inositol-requiring enzyme 1α), PERK (Double-stranded RNA-activated protein kinase (PKR)–like ER kinase) and ATF6α (Activating transcription factor 6α). In a homeostatic state of the cell, all three signal-transducers are in an inactivated form that is maintained by the binding of BiP (Binding immunoglobulin protein), a chaperone of the Hsp70 family (Wang and Kaufman, 2014). However, upon the accumulation of unfolded or misfolded proteins in the ER, BiP dissociates to bind to these proteins and thus the UPR is activated.

The IRE1α branch of the UPR begins with the oligomerization and autophosphorylation of the protein. The activated IRE1α then splices the messenger RNA (mRNA) encoding the transcription factor XBP1 (X-box binding protein 1), which induces the expression of numerous target genes involved in protein folding, secretion and protein degradation (ERAD). Besides, IRE1α is responsible for the activation of JUN N-terminal kinase (JNK) and the degradation of certain mRNAs through the regulated IRE1-dependent decay (RIDD).

ATF6α is an ER-resident transmembrane protein that translocates to the Golgi upon activation. There the S1P and S2P (Site-1 and Site-2 proteases) sequentially remove the luminal- and the transmembrane domains of the protein, respectively, which gives rise to the ATF6f cytosolic fragment. ATF6f is a transcription factor that regulates the expression of proteins assisting in folding and those included in the ERAD.

The PERK branch of the UPR is activated in a similar manner to IRE1α, as it is based on dimerization and trans-autophosphorylation. The activated form of PERK phosphorylates the eukaryotic translation initiator factor 2α (eIF2α) that inhibits protein synthesis and thus reduces the protein folding load on the ER. Apart from this function, the phosphorylated eIF2α allows for the translation of e.g. the activating transcription factor 4 (ATF4), which regulates the expression of genes such as that of the transcription factor C/EBP-homologous protein (CHOP) and the growth arrest and DNA damage-inducible 34 (GADD34) protein.

The UPR has a major effect on the productivity of a production system, as deficient processing and folding of the secreted recombinant product induces aggregation, low product titers and variable glycosylation. Thus, the co-expression of chaperones and folding enzymes involved in the proteolytic processing and post-translational modification can be beneficial for increasing the overall recombinant product yields. Among others, the effect of co-expressing the chaperone calreticulin or the translation initiation factor eIF4E (Eukaryotic translation initiation factor 4E) with an alkaline phosphatase-EGFP fusion protein (SEFP; served as a secreted model product) was tested in *Ac*MNPV-infected *Sf*21 cells (Teng et al., 2013). While the overexpression of calreticulin lead to the expansion of the ER, elevated levels of eIF4E resulted in a boost of functional SEFP expression. Others report the co-expression of the human chaperone Hsp70 and its co-factors Hsdj or Hsp40 in combination with the Epstein-Barr virus replication protein, BZLF1 (Yokoyama et al., 2000). The chaperone Hsp70 itself was able to increase the solubility of the model protein BZLF1, but this effect was several fold

upon including either of the co-factors Hsdj or Hsp40 as well. A more expanded study was conducted using silkworm larvae and cell lines to evaluate the effect of the knockdown or overexpression of five major chaperones involved in protein folding, processing and the UPR (Imai et al., 2015). In overall, apart from the negative effect of BiP depletion on protein secretion, no significant difference was observed in the titers of the model products upon downregulating or overexpressing the chaperones.

The limited improvement in increasing the host´s secretion capacity reported by these studies clearly stress the need for more systematic research. The main goal should be to deepen the understanding of the interdependence and synergistic effects of single chaperones, folding enzymes and proteins involved in protein modification. Although, mammalian cells have been extensively characterized with regard to the regulatory networks of producer cells in a bioprocess environment (Doolan et al., 2008; Nissom et al., 2006; Trummer et al., 2008), no comparable investigation has been conducted in the baculovirus-insect cell system so far. With the identification of the transcriptional and secretory bottlenecks responsible for reduced product titers and the investigation of the metabolic burden of high-level secreted product formation, the improvement of the overall performance of a cell factory becomes possible (Gupta and Lee, 2007; Kuystermans et al., 2007). However, without in-depth knowledge on factors affecting the correct processing and glycosylation of a secreted product, the achievable improvements in the overall productivity will remain strongly limited in the future as well.

1.2.4 Budding of baculoviruses and the bottleneck of product impurities: strategies to downregulate the assembly of baculoviruses in insect cells

The baculovirus-insect cell expression system is suitable for the manufacturing of various industrially relevant products, such as vaccines and gene therapy vectors. However, the therapeutics for human medical use must first go through extensive downstream processing to remove the impurities. Probably the most difficult task is the separation of the co-produced baculoviruses. Although, *Ac*MNPV particles cannot replicate in mammalian cells, they stimulate antiviral effects in these cells, including the induction of pro-inflammatory cytokines and interferons. (Abe and Matsuura, 2010; Gronowski et al., 1999; Kitajima and Takaku, 2008). Additionally, the recombinant baculovirus vectors may also retain some of the promoter activity (Kenoutis et al., 2006; Murges et al., 1997). Current setups for the

downstream purification depend strongly on the characteristics of the product, including structure, glycosylation and whether it is intracellularly or extracellularly located. In general, downstream recovery of the products is costly, time-consuming and may reduce the overall efficiency of the production process.

The existing strategies mainly aim at the reduced formation of baculoviruses during the production processes to facilitate the subsequent purification. In some cases, it also becomes possible to reach elevated levels of recombinant proteins through increasing the metabolic capacities of the cell with the reduced viral load. These studies report mainly the downregulation or complete deletion of genes known to be essential for baculovirus propagation. One example for this approach is the deletion of the *vp80* gene from the viral backbone encoding a capsid-associated protein (Marek et al., 2011). However, when genes involved in baculovirus budding are completely deleted, the generation of helper cell lines becomes necessary that trans-complement the essential gene for the inoculum preparation. Although in this study, reduced baculovirus titers were reported without a decrease in the product yield, the trans-complementation was 25-fold less effective for seed virus generation as compared to the conventional setup. Furthermore, the expression of vp80 decreased with the passages as it induced cytotoxicity in the stable *Sf*9 cell lines. Recently, a similar setup was also developed using gp64null recombinant baculoviruses and was evaluated with regard to VLP production (Chaves et al., 2018).

As the generation of stable cell lines for the trans-complementation of the deleted genes can be quite cumbersome, the knockdown of baculoviral genes may provide a better alternative in some cases. The downregulation of *gp64* with small-interfering RNAs (siRNAs) reduced the baculovirus formation with 30% in *Sf*21 cells, without affecting the recombinant protein expression (Breitbach and Jarvis, 2001). An anti-viral system has also been established in silkworm BmN-SWU1 cells, where *Bm*NPV (*Bombyx mori* nucleopolihedrovirus) contamination was effectively reduced by using artificial microRNA (miRNA) constructs targeting *lef-11* that is involved in DNA replication and late gene transcription (Zhang et al., 2014). These examples clearly support the usefulness of knockdown strategies in insect cells to combat baculovirus contamination.

1.3 RNA INTERFERENCE STRATEGIES FOR CELL AND VIRAL ENGINEERING

Current cell- and viral engineering strategies in the baculovirus-insect cell system usually rely on either the transient co-expression of a target gene on a baculovirus vector (Sokolenko et al., 2012), the generation of stable insect cell lines expressing foreign proteins (Sequeira et al., 2018) or the downregulation of host or baculoviral genes (Mabashi-Asazuma and Jarvis, 2017; Marek et al., 2011). When the reduced level of a certain gene transcript is desired, deletion or gene silencing can be applied. Apart from the classical Lambda RED system (Sharan et al., 2009) that is applicable on the baculoviral backbone harbored by *E. coli* (Marek et al., 2011), the recently developed CRISPR-Cas9 editing tool can be utilized on the host genome (Mabashi-Asazuma and Jarvis, 2017) for deletions. Despite being reliable, these methods are laborious and expensive, not to mention the need for host specific PolII promoter sequences in case of the CRISPR-Cas9 system, which are barely available in insect cells yet. In certain cases, the knockdown of a selected gene might be actually more beneficial compared to a deletion, e.g. when regulating the expression of essential host or viral genes fulfilling a function in basic metabolic processes. For this purpose, RNA interference (RNAi) can be applied.

RNAi is a conserved biological response that has become a popular and valuable tool in recent years for the transient and target-specific knockdown of genes. This mechanism regulates gene expression with short, non-coding RNA molecules including siRNAs and miRNAs; however, there are subtle differences between the two effector molecules (Lam et al., 2015). While the ~21-25 nt long siRNAs are double-stranded molecules of exogenous origin (e.g. viruses, transposons), the ~19-24 nt long miRNAs are purposefully transcribed in the form of single-stranded RNA precursors within the nucleus of the host cell. Furthermore, siRNAs bind perfectly complementary target sequences and thus induce their degradation; in contrast, miRNAs possess more than one target, as they show imperfect pairing with the sequences they repress the translation of. Several methods have been established so far in numerous expression systems using artificial siRNAs, miRNAs and other forms of engineered effector RNA molecules for specific biotechnological purposes; nevertheless, some are considered more advantageous over others.

The earliest and probably most straightforward method established for the manipulation of gene expression with RNAi was based on the delivery of long double-stranded RNA (dsRNA)

molecules into nematode worms that resulted in the silencing of the gene with a complementary sequence (Fire et al., 1998). Since then, with the possibility of other delivery methods (Yu et al., 2013), such as the introduction of a vector encoding the dsRNA for *in vivo* transcription (Huang et al., 2007), this customizable system was successfully transferred to numerous other hosts as well (Gordon and Waterhouse, 2007; Paddison et al., 2002; Sharp, 1999), including insect cells (Huang et al., 2007; Valdes et al., 2003). However, though a simple design is combined with high effectivity, a general weakness of this system is that upon the processing of the long dsRNA molecule, several siRNA duplexes targeting various genes are generated. Thus, the risk of specific off-target effects is high (Haley et al., 2008). Additionally, the introduction of long dsRNAs to mammalian cells has been shown to induce the innate immune response, which eventually leads to a general translational inhibition and mRNA degradation (Wang et al., 2016). Alternatively, customized siRNAs can be transiently transfected into the host to achieve gene silencing (Lee et al., 2015). When using a uniform pool of synthetic siRNAs, the specific off-target effects can be reduced by a proper design, e.g. by avoiding overlaps between the RNA sequence and the host´s genome sequence. However, the exogenously introduced siRNA duplexes are unstable *in vivo*, which can lead to a loss of activity (Hickerson et al., 2008). Additionally, siRNAs may also be immunostimulatory, depending on their sequence composition (Marques and Williams, 2005).

A more target-specific approach for customized RNAi is to embed the siRNA duplex in a naturally occurring precursor structure of the miRNA biogenesis pathway. Thus, the modified hairpin structures assimilate into the miRNA pathway and are being processed accordingly (Bofill-De Ros and Gu, 2016). The “first generation” hairpin constructs, the so-called short hairpin RNAs (shRNAs) mimic the precursor-miRNA (pre-miRNA) structure of a hairpin with a 2-nt overhang at the 3´end. Although, successful studies have been reported in the baculovirus-insect cell system using shRNAs (Kim et al., 2012; Zhang et al., 2018), an essential limitation of their use is the need for well-defined transcript termination. This can be achieved with strong PolIII promoters; however, these sequences are not always available in the popular insect cell lines used for bioprocesses. Furthermore, the large amount of mimics generated by these promoters is often associated with cytotoxicity (Bofill-De Ros and Gu, 2016). The “second generation” constructs mimic the endogenous primary microRNA (pri-miRNA) transcripts comprising a pre-miRNA hairpin structure surrounded by upstream and

downstream flanking sequences. As these regions may be of variable length, the transcription is independent of PolIII promoters that allows for more customization of the silencing system. The few studies reporting the successful establishment of pri-miRNA mimic-based silencing in insect cells (Haley et al., 2008; Zhang et al., 2014) strongly demonstrate the potential of such systems. Especially those setups offering gene silencing in a timely defined manner for the alteration of glycosylation pattern or the downregulation of proteases, essential genes involved in baculovirus assembly would serve as valuable tools in the establishment of more robust production processes.

2 AIMS OF THE THESIS

The first main objective of the thesis was to deepen the understanding of the stress and metabolic burden in insect cells triggered by the viral infection coupled secreted protein production. The thus identified key factors responsible for the correct protein processing should serve as promising targets for molecular engineering to overcome production bottlenecks that derive from the **unfolded protein response** during the viral infection cycle.

Therefore, a comparative transcriptome analysis had to be carried out to reveal the differences in the transcriptional host responses to the production of an intracellular or a secreted model product. Sequencing libraries should be generated using RNA obtained at several time points from infected *Tnms*42 suspension cultures. Deep sequencing should be followed by read alignment and functional annotation of the transcripts. Subsequent Gene Ontology term enrichment analysis should shed light on the most prominent host reactions upon infection with a recombinant baculovirus encoding a secreted model protein.

The second main objective of this work was to develop a tool that allows for the inducible downregulation of essential host or viral genes during an infection process. Such a system could play an essential role in the improvement of the baculovirus-insect cell expression system by targeted **glyco-engineering**, the reduction of **contaminating baculovirus formation** or **the elongation of production processes** through impeding apoptosis of the host cells.

Thus, tailor-made miRNA mimics of baculoviral origin should be evaluated with regard to silencing potency in insect cells. Thereafter, the most efficient construct should be applied for the establishment of an inducible, dual viral vector-based system. The presence of mature artificial miRNAs should be confirmed and the silencing efficiency should be assessed with flow cytometry and real-time quantitative PCR on the protein and mRNA level, respectively.

3 PUBLICATIONS

3.1 PUBLICATION A

Comparative transcriptome analysis of a *Trichoplusia ni* cell line reveals distinct host responses to intracellular and secreted protein products expressed by recombinant baculoviruses

Krisztina Koczka, Philipp Peters, Wolfgang Ernst, Lisa Nika, Reingard Grabherr

Published in Journal of Biotechnology

Journal of Biotechnology 270:61–69 (2018)

doi: 10.1016/j.jbiotec.2018.02.001

Journal of Biotechnology 270 (2018) 61–69

Contents lists available at ScienceDirect

Journal of Biotechnology

journal homepage: www.elsevier.com/locate/jbiotec

Comparative transcriptome analysis of a *Trichoplusia ni* cell line reveals distinct host responses to intracellular and secreted protein products expressed by recombinant baculoviruses

Krisztina Koczka[a,b], Philipp Peters[a,b], Wolfgang Ernst[a,b], Heinz Himmelbauer[a,b], Lisa Nika[a], Reingard Grabherr[a,b,*]

[a] Department of Biotechnology, University of Natural Resources and Life Sciences, Muthgasse 18, 1190 Vienna, Austria
[b] acib - Austrian Centre of Industrial Biotechnology, Muthgasse 11, 1190 Vienna, Austria

ARTICLE INFO

Keywords:
Transcriptome
Insect cells
Baculovirus
Unfolded protein response
Secretion
Expression analysis

ABSTRACT

The baculovirus insect cell expression system has become a firmly established production platform in biotechnology. Various complex proteins, multi-subunit particles including veterinary and human vaccines are manufactured with this system on a commercial scale. Apart from baculovirus infected *Spodoptera frugiperda* (*Sf*9) cells, the *Trichoplusia ni* (HighFive) cell line is alternatively used as host organism. In this study, we explored the protein production capabilities of *Tnms*42 insect cells, a new derivative of HighFive, which is free of latent nodavirus infection. As a model system, a cytosolic (mCherry) and a secreted (hemagglutinin) protein were overexpressed in *Tnms*42 cells. The response of the host cells was followed in a time course experiment over the infection cycle by comparative transcriptome analysis (RNA-seq). As expected, the baculovirus infection *per se* had a massive impact on the host cell transcriptome, which was observed by the huge total number of differentially expressed transcripts (> 14,000). Despite this severe overall cellular reaction, a specific response could be clearly attributed to the overexpression of secreted hemagglutinin, revealing limits in the secretory capacity of the host cell. About 400 significantly regulated transcripts were identified and assigned to biochemical pathways and gene ontology (GO) categories, all related to protein processing, folding and response to unfolded protein. The identification of relevant target genes will serve to design specific virus engineering concepts for improving the yield of proteins that are dependent on the secretory pathway.

1. Introduction

Insect cells are among the most important animal cells used for recombinant protein expression in biotechnology. Applications include not only the production of various viral capsid and envelope proteins for use as vaccines or for analytical purposes, but also many enzymes, membrane proteins and self-assembled nanoparticles have been successfully produced in *Spodoptera frugiperda* (*Sf*9) and *Trichoplusia ni* (HighFive) cells. Insect cells are feasible for the expression of intracellular proteins as well as secreted, often complex and glycosylated proteins. With the market entry of a Human Papilloma virus vaccine (Wang and Roden, 2013) and a hemagglutinin based influenza vaccine (Cox and Hollister, 2009) a few years ago, these cell lines became even more attractive as a biopharmaceutical production platform. Besides being safe and easy to handle, infection with recombinant baculoviruses generally allows for high titer production in batch mode (Thompson et al., 2015).

While mammalian stable cell lines have been well characterized and transcriptional regulatory or secretory bottlenecks during recombinant protein production have been intensively studied (Doolan et al., 2008; Nissom et al., 2006; Trummer et al., 2008), little is known about the stress and metabolic load that occurs in insect cells during virus infection coupled protein production. However, it has been shown that investigation and identification of key players in apoptosis, protein transport, folding and secretion allows for targeted cell engineering and improvement of the overall cell factory's performance (Gupta and Lee, 2007; Kuystermans et al., 2007; Wong et al., 2006). Understanding the basics of the host's metabolic regulation and its reaction to the challenges of overexpressing a foreign gene also facilitates the design and upscaling of a production process (Choi et al., 2003; Kim et al., 2012). Due to the infection with a lytic virus that takes over the cellular synthesis machinery after the onset of the infectious cycle, insect cells

* Corresponding author at: Department of Biotechnology, University of Natural Resources and Life Sciences, Muthgasse 18, 1190 Vienna, Austria.
E-mail addresses: krisztina.koczka@boku.ac.at (K. Koczka), philipp.peters@boku.ac.at (P. Peters), wolfgang.ernst@boku.ac.at (W. Ernst), heinz.himmelbauer@boku.ac.at (H. Himmelbauer), lisa.nika@boku.ac.at (L. Nika), reingard.grabherr@boku.ac.at (R. Grabherr).

https://doi.org/10.1016/j.jbiotec.2018.02.001
Received 4 July 2017; Received in revised form 12 January 2018; Accepted 2 February 2018
Available online 09 February 2018
0168-1656/

hold a special place among the established protein expression systems that are based on stable or transient expression in bacterial, yeast and mammalian cell lines. Upon baculoviral infection, the viral replication, capsid and envelope protein production represent the main stress sources for the host cells. In previous studies, deep sequencing was applied to analyze the dynamics of transcriptional changes of both baculovirus (Chen et al., 2013) and host genes (Chen et al., 2014) upon infection of *Tnms*42 (Granados et al., 2016) cells with a wild type *Autographa californica* multiple nucleopolyhedrovirus (AcMNPV). It was shown that the level of viral transcripts increases dramatically after the first 6 h of infection which is accompanied by an immense decrease in host transcript levels. Among the most highly upregulated host genes were those encoding proteins involved in energy/metabolism, indicating a cellular metabolism changing effect of the viral infection. However, it remains unclear, whether the downregulation of various host genes is due to a cellular defense mechanism or it is caused by the viral replication.

For recombinant protein production in insect cells, generally the strong viral polyhedrin promoter is used to drive the transgene expression in infected insect cells (Smith et al., 1983). Polyhedrin is produced in large quantities during natural infections to form the occlusion derived virus (ODV) in order to contain and protect infectious virions (van Oers et al., 2015). However, ODV particles are unwanted in cell culture applications, thus only budded viruses (BV) are used for recombinant protein expression. While polyhedrin accumulates in the nucleus, recombinant proteins either remain in the cytoplasm or are transported and secreted to the supernatant. In general, any viral infection activates the translation of some host genes, which results in stress due to responses involving unfolded proteins (UPR). Also recombinant overexpression of secreted proteins causes UPR in response to an accumulation of unfolded or misfolded proteins in the lumen of the endoplasmic reticulum (ER). The purpose of the UPR is to restore the normal function of the cell by halting protein translation and activating the signaling pathways that lead to increased production of molecular chaperones, or when this cannot be achieved, the UPR aims towards apoptosis. UPR is based on three different signal transducers: IRE1 (inositol requiring enzyme 1), PERK (double stranded RNA-activated protein kinase), and ATF6 (activating transcription factor 6). The activation of the UPR is mediated by binding immunoglobulin protein (BiP) that constitutively binds to the ER-luminal domains of the three UPR sensors maintaining them in an inactive form. Misfolded proteins accumulating in the ER bind to BiP, which causes its release from the UPR sensors triggering their signaling cascades (Wang and Kaufman, 2014). As a result of this autoregulatory program, chaperones that expand the folding capacity of the ER are upregulated. Among those are e.g. BiP, a chaperon of the Hsp70 family, protein disulfide isomerase (PDI) and the glucose regulated protein 94 (Grp94), which is a chaperon of the Hsp90 family (Walter and Ron, 2011). Yet, many questions about the modes of activation and mechanistic details are unanswered. Still, it has been shown that enveloped virus infections can exploit the UPR to increase the capacity of the ER to assist in viral replication (Li et al., 2007).

Hence, the question arises whether the overexpression of a foreign protein has an impact on the overall stress response during the baculovirus infection cycle and maybe causes changes in the UPR. While such strong effects have been observed in other biotechnologically relevant expression systems, the impact in viral infection systems has not been determined so far. Therefore, to better exploit insect cells as a biotechnological expression system, investigation of differentially regulated genes during expression of foreign proteins might provide strategies for optimizing, fine-tuning or controlling recombinant protein production, especially when it comes to complex secreted proteins. Therefore, we applied comparative transcriptome analysis to baculovirus infections, where either an intracellular, a secreted or no recombinant protein was expressed. Previous observations made by Chen et al. (Chen et al., (2014)) show that while the baculoviral infection takes over control of the insect cells, the overall host transcription levels substantially decrease. As particularly secreted proteins require host factors for trafficking through the secretory pathway, the infected host cell may no longer be able to sufficiently process the recombinant protein, leading to the product being stuck inside the cell. Yet, our hypothesis suggests that the overexpression of complex proteins with different localization should induce differential gene expression as part of various cellular pathways that should be detectable on the transcriptome level and potentially yield cellular genes as markers for process monitoring as well as targets for process optimization. Similar to the study of Chen et al. (Chen et al., (2014)), the alphanodavirus-free *Trichoplusia ni* (*T. ni*) derivative *Tnms*42 cell line (Granados et al., 2016) was selected for our differential transcriptome analysis experiments. Since it is derived from *T. ni*, its performance regarding protein secretion is better in comparison with *Sf*9 cells, furthermore, it is expected to be more stable during virus infection, as has been shown for the alphanodavirus-free *Tnao*38 cells (Wilde et al., 2014). To monitor the transcriptional differences upon production of an intracellular or a secreted protein, on the one hand mCherry – an easy to express and detect, stable and intracellularly located protein – was selected for expression. On the other hand, the influenza A virus derived hemagglutinin H1 was expressed, as it represents a complex, glycosylated protein with biopharmaceutical relevance that may serve as a vaccine candidate. Samples were collected from the different baculovirus infected *T. ni* cultures throughout the experiment until 48 h post infection (h p.i.). Deep sequencing and read alignment was followed by functional annotation of the transcripts. Subsequent GO term enrichment analysis of the datasets revealed protein processing in the ER and the triggering of a stress response as the most prominent host reactions to infection with a baculovirus encoding the secreted version of hemagglutinin.

2. Materials and methods

2.1. Cell lines and culture conditions

*Sf*9 cells (ATCC CRL-1711) and the alphanodavirus-free Tn5B1-4 (High Five) derivative *Tnms*42 cell line (obtained as a kind gift from Gary W. Blissard) were cultivated in HyClone SFM4 insect cell medium (GE Healthcare, Little Chalfont, UK) supplemented with 0.1% Pluronic F68 (Sigma-Aldrich, St. Louis, Missouri, USA). Suspension cultures with a volume of 50 ml were grown in 500 ml flasks at 27 °C and 100 rpm.

2.2. Plasmids and recombinant baculoviruses

The nucleotide sequence encoding the mCherry fluorescent protein (GenBank accession no. ACO48269) was chemically synthetized by IDT (Leuven, Belgium). After PCR amplification, the fragment was cloned into the acceptor vector pACEBac-1 (EMBL, Grenoble, France) resulting in pACEBac-1-mCherry. The pACEBac-1-Cal09HA plasmid carrying the coding sequence for the secreted version of hemagglutinin from Influenza A/California/04/2009 (GenBank accession no. JF915184) including a T4 foldon trimerization domain, but lacking both the C-terminal transmembrane- and endodomains was generated as described previously (Krammer et al., 2012).

An empty pACEBac-1 acceptor vector and the recombinant plasmids pACEBac-1-mCherry and pACEBac-1-Cal09HA were transformed into Max Efficiency DH10Bac competent cells (Invitrogen, Carlsbad, USA). Recombinant mCherry, Cal09HA and empty vector control AcMNPVs were generated by transforming the purified bacmid DNA of the three different clones into *Sf*9 cells with FuGene HD transfection reagent (Promega, Madison, Wisconsin, USA) according to the manufacturer`s instructions. Viral titers of the amplified passage three stocks were determined by plaque assay.

2.3. Infections and sampling

*Tnms*42 cells were grown in 12 parallel suspension cultures with a volume of 50 ml and were infected in triplicates at an initial cell density of 1E + 6 cells/ml with either the mCherry virus encoding the intracellular fluorescent protein or with the Cal09HA virus carrying a secreted soluble protein. The infections were carried out at a multiplicity of infection (MOI) = 5. The time point at which the inoculums were added to the cells was designated 0 h post infection. Samples of 1E + 6 cells were taken in duplicates from the recombinant AcMNPV-infected cultures at time points 0, 6, 12, 24 and 48 h p.i. for subsequent RNA isolation and Western blot analysis. Samples deriving from the non-infected cultures and from those infected with the virus carrying the empty pACEBac-1 vector served as non-infected and empty vector controls, respectively.

2.4. RNA extraction and integrity

Total RNA was extracted from samples using TRI Reagent (Sigma-Aldrich, St. Louis, Missouri, USA) according to the manufacturer`s instructions. RNA concentration was determined with the Nanodrop 1000 (Peqlab, Erlangen, Germany). The quality of the isolated nucleic acid was assessed by the Agilent 2100 Bioanalyzer using the RNA 6000 Nano Kit (Agilent, Santa Clara, California, USA).

2.5. SDS-PAGE and western blots

Samples taken at 5 time points from the recombinant AcMNPV-infected cultures were used to monitor mCherry and Cal09HA product formation by SDS-PAGE and Western blot analysis, according to standard protocols (Gallagher, 2001; Ni et al., 2001). Proteins separated by SDS-PAGE using Novex™ 4–12 % Tris-Glycine Mini Protein Gel (Invitrogen, Carlsbad, USA) were electroblotted onto a PVDF transfer membrane (GE Healthcare Life Sciences, Vienna, Austria). Immunodetection was performed using a primary anti-mCherry rabbit antibody (5993–100, BioVision Inc., San Fransisco, California, USA) and a primary anti-Influenza A virus H1N1 HA rabbit antibody (GTX127357, GeneTex, Irvine, California, USA), both paired with a secondary anti-rabbit IgG alkaline phosphatase labeled goat antibody (A9919, Sigma-Aldrich, St. Louis, Missouri, USA). Development of the PVDF transfer membranes were carried out using BCIP/NBT (Promega, Madison, Wisconsin, USA) and results were evaluated by visual estimation.

2.6. Library preparation and sequencing

Libraries with an average cDNA length of 300 base pairs (bp) were prepared from poly(A +) selected RNA using the SENSE Total RNA-Seq Library Prep Kit (Lexogen GmbH, Vienna, Austria) according to the manufacturer's instructions. Strand specific paired-end sequencing (50 bp reads) was performed on the Illumina HiSeq2500 platform using v4 sequencing chemistry at Vienna Biocenter Core Facilities GmbH.

2.7. Read trimming and alignment

In order to remove the sequencing adapters, Trimmomatic v0.35 (Bolger et al., 2014) was applied to the raw RNA-seq reads (adapter parameters 2:30:10). Furthermore, to infer the expression values for each gene, the trimmed reads were aligned either to the *Tnms*42 transcriptome (Chen et al., 2014) or to the reference sequences of AcMNPV (Ayres et al., 1994), mCherry and the secreted version of Cal09HA by using Bowtie v1.1.2 (Langmead et al., 2009). Reads were trimmed by 5 nucleotides (nt) on both ends and a mismatch up to two nt was allowed per alignment. Counting of mapped reads was then performed by using the featureCounts program of the package Rsubread v1.20.6 (Liao et al., 2013) for R v3.2.2. (R Core Team, 2014).

2.8. Differential expression analysis

The differential expression analysis of *Tnms*42 and viral transcripts was performed using the read counts obtained by featureCounts. For each time point we compared the gene expression levels of all pairwise combinations of the four cultures using the edgeR v3.12.1 package (Robinson et al., 2010) for R. To assess differential expression in the comparisons, the Exact test (Robinson and Smyth, 2008) was applied. Genes with a Benjamini-Hochberg-corrected p-value lower than 0.05 were categorized as differentially expressed.

2.9. Functional annotation

The functional annotation of the transcripts derived from a combination of methods. The already existing annotation compiled by Chen et al. (Chen et al., (2014)) was used and it was complemented by our own blast search. Blastx v2.2.30 + (Altschul et al., 1990; Camacho et al., 2009) was applied to query the unigenes in the NCBI nr protein database with entries from GenPept, Swissprot, PDB, PRF, PIR and NCBI Reference Sequence (RefSeq) project. The E-value cutoff was set to 1E-6.

2.10. Gene ontology term assignment and enrichment

In order to assign GO terms to the identified transcripts, the tool Blast2GO (Conesa et al., 2005) was used. For GO enrichment analysis, a tool described previously (http://bioinfo.bti.cornell.edu/tool/GO/GO_enrich.html) (Chen et al., 2014), based on the GO::TermFinder (Boyle et al., 2004) was applied to reveal significantly enriched terms in selected subgroups of *T.ni* unigenes. The multitest correction method applied for the analysis was the false discovery rate (FDR) with a cutoff of FDR < 0.05.

3. Results and discussion

3.1. Recombinant protein expression

To discover possible differences in the host response of *Tnms*42 cells to different baculovirus expressed recombinant proteins, viruses were generated encoding either the reporter gene mCherry (MC) or a truncated soluble version of the influenza A virus hemagglutinin 1 of the California/04/2009 strain (HA). The two model proteins applied in this study differ in the way how they are processed in the cells. While mCherry being an intracellular protein stays inside the cytoplasm, HA is a complex glycosylated molecule that is being processed, transported and secreted. An overview of the experimental setup can be seen on Fig. 1. Suspension cultures of *Tnms*42 cells were infected with the recombinant baculoviruses in triplicates at MOI = 5, followed by RNA extraction at defined time points. After the quality assessment of the RNA by Agilent 2100 Bioanalyzer, the samples were sequenced on the Illumina HiSeq2500 platform. RNA deriving from infected *Tnms*42 cultures of the non-infected control (NIC) and the empty vector control (EVC) virus served as references at each time point throughout the experiment.

3.2. Detection of recombinant protein production

Expression of the two model proteins throughout the experiment was monitored by using samples of the infected cell pellet and the supernatant, obtained from the MC and HA virus infected cultures for Western blot analysis (Fig. 2 A and B, respectively). It has been shown previously that recombinant protein production under the control of the very late polyhedrin promoter is minimal at 12 h p.i., then expression is initiated 18 h p.i. and at 48 h p.i. a very late burst in yield can be observed (Thiem and Miller, 1990). In accordance with these results, immunoblotting revealed HA (72 kDa) specific bands in samples

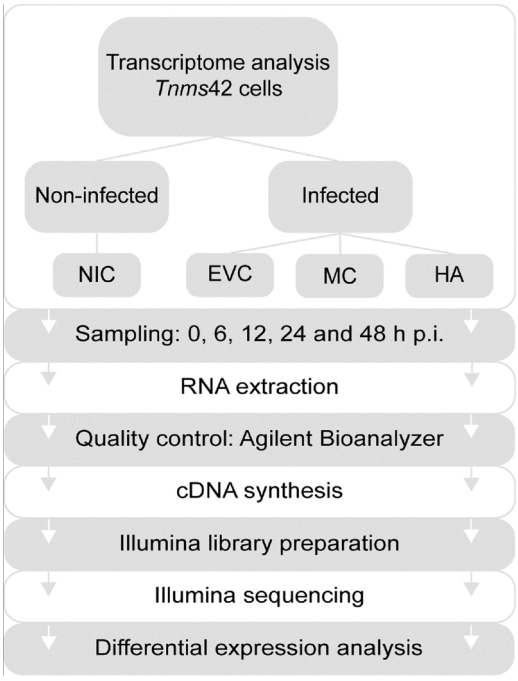

Fig. 1. Experimental outline of recombinant protein expression and transcriptome analysis of baculovirus infected*Tnms*42 cells. Host cells were grown in suspension cultures and were infected in triplicates at a multiplicity of infection (MOI) = 5 with recombinant baculoviruses encoding the intracellular mCherry (MC) protein or the secreted version of the influenza A virus hemagglutinin 1 (HA). Sampling at 5 time points throughout the experiment was followed by RNA extraction, quality control measurements, Illumina sequencing and differential expression analysis. The control samples derived from the triplicate flasks infected by the empty vector control (EVC) virus and the non-infected control (NIC) culture.

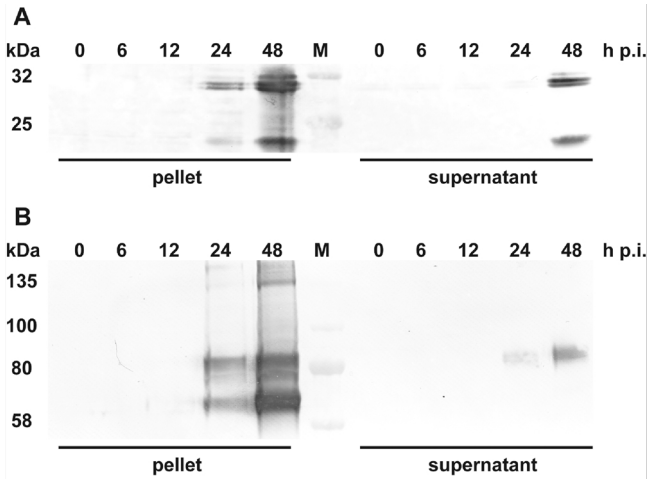

Fig. 2. Western blot analysis of the samples obtained from the recombinant virus infected cultures between 0 and 48 h p.i. (hours post infection). Immunoblotting of heterologous proteins produced in baculovirus infected *T. ni* cells verified that the mCherry protein (A) is present mainly in the cell pellet and slight reactive bands could be detected in the supernatant before the last time point probably due to the virus stock used for the infection. The band at 48 h p.i. presumably results from cell lysis. (B) Analysis of the hemagglutinin glycoprotein revealed that the majority remains in the cells leaving only reduced amounts of the properly folded protein detectable in the supernatant. (M) marker.

of the pellet and the supernatant, collected at 24 h p.i. and at the last time point. Similarly, MC (28.8 kDa) specific strong bands are visible in the pellet at the last two time points, however, the supernatant shows slight bands up to 24 h p.i. and a sharp, defined band at the last time point. The source of the MC detected at the early time points in the supernatant can be mainly the virus stock used for the infection and later on at the last time point MC can be found in larger quantities in the supernatant due to cell lysis. Furthermore, a lower molecular weight band is also observable on the blot at approximately 24 kDa. This is most likely due to an internal translational start site resulting in a truncated, probably not functional molecule (Carroll et al., 2014). Notwithstanding that a secreted version of HA was applied in this experiment, the protein can be found both in the pellet and supernatant fractions. In fact, the amount of HA present in the cells is significantly higher than that found in the supernatant. The intensities of HA reactive bands detected in the cell pellet and supernatant are directly comparable, as the amount of protein loaded corresponds to the same culture volume. It has been observed previously that complex secreted proteins often fail to fold properly and being trapped inside the cells they form large aggregates (Hasemann and Capra, 1990). This phenomenon is well represented by the intracellular HA smear at 48 h p.i. in the cell pellet (Fig. 2B), which seems to be a mixture of hemagglutinin molecules glycosylated and folded to a different extent, whereas in the supernatant the properly processed protein shows a distinct band at the appropriate size of 72 kDa. This heterogeneity is due to the fact that secreted proteins require extensive processing – including various host factors such as those involved in glycosylation, folding or disulfide bridge forming – prior to the secretion of the correct form. Additionally to this, the infection itself represents stress for the cells (Chan, 2014b). Thus, the simultaneous induction of the stress response in the cells and the high demand for active protein processing pathways limit the glycosylation and folding capacity, leading to various glycoforms observed in the pellet.

3.3. Sequencing and read-alignment to reference transcriptome

The sequencing of the samples yielded 758,170,512 read pairs in total, originating from the four different experiments with five separate time points and three replicates each (except for the MC experiment, where one replicate had to be discarded due to insufficient quality). After the removal of sequencing adapters, the reads were aligned to the reference transcriptome containing 70,322 *T. ni* host unigenes, 156 AcMNPV genes (Chen et al., 2014) and the two recombinant genes (MC and HA). 449,465,326 read pairs (59.3%) mapped to the transcripts and thus remained in the datasets for analysis. The relatively low number of mapped reads in the infected datasets can be attributable to the baculovirus infection in the host cells, which is supported by the fact that in the non-infected control a higher ratio (77.9%) of the reads could be mapped. Transcripts were annotated using blastx against all organisms in the NCBI protein database, with an E-value cutoff of 1E-6 that resulted in 27,805 hits (40% of all unigenes). Approximately 53% and 16% of the unigenes with a length shorter than 300 bp and with 300 bp or longer were annotated, respectively. GO terms were assigned to the annotated unigenes with Blast2GO. In overall 20,580 (29%) genes obtained at least one GO term and more than half of these (13,905 unigenes, 20%) were present in more than one GO category. The GO term assignment resulted in 13,307 (19%), 11,145 (16%) and 16,313 (23%) genes in the GO categories biological process, cellular component and molecular function, respectively.

3.4. Transcriptional host responses to recombinant baculovirus infections

In order to reveal the differences in the transcriptional pattern of the host *Tnms*42 in response to an infection with a baculovirus encoding an intracellular or a secreted protein, the reads passing the quality restraints were mapped to the reference *Tnms*42 transcriptome (70,322 unigenes). In case of an infection with the EVC or MC viruses, the trends of the host and viral read counts (Fig. 3A and B, respectively) progress similar to that reported previously (Chen et al., 2014). Namely, at 6 h p.i. an increase in viral mRNA levels (including reads mapped to recombinant protein, if present) is perceivable along with a decrease in

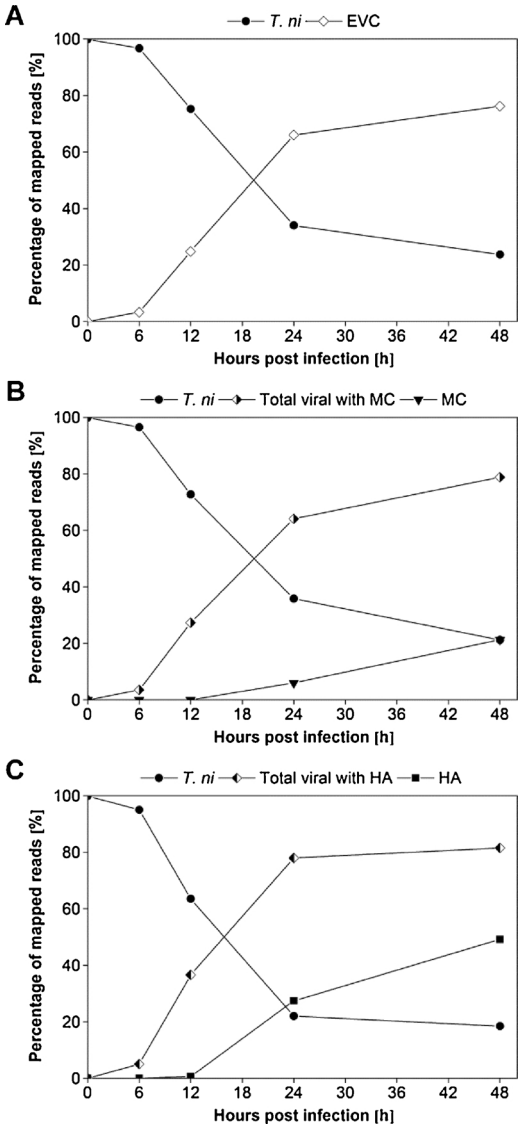

Fig. 3. Percentage of mapped reads to the host cells (*T. ni*) and baculoviral expressed genes. Each time point represents the proportion of host cell versus baculovirus transcripts. The viral read counts increase abruptly after 6 h p.i. and by 48 h p.i. raise to more than 75%. This profile can be observed for all three datasets of virus infected *T. ni* cells. (A) Baculovirus empty vector expression control (EVC). (B) Baculovirus expressing recombinant mCherry (MC). Transcripts for MC are shown separately and together with all viral genes (C) Baculovirus expressing recombinant hemagglutinin (HA). Transcripts for HA are shown separately and together with all viral genes. The highest percentage of mRNAs is reached by the HA virus at all time points throughout the experiment. Recombinant protein expression controlled by the polyhedrin promoter is initiated around 12 h p.i. leading to approximately 21% and 49% product specific reads of the overall transcripts in the MC and HA datasets, respectively.

host mRNA levels. The growth continues in a similar manner until 24 h p.i., when a more moderate increase begins. At 48 h p.i. approximately 24% and 21% of the mRNAs from the EVC and MC datasets belong to the host *Tnms*42, respectively. In comparison, an even steeper increase in the viral mRNA levels can be observed when *Tnms*42 cells are infected with the secreted HA expressing baculovirus (Fig. 3C). As seen before, the viral read count (including reads mapped to HA) increases abruptly from 6 h p.i. onward until 24 h p.i. when it reaches 78% of the total reads. After this time point, a gentler increase of the viral read count leads to a final ratio of 82%, leaving only 18% for the host derived mRNA level. Notwithstanding that the expression of the two recombinant proteins used in this experiment is controlled by the same AcMNPV polyhedrin promoter in both the MC and HA viral constructs,

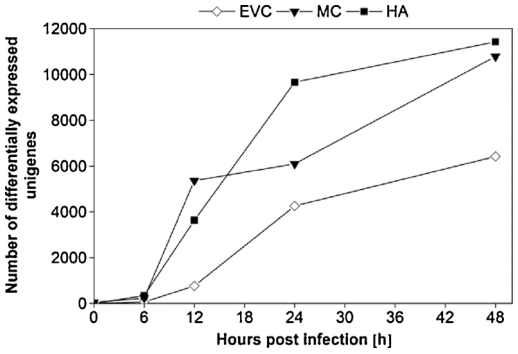

Fig. 4. Overview of the total number of up- and downregulated unigenes throughout the experiment. An increasing number of regulated genes is perceivable in the empty vector control (EVC), mCherry (MC) and hemagglutinin (HA) datasets against the non-infected control (NIC) as the infection proceeds. The number of significantly regulated unigenes ($p < 0.05$) is higher in the datasets of both viruses expressing the recombinant model proteins at all time points compared to the EVC. At 48 h p.i. 10,789 unigenes and 11,422 unigenes are regulated in the MC and HA datasets, respectively, whereas the EVC reaches only 6421 unigenes at the same time point.

there is a difference in the development of the number of reads mapped to these genes. Transcription of the recombinant genes starts around 12 h p.i. for both constructs, but the number of reads mapped to HA shows a sharper increase reaching around 49% of the total read count at 48 h p.i., whereas the growth of MC mRNA level is more modest with a final value of around 21% at the last time point.

3.5. Specifically regulated genes

In order to identify the host genes specifically regulated in response to the different baculovirus infections, the three separate viral datasets (MC, HA, EVC) were compared to time point matched controls of NIC cells. Significantly differentially expressed genes were identified among the three viral sets at each time point. An overview of the total number of up- and downregulated host genes in the infected datasets (Fig. 4) shows increasing numbers of regulated genes as the infections proceed. In case of all three viral constructs, a rapid elevation of differentially expressed genes is perceivable starting from 6 h p.i. and at 12 h p.i. the MC virus reaches the highest number of 5364 unigenes. At later time points the regulated gene count of MC increases slower (6,096 unigenes at 24 h p.i.), summing up to 10,789 unigenes at the last time point. At 24 h p.i. the count of up- and downregulated genes is the highest in the HA dataset with a final value of 11,422 unigenes. The number of significantly regulated transcripts in the EVC infection is much lower throughout the infection cycle compared to those of the two recombinant viruses. At the last time point, approximately only half as many unigenes were affected in the control virus as observed for MC or HA, indicating that the production of a recombinant protein requires additional host factors involved in protein processing and post-translational modifications.

As a next step, in order to examine the differences in expression patterns induced by the different infections, the *T. ni* host genes showing the highest fold change (FC) in expression were examined. The recombinant virus specific top 25 upregulated unigenes (EVC25, MC25, HA25) were collected for each baculoviral expression construct. Fig. 5 shows the expression values as transcript per million reads (TPM) grouped by the three different viruses, with the FC values increasing along the x axis from left to right.

The three sets share 7 common unigenes, out of which 5 are annotated and two are without annotation (UN003339 – N.A., UN006154 – KLV34194, UN026052 – N.A., UN008507 – Pxd, UN063845 – EZA54533, UN065390 – JAT08020, UN009398 – EZA54533). Among the three datasets, the HA25 TPM values are the highest with a maximum of 3295, whereas the EVC25 and MC25 TPM values never exceed

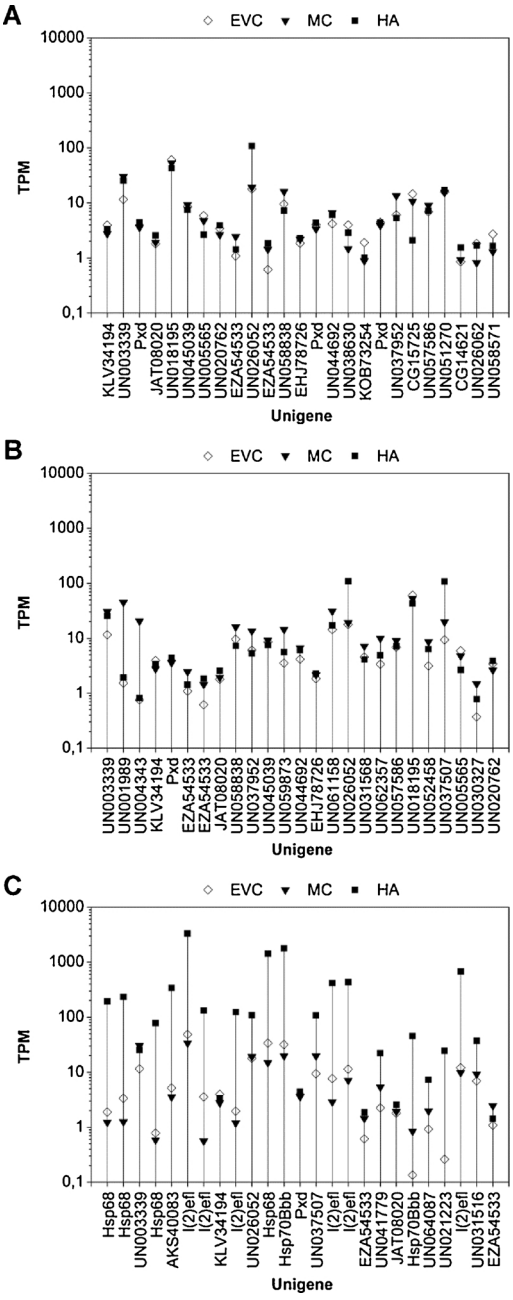

Fig. 5. Transcript per million (TPM) expression values of the top 25 upregulated host genes in the three different viral datasets. (A) Empty vector control top 25 (EVC25) dataset, (B) mCherry top 25 (MC25) dataset, (C) hemagglutinin top 25 (HA25) dataset. Values of the non-infected control samples are not indicated on the graphs, as they stay close to zero in all three viral sets. The top 25 unigenes ($p < 0.05$) of the three viral sets are represented by their *Drosophila melanogaster* protein IDs. If a *D. melanogaster* protein ID was not available, the accession number of the best BLAST hit was applied. In case there is no annotation applicable, the unigene IDs were used. Hsp68 (Heat shock protein 68), Hsp70Bbb (Major heat shock 70 kDa protein Bbb), l(2)efl (Lethal (2) essential for life), Pxd (Peroxidase).

60 and 52, respectively. The highest TPM values in the HA25 dataset belong to l(2)efl (Lethal (2) essential for life; UN039179, FC 2352.5), Hsp68 (Heat shock protein 68; UN001910, FC 1663.5) and Hsp70Bbb (Major heat shock 70 kDa protein Bbb; UN001769, FC 1552.1). Furthermore, in the HA25 set 10 unigene IDs could be assigned to the heat shock protein family Hsp70 and small heat shock chaperones (UN002605 – Hsp68, UN002604 – Hsp68, UN015812 – Hsp68, UN039179 – l(2)efl, UN001910 – Hsp68, UN001769 – Hsp70Bbb, UN062469 – l(2)efl, UN063826 – l(2)efl, UN045506 – Hsp70Bbb, UN029422 – l(2)efl).

Table 1
Overview of the sum of significantly up- and downregulated genes ($p < 0.05$) among the viral datasets at the different time points. Empty vector control (EVC), mCherry (MC), hemagglutinin (HA).

	0 h	6 h	12 h	24 h	48 h
EVC vs. HA	0	0	0	3	183
EVC vs. MC	0	0	2	2	2
MC vs. HA	0	0	5	3	319

3.6. Analysis of host gene set involved in secreted recombinant protein production

To identify potential target genes that limit secreted protein production in the *T. ni* host cell line and might serve as tools for process monitoring, the two datasets of HA and MC were analyzed, considering the type of protein as the discriminating variable. Data from the 48-h time point were selected for this purpose, taking into account the very late polyhedrin promoter activity controlling the expression of the two recombinant model proteins (Thiem and Miller, 1990). The number of significantly regulated genes (compared to NIC) is the highest at 48 h p.i. (see Fig. 4), furthermore, the highest fold change values derive also from this time point. To identify the genes regulated specifically in response to the expression of a secreted glycoprotein, an intracellular and an empty control virus, all three viral datasets were also compared against each other at the last time point. For all time points, Table 1 shows an overview of the numbers of differentially expressed unigenes in the MC and HA datasets, each compared to the EVC, and also those of the HA to MC comparison. Obviously, all three comparisons up to 24 h p.i. are not very informative, since they contain maximum three genes. This is not entirely surprising, as this specific host cell response occurs subsequently to the formation of the recombinant protein, expressed under the polyhedrin promoter. In case of the HA infection, the last time point provides clearly the most information, based on the number of significantly regulated genes. When compared to the EVC infection, the HA virus causes the significant up- and downregulation of 162 and 21 unigenes at 48 h p.i., respectively. For the comparison HA versus MC, these numbers change to 211 upregulated and 108 downregulated unigenes and for MC versus EVC only two unigenes met the criterion for being significantly upregulated at the last time point ($p < 0.05$; probably due to the removal of one replicate). The number of mapped transcripts of the two recombinant proteins (Fig. 3) is different, although their expression is controlled by the same promoter. At 24 h p.i. the number of transcripts mapped to the recombinant products reaches 157,233 TPM for HA and 65,301 TPM for MC. However, this does not seem to have an impact on the differential gene maps derived, since only two-three genes are detected at 24 h p.i. in contrast to the 48-hour time point, where the numbers are 183 (EVC vs. HA) and 319 (MC vs. HA). This shows that the difference in the transcriptome data is merely a response to the type of protein rather than a result of the different mRNA levels detected.

The 319 differentially expressed unigenes of the MC-HA comparison dataset were evaluated with emphasis on the differences arising from the production of a secreted protein compared to an intracellular product. This specific set of 211 upregulated and 108 downregulated host genes was induced only in response to the secreted HA model protein as late as 48 h p.i., when the maturing protein is on its route through the secretory pathway. To identify the most important processes these regulated genes engage in, the set of both the up- and downregulated unigenes was analyzed with a GO term enrichment tool (see Materials and methods). Fig. 6 shows the most significantly enriched GO categories in the ontology “biological process” obtained for the 319 regulated genes with the expected and observed amounts of elements in the

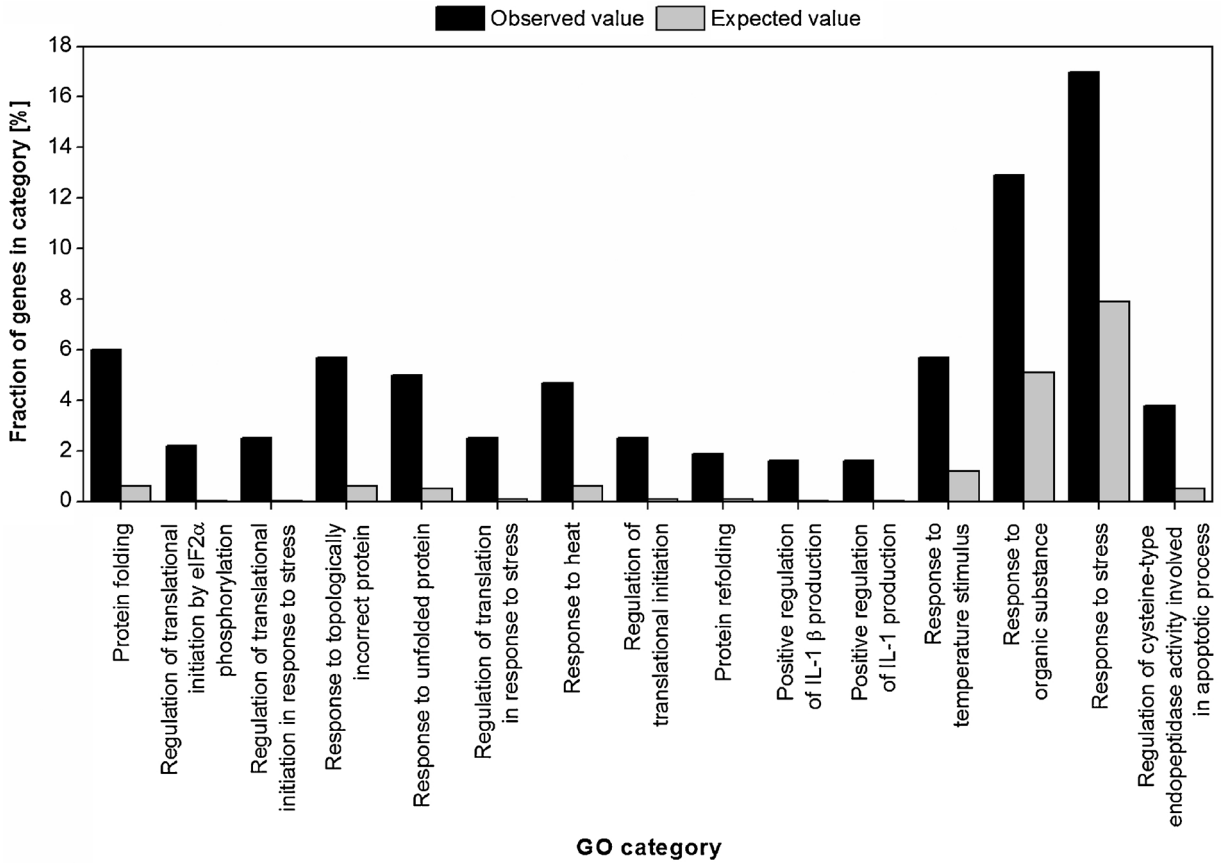

Fig. 6. GO term enrichment results of the 319 MC-HA comparison gene set. The bar chart shows the observed and expected number of genes in the top 15 GO categories (FDR < 0.05) with an increasing p value from left to right along the horizontal axis. The most highly enriched GO categories include those involved in the stress response to unfolded proteins and protein folding, supporting the theory that the host cells are under stress due to the parallel infection and secreted protein production.

groups. The enrichment analysis revealed that many of the regulated unigenes are involved in the stress response to unfolded proteins, supporting the assumption that the cells' processing capacity is at its limit with the elevated level of secreted recombinant protein production. Among the 15 most highly enriched GO categories can be found e.g. protein folding (10-fold enrichment; GO:0006457), response to unfolded protein (10-fold enrichment; GO:0006986), and response to topologically incorrect protein (10-fold enrichment; GO:0035966), reflecting the cells' reaction to the increased amount of incorrectly folded proteins present in the ER. Additionally, to reduce the protein folding load on the ER, general translational attenuation occurs by the phosphorylation of eIF2α (α-subunit of eukaryotic translation initiation factor 2) as part of the UPR (Walter and Ron, 2011), represented by the enriched GO categories of e.g. regulation of translational initiation by eIF2 alpha phosphorylation (96-fold enrichment; GO:0010998) and regulation of translation in response to stress (63-fold enrichment; GO:0043555). Furthermore, the gene set also contains all the most highly upregulated unigenes with a heat shock protein annotation of the HA25 dataset presented in Fig. 5, indicating the protein folding and the stress response to be the most prominent reactions of the host cells to the infection and heterologous protein production.

To further investigate the characteristics of the host cells` stress response to simultaneous baculovirus infection and secreted protein production, the enriched pathways were identified with using solely *D. melanogaster* annotations. As expected, if the HA specific regulated gene set is analyzed with the KEGG pathway mapping tool, "Protein processing in endoplasmic reticulum" is among the top ranked pathways at position 2 after "Metabolic pathways". Homologues of two key players of the UPR (Grootjans et al., 2016) can be found among these genes: BiP (Hsc70-3; UN016518) and PERK (PEK; UN064014). At physiological conditions, BiP can be found bound to the ER luminal domains of IRE1α, ATF6α and PERK, the three stress sensors of the UPR. During heterologous protein production, as the ER exceeds its folding capacity, the amount of misfolded proteins rises and the UPR is activated. BiP preferentially binds to the misfolded proteins, therefore upon elevated levels of incorrectly folded proteins it dissociates from the stress sensors and thereby activates them. The function of the UPR is to return the cells to a homeostatic state through various mechanisms, of which some were found to be upregulated in *Tnms*42 cells in response to secreted HA production. One of these aims to reduce the protein folding load on the ER by general translational arrest through the phosphorylation of eIF2α by PERK. Furthermore, apart from BiP and PERK, another group of unigenes, mainly heat shock proteins were specifically upregulated upon infection with the HA virus. These genes encode the Droj2 (DNA-J-like-2; UN063888), Hsp68 (Heat shock protein 68; UN001910, UN002604, UN002605, UN015812), Hsp70Bbb (Major heat shock 70 kDa protein Bbb; UN001769, UN045506), Hsp83 (Heat shock protein 83; UN009070), Hsc70Cb (Hsp70 interacting protein; UN065785) and l(2)efl (Lethal (2) essential for life; UN002579, UN026941, UN028365, UN029422, UN039179, UN062469, UN063826) *D. melanogaster* homologs and as part of ERAD (ER-associated degradation) they contribute to the removal of incorrectly folded proteins from the ER, followed by ubiquitination and degradation in the cytoplasm by the ubiquitin-proteasome system. Analysis of the 183 regulated unigenes of the EVC-HA comparison (sharing 121 unigenes with the MC-HA comparison) yielded similar results with regard to the activation of the UPR. The main GO categories related to the stress response induced by secreted protein production were also present in the most highly enriched terms with a nearly identical p-value ranking (data not shown). Furthermore, KEGG pathway mapping revealed "Protein processing in

endoplasmic reticulum" to be the most highly enriched pathway when compared to the non-producing infected control cells. The upregulation of these genes and the activation of the UPR in case of an infection with the HA virus is a clear indication of the additional stress caused by secreted protein production in comparison to intracellular products or non-expressing cells.

Although the cellular transcription decreases due to the baculovirus replication, the additional burden of folding and protein processing is specifically visible in the host cell transcriptome. UPR has been described for recombinant protein expression in animal cells before (Hussain et al., 2014), as well as for viral infection (Chan, 2014a). However, in this study we showed that UPR is even more pronounced when a secreted protein is recombinantly produced during a viral infection. In addition, there is a major difference between a recombinant protein that is being processed and secreted and a protein that stays in the cytoplasm. Future studies, including quantitative PCR (polymerase chain reaction) experiments will serve to identify and verify chosen target transcripts. The expected increasing availability of *T. ni* genome sequence data and gene annotations will facilitate further investigations. Once the activation of the UPR has been quantified in more detail, overexpression of some key players might help to increase the protein processing capacity of insect cell lines.

4. Conclusions

In the framework of this study, the alphanodavirus-free *Tnms*42 cell line was investigated with regard to differentially regulated host genes, triggered by various recombinant baculoviral infections. Comparative transcriptome analysis was conducted to reveal the differences in the specific host response to a viral infection on the one hand inducing the production of a complex, glycosylated protein, the secreted version of influenza A virus derived hemagglutinin H1. On the other hand, mCherry was selected as an intracellular model protein, an easy to express and detect, stable fluorescent molecule. Samples were collected throughout the 48-h long experiment that was followed by deep sequencing, read alignment and subsequent functional annotation of the transcripts. Detection of the recombinant products by immunoblotting revealed that in case of HA, high amounts of the protein was stuck in the cell pellet in the form of aggregates and not properly folded or glycosylated molecules, reducing the yield of functional protein in the supernatant. Furthermore, among the most highly upregulated unigenes, numerous chaperones and heat shock proteins were identified, mainly emerging from 48 h p.i. and one of the recombinant datasets (MC, HA). These results imply that the cells specifically react to the stress caused by the viral infection and the parallel secreted protein production, by upregulating various host factors responsible for the correct folding, glycosylation and proper disulfide bridge forming. This assumption was proven to be correct as the GO enrichment analysis of the subset of 319 unigenes specifically regulated in the HA dataset at 48 h p.i. compared to MC identified UPR and protein folding related categories among the most highly enriched terms. KEGG pathway analysis further supported these findings as the second most prominent category related to these unigenes is protein processing in the ER with upregulated unigenes encoding proteins such as BiP and PERK. The key proteins identified to be involved in this severe reaction of the host might serve as promising targets for molecular engineering to achieve a cell line overcoming the bottlenecks of secreted protein production and thus achieving higher yields.

Funding

This work has been supported by the Federal Ministry of Science, Research and Economy (BMWFW), the Federal Ministry of Traffic, Innovation and Technology (bmvit), the Styrian Business Promotion Agency SFG, the Standortagentur Tirol, the Government of Lower Austria and Business Agency Vienna through the COMET-Funding Program managed by the Austrian Research Promotion Agency FFG. This work was also funded by the PhD programme "BioTop – Biomolecular Technology of Proteins" (Austrian Science Funds, Project number FWF W1224).

References

Altschul, S.F., Gish, W., Miller, W., Myers, E.W., Lipman, D.J., 1990. Basic local alignment search tool. J. Mol. Biol. 215, 403–410.
Ayres, M.D., Howard, S.C., Kuzio, J., Lopez-Ferber, M., Possee, R.D., 1994. The complete DNA sequence of Autographa californica nuclear polyhedrosis virus. Virology 202, 586–605.
Bolger, A.M., Lohse, M., Usadel, B., 2014. Trimmomatic: a flexible trimmer for Illumina sequence data. Bioinformatics 30, 2114–2120.
Boyle, E.I., Weng, S., Gollub, J., Jin, H., Botstein, D., Cherry, J.M., Sherlock, G., 2004. GO::TermFinder–open source software for accessing Gene ontology information and finding significantly enriched Gene ontology terms associated with a list of genes. Bioinformatics 20, 3710–3715.
Camacho, C., Coulouris, G., Avagyan, V., Ma, N., Papadopoulos, J., Bealer, K., Madden, T.L., 2009. BLAST+: architecture and applications. BMC Bioinform. 10, 421.
Carroll, P., Muwanguzi-Karugaba, J., Melief, E., Files, M., Parish, T., 2014. Identification of the translational start site of codon-optimized mCherry in mycobacterium tuberculosis. BMC Res. Notes 7, 366.
Chan, S.W., 2014a. The unfolded protein response in virus infections. Front. Microbiol. 5.
Chan, S.W., 2014b. The unfolded protein response in virus infections. Front. Microbiol. 5.
Chen, Y.R., Zhong, S., Fei, Z., Gao, S., Zhang, S., Li, Z., Wang, P., Blissard, G.W., 2014. Transcriptome responses of the host Trichoplusia ni to infection by the baculovirus Autographa californica multiple nucleopolyhedrovirus. J. Virol. 88, 13781–13797.
Chen, Y.R., Zhong, S., Fei, Z., Hashimoto, Y., Xiang, J.Z., Zhang, S., Blissard, G.W., 2013. The transcriptome of the baculovirus autographa californica multiple nucleopolyhedrovirus in trichoplusia ni cells. J. Virol 87, 6391–6405.
Choi, J.H., Lee, S.J., Lee, S.J., Lee, S.Y., 2003. Enhanced production of insulin-like growth factor I fusion protein in Escherichia coli by coexpression of the down-regulated genes identified by Transcriptome profiling. Appl. Environ. Microbiol. 69, 4737–4742.
Conesa, A., Gotz, S., Garcia-Gomez, J.M., Terol, J., Talon, M., Robles, M., 2005. Blast2GO: a universal tool for annotation, visualization and analysis in functional genomics research. Bioinformatics 21, 3674–3676.
Cox, M.M.J., Hollister, J.R., 2009. FluBlok, a next generation influenza vaccine manufactured in insect cells. Biologicals 37, 182–189.
Doolan, P., Melville, M., Gammell, P., Sinacore, M., Meleady, P., McCarthy, K., Francullo, L., Leonard, M., Charlebois, T., Clynes, M., 2008. Transcriptional profiling of gene expression changes in a PACE-transfected CHO DUKX cell line secreting high levels of rhBMP-2. Mol. Biotechnol. 39, 187–199.
Gallagher, S.R., 2001. One-dimensional SDS gel electrophoresis of proteins. Current Protocols in Molecular Biology. John Wiley & Sons, Inc.
Granados, R., Blissard, G., Debbie, P., (2016) Cell Lines That Are Free of Viral Infection and Methods for Their Production. Google patents.
Grootjans, J., Kaser, A., Kaufman, R.J., Blumberg, R.S., 2016. The unfolded protein response in immunity and inflammation. Nat. Rev. Immunol. 16, 469–484.
Gupta, P., Lee, K.H., 2007. Genomics and proteomics in process development: opportunities and challenges. Trends Biotechnol. 25, 324–330.
Hasemann, C.A., Capra, J.D., 1990. High-level production of a functional immunoglobulin heterodimer in a baculovirus expression system. Proc. Natl. Acad. Sci. U.S.A. 87, 3942–3946.
Hussain, H., Maldonado-Agurto, R., Dickson, A.J., 2014. The endoplasmic reticulum and unfolded protein response in the control of mammalian recombinant protein production. Biotechnol. Lett. 36, 1581–1593.
Kim, I.K., Roldao, A., Siewers, V., Nielsen, J., 2012. A systems-level approach for metabolic engineering of yeast cell factories. FEMS Yeast Res. 12, 228–248.
Krammer, F., Margine, I., Tan, G.S., Pica, N., Krause, J.C., Palese, P., 2012. A carboxy-terminal trimerization domain stabilizes conformational epitopes on the stalk domain of soluble recombinant hemagglutinin substrates. PloS One 7, e43603.
Kuystermans, D., Krampe, B., Swiderek, H., Al-Rubeai, M., 2007. Using cell engineering and omic tools for the improvement of cell culture processes. Cytotechnology 53, 3–22.
Langmead, B., Trapnell, C., Pop, M., Salzberg, S.L., 2009. Ultrafast and memory-efficient alignment of short DNA sequences to the human genome. Genome Biol. 10, R25.
Li, B., Gao, B., Ye, L., Han, X., Wang, W., Kong, L., Fang, X., Zeng, Y., Zheng, H., Li, S., Wu, Z., Ye, L., 2007. Hepatitis B virus X protein (HBx) activates ATF6 and IRE1-XBP1 pathways of unfolded protein response. Virus Res. 124, 44–49.
Liao, Y., Smyth, G.K., Shi, W., 2013. The subread aligner: fast, accurate and scalable read mapping by seed-and-vote. Nucleic Acids Res. 41, e108.
Ni, D., Xu, P., Gallagher, S., 2001. Immunoblotting and immunodetection. Current Protocols in Molecular Biology. John Wiley & Sons, Inc.
Nissom, P.M., Sanny, A., Kok, Y.J., Hiang, Y.T., Chuah, S.H., Shing, T.K., Lee, Y.Y., Wong, K.T., Hu, W.S., Sim, M.Y., Philp, R., 2006. Transcriptome and proteome profiling to understanding the biology of high productivity CHO cells. Mol. Biotechnol. 34, 125–140.
Core Team, R., 2014. R: A Language and Environment for Statistical Computing. http://www.R-project.org.
Robinson, M.D., McCarthy, D.J., Smyth, G.K., 2010. edgeR: a bioconductor package for differential expression analysis of digital gene expression data. Bioinformatics 26, 139–140.

Robinson, M.D., Smyth, G.K., 2008. Small-sample estimation of negative binomial dispersion, with applications to SAGE data. Biostatistics 9, 321–332.
Smith, G.E., Summers, M.D., Fraser, M.J., 1983. Production of human beta interferon in insect cells infected with a baculovirus expression vector. Mol. Cell. Biol. 3, 2156–2165.
Thiem, S.M., Miller, L.K., 1990. Differential gene expression mediated by late, very late and hybrid baculovirus promoters. Gene 91, 87–94.
Thompson, C.M., Petiot, E., Mullick, A., Aucoin, M.G., Henry, O., Kamen, A.A., 2015. Critical assessment of influenza VLP production in Sf9 and HEK293 expression systems. BMC Biotechnol. 15, 31.
Trummer, E., Ernst, W., Hesse, F., Schriebl, K., Lattenmayer, C., Kunert, R., Vorauer-Uhl, K., Katinger, H., Müller, D., 2008. Transcriptional profiling of phenotypically different Epo-Fc expressing CHO clones by cross-species microarray analysis. Biotechnol. J. 3, 924–937.
van Oers, M.M., Pijlman, G.P., Vlak, J.M., 2015. Thirty years of baculovirus-insect cell protein expression: from dark horse to mainstream technology. J. Gen. Virol. 96, 6–23.
Walter, P., Ron, D., 2011. The unfolded protein response: from stress pathway to homeostatic regulation. Science 334, 1081–1086.
Wang, J.W., Roden, R.B.S., 2013. Virus-like particles for the prevention of human papillomavirus-associated malignancies. Expert Rev. Vaccines 12.
Wang, M., Kaufman, R.J., 2014. The impact of the endoplasmic reticulum protein-folding environment on cancer development. Nat. Rev. Cancer 14, 581–597.
Wilde, M., Klausberger, M., Palmberger, D., Ernst, W., Grabherr, R., 2014. Tnao38, high five and Sf9–evaluation of host-virus interactions in three different insect cell lines: baculovirus production and recombinant protein expression. Biotechnol. Lett. 36, 743–749.
Wong, D.C., Wong, K.T., Nissom, P.M., Heng, C.K., Yap, M.G., 2006. Targeting early apoptotic genes in batch and fed-batch CHO cell cultures. Biotechnol. Bioeng. 95, 350–361.

3.2 PUBLICATION B

Development of a dual-vector system utilizing microRNA mimics of the *Autographa californica* miR-1 for an inducible knockdown in insect cells

Krisztina Koczka, Wolfgang Ernst, Dieter Palmberger, Miriam Klausberger, Lisa Nika, Reingard Grabherr

Published in International Journal of Molecular Sciences

International Journal of Molecular Sciences 20(3):533 (2019)

doi: 10.3390/ijms20030533

International Journal of
Molecular Sciences

MDPI

Article

Development of a Dual-Vector System Utilizing MicroRNA Mimics of the *Autographa californica* miR-1 for an Inducible Knockdown in Insect Cells

Krisztina Koczka [1,2], Wolfgang Ernst [1,2], Dieter Palmberger [1], Miriam Klausberger [1,2], Lisa Nika [2] and Reingard Grabherr [1,2,*]

[1] Austrian Centre of Industrial Biotechnology - acib, A-1190 Vienna, Austria; krisztina.koczka@boku.ac.at (K.K.); wolfgang.ernst@boku.ac.at (W.E.); dieter.palmberger@boku.ac.at (D.P.); miriam.klausberger@boku.ac.at (M.K.)

[2] Department of Biotechnology, University of Natural Resources and Life Sciences, A-1190 Vienna, Austria; lisa.nika@boku.ac.at

* Correspondence: reingard.grabherr@boku.ac.at; Tel.: +43-1-47654-79006

Received: 7 January 2019; Accepted: 24 January 2019; Published: 27 January 2019

Abstract: The baculovirus-insect cell expression system is a popular tool for the manufacturing of various attractive recombinant products. Over the years, several attempts have been made to engineer and further improve this production platform by targeting host or baculoviral genes by RNA interference. In this study, an inducible knockdown system was established in insect (*Sf*9) cells by combining an artificial microRNA precursor mimic of baculoviral origin and the bacteriophage T7 transcription machinery. Four structurally different artificial precursor constructs were created and tested in a screening assay. The most efficient artificial microRNA construct resulted in a 69% reduction in the fluorescence intensity of the target enhanced yellow fluorescent protein (eYFP). Next, recombinant baculoviruses were created carrying either the selected artificial precursor mimic under the transcriptional control of the T7 promoter or solely the T7 RNA polymerase under a baculoviral promoter. Upon co-infecting *Sf*9 cells with these two viruses, the fluorescence intensity of eYFP was suppressed by ~30–40% on the protein level. The reduction in the target mRNA level was demonstrated with real-time quantitative PCR. The presented inducible knockdown system may serve as an important and valuable tool for basic baculovirus-insect cell research and for the improvement of production processes using this platform.

Keywords: artificial miRNA; baculovirus-insect cell expression system; RNA interference

1. Introduction

The baculovirus-insect cell expression system (BEVS) is widely used for the manufacturing of various recombinant products, e.g., virus-like particles to be applied as vaccines [1] or display scaffolds [2], viral vectors for gene therapy [3], gene delivery vectors [4], and various other complex proteins. The popularity of this platform lies in its advantageous properties that allow for high product titers in combination with lower production costs as compared to production in mammalian cells [5] as well as proper post-translational modifications such as glycosylation [6]. Additionally, several attempts have been made over the years to make this expression system even more appealing for industrial use. Besides the establishment of efficient expression vectors along with easy transfection and cloning procedures, RNA interference (RNAi) has been exploited to specifically downregulate selected genes during the production process.

RNAi is a conserved biological process using short RNA molecules that include small-interfering RNAs (siRNAs) and microRNAs (miRNAs) for the regulation of gene expression [7]. siRNAs are

~21–25 nucleotide (nt) long non-coding double-stranded RNA (dsRNA) molecules that are produced in response to foreign nucleic acid originating from exogenous invaders (such as viruses or transposons) to sequence-specifically degrade perfectly complementary target messenger RNAs (mRNAs) [8]. In contrast, miRNAs are ~19–24 nt long non-coding RNA pieces originating from purposefully expressed stem-loop precursors with an incomplete double-stranded character, called primary miRNA (pri-miRNA) transcripts. Unlike siRNAs, miRNAs show imperfect complementarity to their target mRNA sequences, and they mediate translational repression and transcript degradation [9].

In general, several studies have been carried out in insect cells focusing on the exploitation of the RNAi pathway to create a tool for gene function studies and to improve the production system by specific regulation of host or baculoviral gene expression. Huang et al. [10] established a baculovirus-based system in *Spodoptera frugiperda Sf*9 cells to achieve the synthesis of long hairpin dsRNAs in vitro that might serve as a reverse genetics tool. Although long dsRNAs are easy to design and they abolish the expression of a target gene effectively, the processing of a long hairpin may result in multiple siRNA duplexes targeting various genes, which carries the risk of severe off-target effects [11]. Another, possibly more target-specific approach utilizes short hairpin RNAs (shRNAs). Studies [12] report the successful downregulation of *N*-acetylglucosaminidase to generate more mammalian-like glycosylation in *Trichoplusia ni* cells using shRNAs delivered by DNA vectors. Others [13] aimed at an improved production platform by targeting *S. frugiperda* caspase-1 using a baculoviral shRNA vector. However, in order to obtain well-defined transcript termination, the expression of shRNAs in vivo necessitates the use of strong Pol III promoters, which not only limits the application of the system but may also cause cytotoxicity in the host cells [14].

Alternatively, synthetic siRNAs that target a chosen gene can be embedded within endogenous pri-miRNA transcripts that serve as backbones. The expression of such mimics can be driven by Pol II promoters to overcome the cytotoxicity linked to Pol III promoters [14]. The pri-miRNA carrying the synthetic siRNA—or the so-called artificial microRNA (amiRNA)—mimics the natural transcript and is recognized and processed by the host cell´s microRNA biogenesis pathway [15]. Briefly, concurrently with transcription by RNA polymerase II, the natural pri-miRNA transcript (or a mimic) is cleaved by the microprocessor complex comprising one molecule of Drosha and two molecules of its cofactor Pasha [16]. The resulting ~70 nt long precursor hairpin structure, known as the pre-miRNA, is thereafter exported to the cytoplasm by the transporter protein Exportin-5 together with Ran-GTP. Here, another processing complex consisting of Dicer-2 and its cofactors the dsRNA-binding proteins Loquacious PD isoform (Loqs-PD) and R2D2 cleaves the pre-miRNA to short double-stranded RNA fragments [17]. Next, through the binding of Argonaute 2 (Ago2) protein with the RNA duplex, the precursor RNAi-induced silencing complex (pre-RISC) is formed [18]. The mature RISC contains only the strand with the less stable base pair (bp) at the 5´ end, called the guide strand, whereas the other strand of the RNA duplex (passenger strand) is cleaved. When a pri-miRNA transcript mimic is processed, the customized amiRNA sequence is loaded into the mature complex [15]. Finally, this activated multi-enzyme complex cleaves complementary mRNA sequences [7]. Haley et al. [11] established such a system in *Drosophila melanogaster* S2 cells and transgenic flies. Moreover, Zhang et al. [19] reported that the use of *Bombyx mori* nucleopolyhedrovirus pri-miRNA mimics to effectively inhibit viral replication in silkworm.

The pri-miRNA transcript of *Autographa californica* nucleopolyhedrovirus miR-1 (*Ac*MNPV-pri-miR-1) is the first and, to our knowledge, so far only miRNA discovered in the genome of *Ac*MNPV [20]. To reveal and assess its silencing capabilities as a pri-miRNA mimic backbone, the original siRNA duplex within the stem-loop structure was replaced by a synthetic sequence targeting eYFP. Additionally, four different structural versions of the natural transcript were created by applying small changes in the stem sequences and the flanking regions according to general design rules [14]. To evaluate the silencing potency of these customized constructs, a plasmid-based screening was carried out. According to this data, the most effective stem-loop structure was selected for insertion into the genome of *Ac*MNPV. For the transcriptional control of the most effective silencer

mimic, a T7-based expression system was developed. The bacteriophage T7 transcription machinery is an attractive system due to its strict promoter selectivity and high catalytic activity [21]. Several successful attempts have been made in past years with the aim of utilizing this 100 kDa prokaryotic enzyme for protein expression in eukaryotic cells, including mammalian [22], insect [23,24], and plant [25] cell lines.

The experimental setup presented here relies on two viral vectors. One recombinant baculovirus was designed to harbor an amiRNA construct linked to the bacteriophage T7 promoter, while the corresponding T7 RNA polymerase (T7 RNAP) with an additional nuclear localization signal was expressed by a second viral vector. The selective transcriptional activity, together with the fact that the functional expression of the amiRNA construct depends on the presence of the T7 RNAP that is encoded on a separate virus constitute an inducible system. Even when essential genes are targeted for downregulation, the two viral expression vectors can be produced efficiently whenever they are separate from each other. We could show that the T7 RNAP is functional in *Sf*9 cells as it activates the transcription of genes that are under control of the T7 promoter. We further demonstrated that amiRNAs are functional after transcription by the T7 RNAP as they successfully downregulated the reporter gene eYFP. Our T7-based inducible expression system may serve as a valuable tool for gene regulation during a production process, e.g., by altering the glycosylation pattern or downregulating essential genes such as proteases or proteins involved in baculovirus assembly.

2. Results and Discussion

2.1. amiRNA Construct Design

Here we describe a novel, inducible knockdown system established in *Sf*9 cells. Our approach is based on combining the transcription machinery of the prokaryotic bacteriophage T7 [23] with RNAi-based amiRNA constructs derived from the *Ac*MNPV-pri-miR-1 transcript [20]. One common way to establish a targeted RNAi system is to exploit the endogenous miRNA biogenesis pathway by embedding a small, artificial RNA molecule into the hairpin structure of a natural pri-miRNA transcript. This method is considered more advantageous over the traditional siRNA-based approaches, as it confers higher gene silencing efficiency in combination with reduced off-target effects [26]. Since baculoviruses take control of the host cell synthesis machinery as part of the infectious cycle and downregulate almost all cellular genes [27], it was of importance to select a viral miRNA precursor, which is highly abundant during the infection cycle. Thus, the 58 nt long precursor hairpin of the baculovirus-encoded *Ac*MNPV-miR-1 (*Ac*MNPV-pre-miR-1) was selected. The 20 nt long processed miR-1 targets the viral gene *ac94* (ODV-E25) [28]. In our experimental setup, the eYFP was chosen as a model target for the amiRNA. Therefore, each hairpin harbored a highly effective, previously described customized siRNA sequence targeting enhanced green fluorescent protein (eGFP) [29]. Notwithstanding that a slightly different eGFP variant was applied in this study, the synthetic duplex embedded in the amiRNA constructs was still applicable to estimate the silencing capacity of the proposed system, as the eYFP sequence used in these experiments also contained the target nucleotides of the published synthetic siRNA.

Overall, four artificial versions of the *Ac*MNPV-pri-miR-1 transcript were generated: amiR-1A, amiR-1B, amiR-1C, and amiR-1D (amiR-1A-D). Sequences of the amiRNA constructs are listed in Table 1, and the precursor hairpin structures (without the flanking regions) are presented in Figure 1. The 58 nt long amiR-1A hairpin construct mimics the natural *Ac*MNPV-miR-1 in all aspects, as they share the same internal structure and the nucleotide composition of the pre-miRNA backbone stem and loop. Moreover, amiR-1A contained 31 nt long flanking regions of the natural *Ac*MNPV-pri-miR-1 transcript upstream and downstream of the hairpin without internal restriction sites, since the construct was synthesized as a single piece of DNA fragment. The processing of the artificial construct by the miRNA biogenesis pathway should result in a 20 nt long guide strand. This small RNA contains a base pair mismatch to the target eYFP sequence at the terminal 3′ nucleotide (T→C). Thereby, the 3′-end

becomes more stably paired to the passenger strand (in comparison to the 5′ end starting with A) and facilitates its incorporation into the RISC. Additionally, a mismatch at the 3′ end of the guide strand was shown to be advantageous, as it induces more potent silencing in mammalian cells [30].

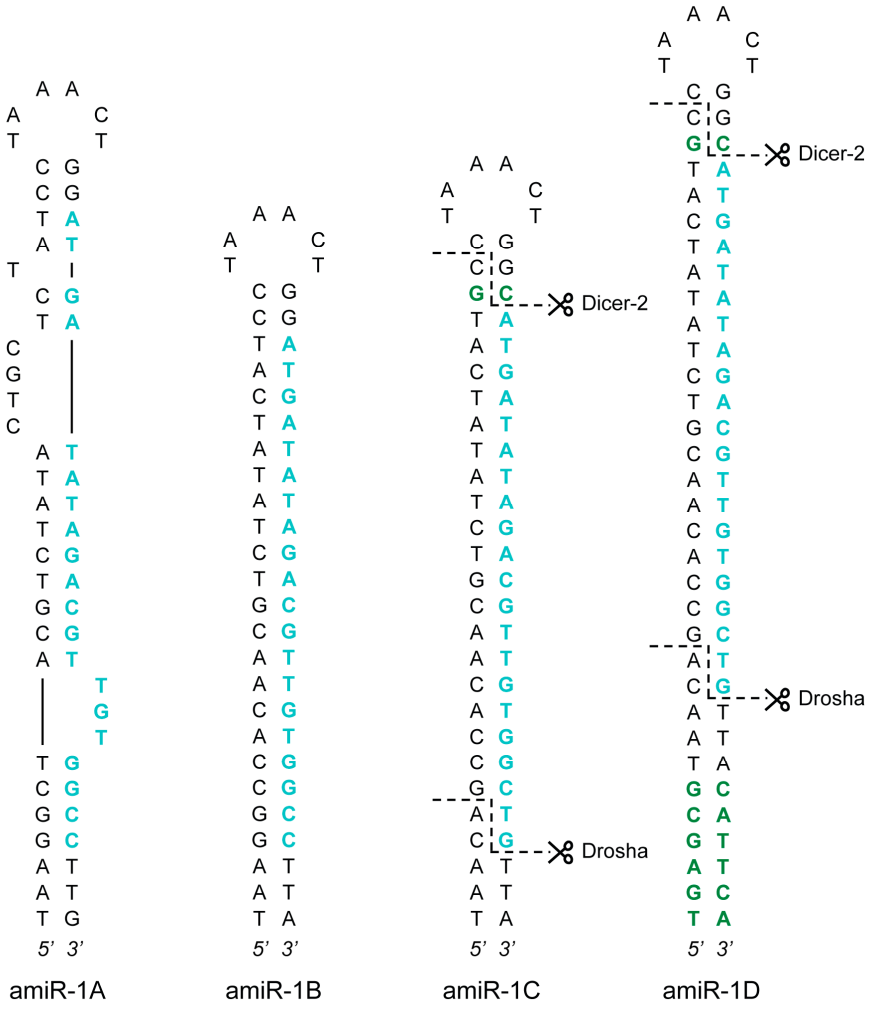

Figure 1. amiRNA precursor hairpin structures. Four structural versions of the *Ac*MNPV-pri-miR-1 transcript were created: amiR-1A-D. The guide strands targeting eYFP are highlighted in blue, whereas the additional nucleotides in the stem regions (in comparison to the *Ac*MNPV-pre-miR-1 hairpin) are showed in green. The anticipated Drosha and Dicer-2 cut sites (as a result of the extra nucleotides) are marked with dashed lines in the amiR-1C and amiR-1D structures.

Based on the effectiveness of similar setups [11,31], the internal structure of the stem-loop constructs amiR-1B-D was substantially different from that of amiR-1A (Figure 1), as the stem region of these hairpins showed perfect complementarity, thereby lacking the bulges and mismatches that can be found in the pre-miR-1. Furthermore, the longer flanking regions of 120 nt upstream and downstream of the stems necessitated a different, but commonly used cloning procedure (see Section 3.2), where the insertion of the hairpins, as annealed oligonucleotides (oligos), was facilitated by restriction sites between the flanking regions, resulting in short scar sequences between the hairpin's ends and the flanking sequences. This, however, did not seem to interfere with the processing of the amiRNA as shown for the amiR-1C construct (see Appendix A section "Detection of Mature amiRNAs"). Apart from these differences, the 56 nt long amiR-1B construct shares the exact same embedded 20 nt guide strand with the amiR-1A hairpin structure, including the above-mentioned mismatch at Position 20. The amiR-1C and amiR-1D constructs were modified based on previous findings regarding the two possible mechanisms of cleavage site recognition of the microprocessor complex (consisting of

Drosha and its cofactor Pasha) in the early steps of the miRNA biogenesis pathway. According to this data [32–34], the dominant process is that, with Pasha serving as a molecular ruler, the enzyme complex cuts 11 nt distant from the basal junction along the stem of the pri-miRNA hairpin structure. In contrast, the less governing cleavage mechanism initiates the cleavage 22 nt distant from the apical junction. Theoretically, in order to achieve precise cleavage, pri-miRNA transcript mimics should be designed in such a way that both mechanisms lead to the same cleavage sites. However, neither the natural hairpin structure of *Ac*MNPV-pri-miR-1 nor the mimic constructs amiR-1A or amiR-1B fulfills the 11 nt or the 22 nt distance criterion mentioned above. The amiR-1C and amiR-1D stem-loop constructs were nevertheless designed with regard to these distance constraints. The guide strand embedded in the 60 nt long amiR-1C hairpin was identical to the original 21 nt long siRNA published previously [29]. It contained no mismatches to the target eYFP (as opposed to amiR-1A-B), and an extra C-G bp was inserted into the stem region of the construct between the artificial RNA duplex and the loop. These two modifications increase the distance between the basal and apical junctions to 22 nt, making the structure accessible to the secondary microprocessor cleavage mechanism. The 72 nt long amiR-1D construct includes the complete hairpin of the amiR-1C stem-loop structure with an additional 6 nt stem extension to increase the distance between the basal junction and the required cut site to 11 nt. Thus, regardless of the preferred cleavage process of the microprocessor complex, the processing of the amiR-1D construct should lead to the same precursor hairpin product. For the precise assessment of the four constructs (amiR-1A-D), controls with matching structures and scrambled embedded siRNA sequences were created: amiR-1As, amiR-1Bs, amiR-1Cs, and amiR-1Ds (amiR-1As-Ds).

2.2. Plasmid-Based Evaluation of the amiRNA Constructs

A plasmid-based screening assay was carried out, to evaluate and select the best amiRNA construct. *Sf*9 cells seeded into 6-well plates were transfected with 200 ng of the reporter plasmid pACEBac1ie1-eYFP in combination with 2 µg of one of the eight following plasmids: pACEBac1ie1amiR-1A-D or pACEBac1ie1amiR-1As-Ds (control). Forty-eight hours post-transfection (h p.t.), the silencing efficiency was evaluated by microscopy and flow cytometry. Figure 2 shows the matching phase contrast and fluorescence images of the co-transfections. A merely visual estimation of the images suggests that the strongest silencing on the protein level was achieved (in comparison to the structure-specific scrambled controls), when either the amiR-1B or amiR-1C construct was applied, whereas in the case of amiR-1A or amiR-1D hardly any difference could be observed between the control and sample fluorescence images. These results were further supported by the data obtained by flow cytometry measurements (Figure 2). As a basis of comparison, the sum of intensity (overall fluorescence intensity) values was calculated by multiplying the fluorescent cell count with the arithmetic mean of the fluorescence intensity. According to this, the amiR-1B and amiR-1C hairpin constructs were the most efficient mimics in silencing the target gene eYFP, with 59% and 69% reductions in the overall fluorescence, respectively. The increased distance between the hairpin's apical and basal junctions in amiR-1C might have increased the processing efficiency by the microprocessor complex, leading to a greater decrease in eYFP fluorescence intensity as compared to amir-1B. In contrast, the lowest efficiency of 14% reduction in eYFP intensity was achieved with amiR-1D, containing the most modifications as compared to the original *Ac*MNPV-miR-1 precursor structure. This suggests that certain changes or too many modifications are not tolerated by the endogenous miRNA processing pathway. Surprisingly, the amiR-1A construct achieved only a 20% reduction in eYFP intensity, despite a high resemblance to the original *Ac*MNPV-miR-1 precursor hairpin. A reason behind this could be the rather short flanking regions included in this construct. As the amiR-1A mimic contains only 31 nt single stranded flanking RNA upstream and downstream of the hairpin structure, it is possible that this has an impact on the secondary structure of the construct. Based on these results, the amiR-1C hairpin construct was considered most effective for the downregulation of the target eYFP with the embedded amiRNA and was selected for further studies. However, it must

be noted that the embedded amiRNA might affect its processing in the hairpin; thus, one of the other constructs may prove to be more effective in combination with other amiRNA sequences.

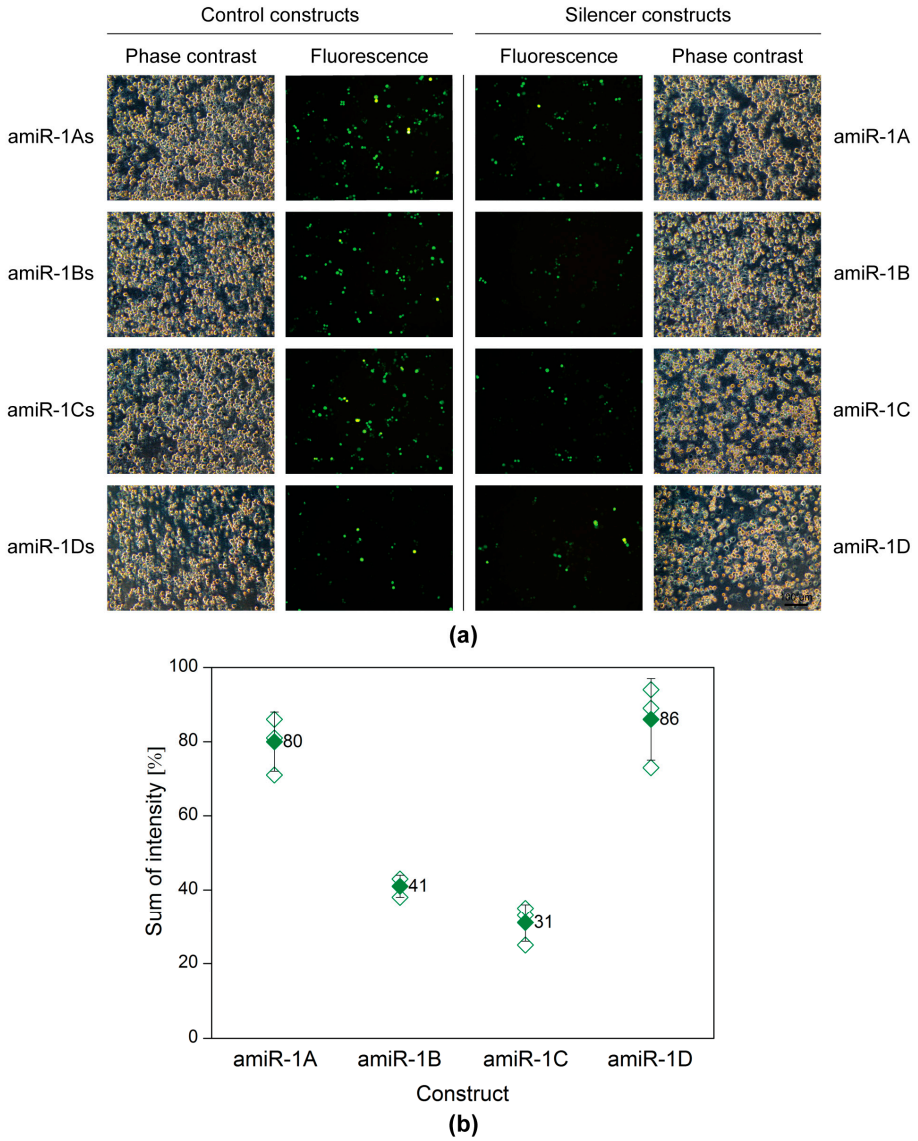

Figure 2. Plasmid-based screening of the amiRNA constructs with fluorescence microscopy (**a**) and flow cytometry (**b**). *Sf*9 cells were co-transfected with the reporter plasmid pACEBac1ie1-eYFP (200 ng) in combination with one of the four artificial hairpin constructs (pACEBac1ie1amiR-1A-D; 2 µg) or the four controls (pACEBac1ie1amiR-1As-Ds; 2 µg). The silencing efficiency was evaluated at 48 h p.t. (**a**) The microscopy images (100× magnification) imply that the highest silencing activity was achieved by amiR-1B and amir-1C, whereas amir-1A and amiR-1D seemed to have no remarkable effect on the overall eYFP fluorescence, when compared to the structure-specific scrambled controls. (**b**) Data obtained by flow cytometry show that amiR-1B and amir-1C reduced the overall eYFP fluorescence by 59% and 69%, respectively. In comparison, amiR-1A and amiR-1D resulted only in fluorescence reductions of 20% and 14%, respectively. The hollow diamonds represent values of the individual measurements, whereas the full diamonds stand for the average sum of intensity value for a given construct.

2.3. The Inducible Knockdown System

The amiR-1C hairpin structure was selected based on the preliminary screening experiments as the most efficient gene silencer. The baculoviruses *Ac*-T7amiR-1C_ ie1eYFP and *Ac*-T7amiR-1Cs_ ie1eYFP

harboring the eYFP under the control of the ie1 promoter, together with either the amiR-1C or the amiR-1Cs pri-miRNA under the control of T7 promoter, respectively. The inducibility of the system lies in the fact that, in the absence of the T7 RNAP, the hairpin structures are not transcribed, as the T7 promoter is inactive without its corresponding T7 polymerase. Therefore, the *Ac*-ie1T7RNAP virus served as the inducer of the silencing effect. Before the setup of the inducible system, the expression and the functionality of the *Ac*-ie1T7RNAP virus was confirmed with immunoblotting and an in vitro transcription assay (see Figure A1). The system's mechanism of action is illustrated in Figure 3. Briefly, for the transcription of a pri-miRNA transcript mimic and the subsequent production of a mature amiRNA, the simultaneous presence of either the *Ac*-T7amiR-1C_ ie1eYFP or the *Ac*-T7amiR-1Cs_ ie1eYFP (control) baculovirus (Virus A) and the *Ac*-ie1T7RNAP virus (Virus B) is necessary. Upon co-infection of *Sf*9 cells with the two recombinant baculoviruses, the T7 RNAP expressed from Virus B transcribes the pri-miRNA transcript mimic encoded by Virus A. The entry of this transcript into the host's endogenous miRNA processing pathway is followed by the digestion with the Drosha and Dicer-2 nucleases, resulting in an amiRNA duplex containing either an eYFP targeting (amiR-1C) or a scrambled control (amiR-1Cs) guide amiRNA strand. The mature RISC containing only the guide amiRNA strand initiates the degradation of perfectly complementary mRNA sequences and thereby impedes translation and product formation of eYFP (provided that the *Ac*-T7amiR-1C_ ie1eYFP virus was used as Virus A).

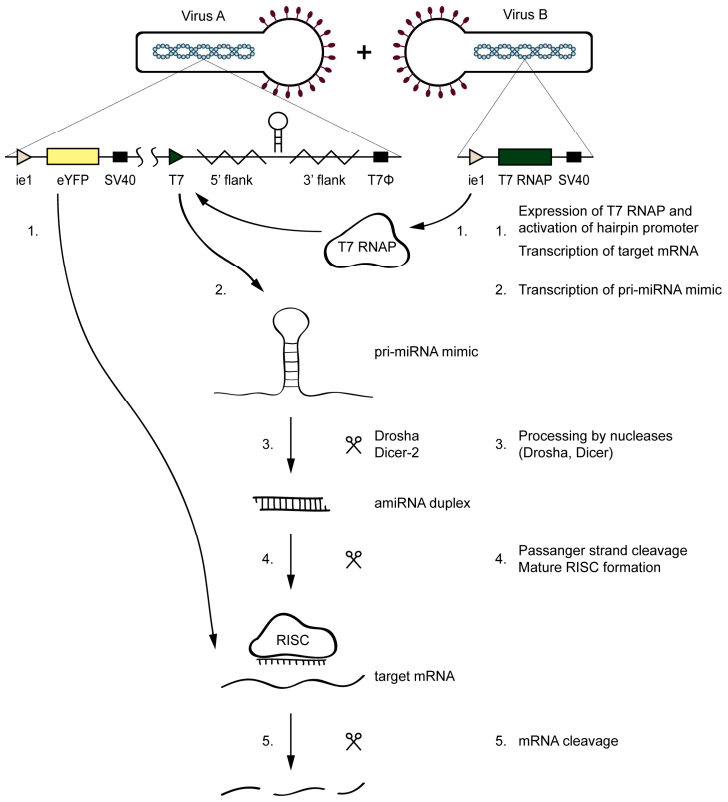

Figure 3. Mechanism of the inducible silencing system targeting eYFP. Upon the co-infection of the *Ac*-T7amiR-1C_ ie1eYFP virus (Virus A) and the *Ac*-ie1T7RNAP virus (Virus B), the T7 RNAP expressed from Virus B (**1**) transcribes the pri-miRNA transcript mimic harboring the eYFP targeting amiR-1C on Virus A (**2**). The transcript enters the host's miRNA biogenesis pathway, where it is processed by the Drosha and Dicer-2 nucleases (**3**). The resulting amiRNA duplex provides the guide strand (**4**) and thereby activates the RNA-induced silencing complex (RISC) that cleaves the perfectly complementary mRNAs of eYFP (**1**,**5**), thereby impeding its translation and the product formation. No silencing occurs in the control reaction, where the *Ac*-T7amiR-1Cs_ ie1eYFP is used as Virus A.

*Sf*9 cells were co-infected at various multiplicity of infection (MOI) combinations with the *Ac*-ie1T7RNAP virus and either the *Ac*-T7amiR-1C_ ie1eYFP or the *Ac*-T7amiR-1Cs_ ie1eYFP (control) baculovirus. Samples were collected 48 h post-infection (h p.i.) to evaluate the silencing efficiency of the selected artificial hairpin structure (amiR-1C) in comparison to its scrambled sequence control (amiR-1Cs) on the protein level. Figure 4 shows the flow cytometry results of co-infections, where the MOI of the *Ac*-T7amiR-1C_ ie1eYFP and *Ac*-T7amiR-1Cs_ ie1eYFP (control) viruses was either 1 or 5, whereas the *Ac*-ie1T7RNAP was added to the cultures at either MOI 5 or MOI 10. The 5-fold excess of the *Ac*-ie1T7RNAP virus resulted in a 37% decrease in the overall eYFP fluorescence intensity, whereas upon applying a 10-fold excess, a 31% reduction was observed. However, the combination of both viruses at MOI 5 turned out to be a less efficient setup, since only a minor reduction of 8% was perceivable in the fluorescence intensity. There are several possible reasons behind the relatively low efficiency of silencing observed with the virus-based inducible system in comparison to the results of the plasmid experiments. First, as the plasmid-based mimic vectors silence the target eYFP in a dose-dependent manner, the ratio between the target and the mimic is essential. However, the inducible system utilizes the T7 promoter for the transcription of the mimics and the ie1 promoter for eYFP, which changes the relative amounts of the silencer and the target. Second, a prerequisite for the expression of the mimics is the presence of a functional T7 RNAP in the same cell. However, the viruses are added concurrently to the insect culture, thus the RNAP and the target eYFP are being expressed simultaneously. This leads to a certain amount of pre-existing target protein, before the processing of the mimic. Furthermore, the eYFP is known to be a rather stable protein [35], which also contributes to the observed effects. Nevertheless, the flow cytometry data on the protein level indicate the functionality of the inducible system on a viral basis, which was further confirmed on the RNA level with real-time quantitative PCR (RT-qPCR).

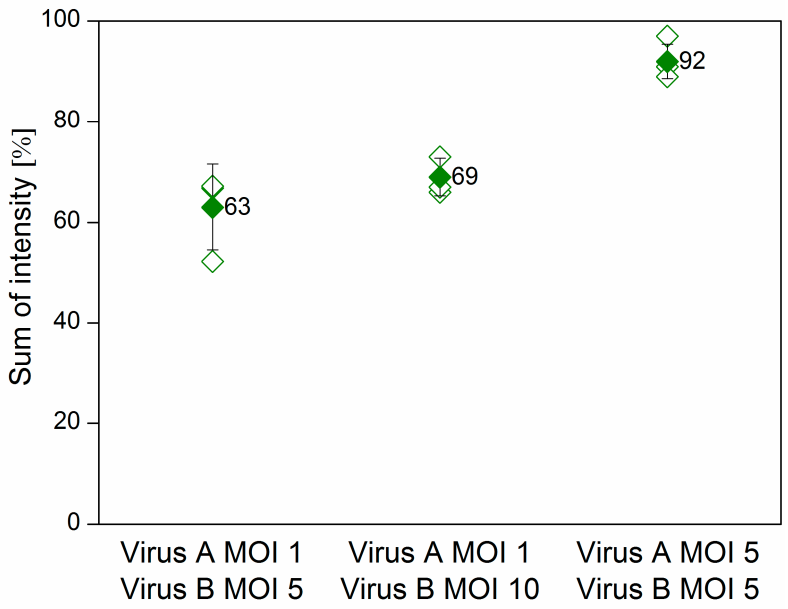

Figure 4. Flow cytometry results of the virus-based inducible system. *Sf*9 cells were co-infected with the fusion virus *Ac*-T7amiR-1C_ ie1eYFP (Virus A) at MOI 1 in combination with the *Ac*-ie1T7RNAP virus (Virus B) in either 5-fold or 10-fold excess (MOI 5 or MOI 10), resulting in a reduction of 37% and 31% in the overall fluorescence intensity, respectively. In case both viruses were added at MOI 5 to the culture, only a slight decrease of 8% was observable. All values are calculated and compared to co-infections with the construct-specific scrambled control virus *Ac*-T7amiR-1Cs_ ie1eYFP (100%) under the same conditions. All co-infections were repeated three times. The hollow diamonds represent values of the individual measurements, whereas the full diamonds stand for the average sum of intensity value for a given construct.

2.4. Evaluation of the Inducible System on the RNA Level

To reveal, whether the reduction in overall eYFP fluorescence intensity was indeed the effect of specific downregulation, the processing and presence of mature amiRNAs was confirmed (see Figure A2) and the decrease in the eYFP mRNA level was quantified by RT-qPCR. Again, samples were obtained from co-infected (*Ac*-T7amiR-1C_ ie1eYFP or *Ac*-T7amiR-1Cs_ ie1eYFP virus at MOI 1 or 5 in combination with *Ac*-ie1T7RNAP virus at MOI 5 or 10) *Sf*9 cultures. After total RNA extraction and genomic DNA removal, a one-step reverse transcription and RT-qPCR reaction was carried out using specific primers for eYFP. The data were evaluated using the $2^{-\Delta\Delta Cq}$ method [36]. For the calculation of ΔΔCq values and corresponding fold change values presented in Figure 5, ΔCq control values originating from co-infections with the construct-specific scrambled control virus *Ac*-T7amiR-1Cs_ ie1eYFP (ΔΔCq = 0 or fold change of −1) under the same conditions were applied. The results were consistent with those from flow cytometry analysis. The co-infection with 5-fold excess (MOI 5) of the *Ac*-ie1T7RNAP virus compared to *Ac*-T7amiR-1C_ie1eYFP (MOI 1) resulted in a ΔΔCq value of −0.34 corresponding to a 1.3-fold reduction in the eYFP mRNA level, whereas applying the RNAP virus in 10-fold excess (MOI 10) lead to a stronger decrease with a ΔΔCq value of −0.59, indicating a 1.5-fold reduction in eYFP mRNA. However, the co-infection containing the same amounts of both viruses (MOI 5) did not result in a statistically significant suppression in the target mRNA level with a ΔΔCq value of −0.11 and a corresponding 1.1-fold reduction.

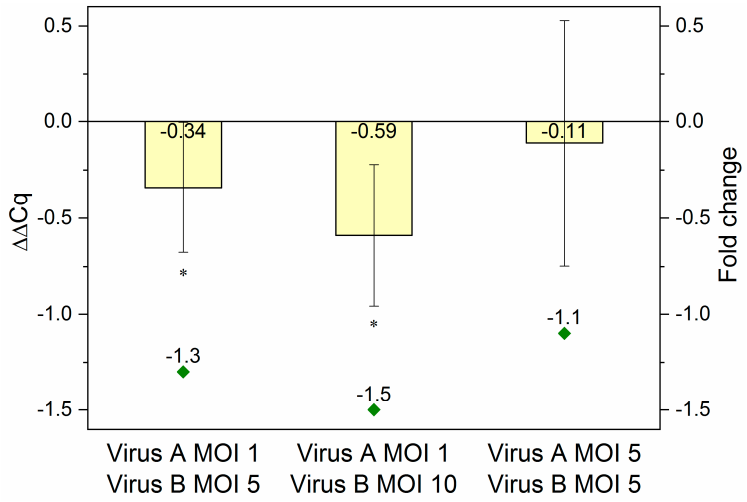

Figure 5. RT-qPCR results. RNA samples originating from *Sf*9 cells co-infected with *Ac*-T7amiR-1C_ ie1eYFP virus (Virus A) at MOI 1 or MOI 5 in combination with *Ac*-ie1T7RNAP virus (Virus B) at MOI 5 or MOI 10 were used for RT-qPCR analysis. In case a lower MOI of 1 was applied from the fusion virus *Ac*-T7amiR-1C_ ie1eYFP together with a 5-fold (MOI 5) or 10-fold (MOI 10) excess of the *Ac*-ie1T7RNAP virus, ΔΔCq values of –0.34 (fold change –1.3) and –0.59 (fold change –1.5) were observed, respectively. The co-infection with MOI 5 of both viruses yielded only a slight reduction in the eYFP mRNA level with a ΔΔCq value of –0.11 (fold change –1.1). All co-infections and RT-qPCR measurements were repeated three times. Statistically significant differences in comparison to the construct-specific scrambled control infections with *Ac*-T7amiR-1Cs_ ie1eYFP virus under the same conditions: * $p < 0.05$.

3. Materials and Methods

3.1. Insect Cells and Culture Conditions

*Sf*9 cells (ATCC CRL-1711) were propagated in HyClone SFM4 insect cell medium (GE Healthcare, Little Chalfont, UK) supplemented with 0.1% Pluronic F68 (Sigma-Aldrich, St. Louis, MO, USA). Fifty-milliliter suspension cultures were cultivated in 500 mL flasks at 27 °C with a shaker speed of 100 rpm.

3.2. amiRNA Plasmid Constructs

The 600 nt long promoter sequence upstream of the baculoviral immediate-early gene (*ie1*) was PCR amplified using the baculovirus shuttle vector originating from Max Efficiency DH10Bac cells (Invitrogen, Carlsbad, CA, USA) as template. The fragment was then cloned between the ClaI and BamHI restriction sites of the MultiBac acceptor vector pACEBac1 (EMBL, Grenoble, France), thereby replacing the original polyhedrin (polh) promoter and resulting in the pACEBac1ie1 vector. The baculovirus shuttle vector harbored by DH10MultiBacY cells (EMBL, Grenoble, France) was used as template to obtain a PCR fragment of the gene encoding the eYFP (KT878739), which was cloned into the pACEBac1ie1 vector and thus gave rise to the pACEBac1ie1eYFP reporter plasmid.

To facilitate the setup of the inducible system, a special donor vector was created. A 344 nt long fragment containing (in order) the T7 RNAP promoter sequence, 120 nt-s of the 5′ flanking region of the natural miR-1 precursor hairpin [20], a mini multi cloning site (MCS), 120 nt-s of the 3′ flanking region of the pre-miR-1 hairpin, and the TΦ terminator sequence was chemically synthetized by IDT (Leuven, Belgium). After PCR amplification, the product was cloned between the SpeI and PmeI sites of the MultiBac donor vector pIDS (EMBL, Grenoble, France), thus replacing the original cloning cassette and resulting in the pIDST7amiR plasmid. The sequence of the above-described T7amiR fragment embedded in pIDS is presented in Table 1.

Table 1. Sequences used for the cloning of the artificial miRNA constructs.

Fragment Name	Nucleotide Sequence 5′ to 3′
T7amiR fragment	TAATACGACTCACTATAGGGCTGCAGGTCTATAGATAGCGGTTTTTC GGCAATATACACTTGGCTCAATTTATTATCGCCGTGTGCGATGCGCAAG TTGGCCACCCGGCCGTTATTCAGCTTTACGTTTAATTGTTTGTTCTCGTC *ggatccgaattcctcgagtctaga*AAATTTAATGCATTCGTCCAATAAAGATAA AACAGTATGAGCAAAACGATAAGTAACACGATTCC CCACATGATTTGTTTTAATTTACAATTTCAATTCCAATGAGATTTAGGTT GTGCA*GGTAC*CCTAGCATAACCCCTTGGGGCCTCTAAACGGGTCTT GAGGGGTTTTTTG
amiR-1A hairpin construct	TCAGCTTTACGTTTAATTGTTTGTTCTCGTCTAAGGCTACGTCTATACTG CTCTATCCTAAACTGGATGATATAGACGTTGTGGCCTTGAAATTT AATGCATTCGTCCAATAAAGATAAA
amiR-1As hairpin construct	TCAGCTTTACGTTTAATTGTTTGTTCTCGTCTAAACACTCTCAGTAACT GCGACTCCCTAAACTGGGATCTTACTGAGACAGGTGTTTGAAATTTA ATGCATTCGTCCAATAAAGATAAA
amiR-1B hairpin construct	*ggatcc*TAAGGCCACAACGTCTATATCATCCTAAA CTGGATGATATAGACGTTGTGGCCTTA*tctaga*
amiR-1Bs hairpin construct	*ggatcc*TAAACACTCTCTCGGGTAAAATCCCTAAACTGG GATTTTACCCGAGAGAGTGTTTA*tctaga*
amiR-1C hairpin construct	*ggatcc*TAACAGCCACAACGTCTATATCATGCCTAAACTGGC ATGATATAGACGTTGTGGCTGTTA*tctaga*
amiR-1Cs hairpin construct	*ggatcc*TAAACACCTCTCTCAGGTAAAATCGCCTAAACTGGC GATTTTACCTGAGAGAGGTGTTTA*tctaga*
amiR-1D hairpin construct	*ggatcc*TGAGCGTAACAGCCACAACGTCTATATCATGCCTAAACTGGC ATGATATAGACGTTGTGGCTGTTACATTCA*tctaga*
amiR-1Ds hairpin construct	*ggatcc*TGAGCGTAAACACCTCTCTCAGGTAAAATCGCCTAAACTGGC GATTTTACCTGAGAGAGGTGTTTACATTCA*tctaga*

The restriction enzyme sites are in italic small caps. The guide strands of the synthetic siRNA duplexes embedded in the amiRNA hairpins are underlined.

As a basis for the amiRNA constructs, the *Ac*MNPV-pri-miR-1 transcript served as a backbone [20]. The original siRNA duplex within the transcript was replaced with a synthetic one containing a siRNA sequence previously proven to be highly effective against its original target eGFP [29]. Furthermore, small changes were applied to the stem sequences, to create overall four altered versions of the *Ac*MNPV-miR-1 hairpin structure: amiR-1A, amiR-1B, amiR-1C, and amiR-1D. In addition to the diversity in the stem-loop structures, there are differences in the length of the flanking regions that were obtained from the natural *Ac*MNPV-pri-miR-1 transcript. Moreover, for each of the amiRNA constructs, a corresponding control was also created by scrambling up the sequence of the given eGFP

targeting siRNA duplex incorporated in the amiRNA backbone: amiR-1As, amiR-1Bs, amiR-1Cs, and amiR-1Ds. Sequences of the modified amiRNA hairpin constructs and the scrambled controls are listed in Table 1.

The diverse design of the amiRNA constructs necessitated different cloning procedures for the structures. For amiR-1B, amiR-1C, and amiR-1D (amiR-1B-D) and amiR-1Bs, amiR-1Cs, and amiR-1Ds (amiR-1Bs-Ds), a method described previously was applied. Briefly, each of the stem-loop structures was ordered as two single-stranded, complementary, synthetic oligos from Sigma-Aldrich (St. Louis, MO, USA). The oligos were then pairwise annealed according to the manufacturer´s instructions and subsequently cloned between the BamHI and XbaI sites of the mini MCS in between the 120 nt long flanking regions of the pre-miR-1 hairpin in the donor vector pIDST7amiR, thus resulting in the plasmids pIDST7amiR-1B-D and pIDST7amiR-1Bs-Ds. Furthermore, for the transfection experiments carried out in *Sf*9 cells that served as a preliminary screening of the constructs (see Section 3.3), the backbone of the pACEBac1ie1 vector was used. To this end, the plasmids pIDST7amiR-1B-D and pIDST7amiR-1Bs-Ds served as template for the PCR amplification of the six different fragments, each containing the 120 nt 5´ flank, the stem-loop, and the 120 nt 3´ flank (without the T7 RNAP promoter and terminator sequences). The amplified products were subsequently cloned between the SalI and NotI sites of pACEBac1ie1, giving rise to the plasmids pACEBac1ie1amiR-1B-D and pACEBac1ie1amiR-1Bs-Ds.

The nucleotide sequences encoding the stem-loops amiR-1A and amiR-1As, including the 31 nt long flanking regions of the natural *Ac*MNPV-pri-miR-1 transcript on both sides of the stems, were chemically synthetized as single pieces by IDT (Leuven, Belgium). For the screening experiments, the fragments were cloned, after PCR amplification, between the BamHI and EcoRI sites of the pACEBac1ie1 vector to create the pACEBac1ie1amiR-1A and pACEBac1ie1amiR-1As plasmids, respectively. Furthermore, for the setup of the inducible system, the pIDST7amiR backbone was used and following another PCR amplification, the resulting stem-loop fragments were cloned between the T7 RNAP promoter and terminator sequences (PstI and KpnI sites) of the donor plasmid. This removed the 120 nt 5′ flank, the mini MCS, and the 120 nt 3′ flank necessary for the insertion of the annealed oligos and resulted in the vectors pIDST7amiR-1A and pIDST7amiR-1As. All of the plasmids described here were confirmed with sequencing.

3.3. Screening of amiRNA Constructs

The preliminary screening experiments for the estimation of the silencing effectiveness of the different stem-loop constructs comprised of the transfection of insect cells followed by visual estimation by fluorescence microscopy and subsequent flow cytometry analysis. *Sf*9 cells were seeded to 6-well plates with a density of 9×10^5 cells/well and were then pairwise co-transfected with 200 ng of the reporter plasmid pACEBac1ie1-eYFP in combination with 2 µg of one of the eight following plasmids: pACEBac1ie1amiR-1A-D or pACEBac1ie1amiR-1As-Ds. The co-transfections were done with FuGene HD transfection reagent (Promega, Madison, WI, USA) according to the manufacturer's instructions. Forty-eight hour post-transcription, the eYFP fluorescence intensity was first evaluated using a Leica DM IL LED Inverted Laboratory Microscope and the Leica Application Suite v4.6 software (Leica Microsystems, Wetzlar, Germany). After harvesting the cells, flow cytometry analysis was carried out using a Gallios Flow Cytometer (Beckman Coulter, Vienna, Austria). For the evaluation of the raw data, the Kaluza1.2 software (Beckman Coulter) was applied. All co-transfection experiments were repeated thrice.

3.4. Cloning of the Bacteriophage T7 RNA Polymerase

The *T7 gene1* encoding the bacteriophage T7 RNAP (AM946981) was PCR amplified using the lambda DE3 prophage as a template present in *Escherichia coli* BL21(DE3) cells (New England Biolabs, Ipswich, MA, USA). To target the mature RNA polymerase into the nucleus of *Sf*9 cells, where it is needed for the generation of pri-miRNA transcript mimics harboring the amiRNAs, the forward

primer used for the PCR amplification contained extra 36 nt encoding the SV40 T antigen nuclear location signal [23,37]. The obtained fragment was cloned within the BamHI and XbaI sites of the pACEBac1ie1 vector, resulting in the pACEBac1ie1T7RNAP construct.

To generate the *Ac*-ie1T7RNAP recombinant *Ac*MNPV, the pACEBac1ie1T7RNAP vector was transformed into Max Efficiency DH10Bac competent cells (Invitrogen). The purified bacmid DNA was then transfected into *Sf*9 cells with FuGene HD transfection reagent (Promega) according to the manufacturer's instructions. The amplified viral stock of passage three was used to determine the viral titer by plaque assay.

3.5. Setup of the Inducible Knockdown System

Acceptor–donor fusion constructs were generated via Cre-LoxP recombination by merging the reporter plasmid pACEBac1ie1eYFP with either pIDST7amiR-1C or pIDST7amiR-1Cs, resulting in the T7amiR-1C_ ie1eYFP and T7amiR-1Cs_ ie1eYFP vectors, respectively. By transforming the fusions into Max Efficiency DH10Bac competent cells (Invitrogen) with FuGene HD transfection reagent (Promega) according to the manufacturer's instructions, the *Ac*-T7amiR-1C_ ie1eYFP and *Ac*-T7amiR-1Cs_ ie1eYFP recombinant viruses were created. The titers of the amplified viral stocks of passage three were determined by plaque assay.

The silencing of eYFP using the inducible viral system was evaluated on the protein level with flow cytometry. To this end, *Sf*9 cells seeded into T25 flasks at a cell density of 2.5×10^6 cells/flask were co-infected with *Ac*-ie1T7RNAP together with the *Ac*-T7amiR-1C_ ie1eYFP or *Ac*-T7amiR-1Cs_ ie1eYFP virus at various MOI combinations. Forty-eight hours post-infection, the cells were harvested and the eYFP fluorescence intensity was measured with a Gallios Flow Cytometer (Beckman Coulter). For the data analysis, the Kaluza1.2 software (Beckman Coulter) was used. The co-infections were set up three times.

3.6. Real-Time Quantitative PCR

Total RNA was extracted from 1×10^6 cells with TRIzol Reagent (Invitrogen) according to the manufacturer's instructions. The genomic DNA contamination of the RNA samples was removed with the TURBO DNA-free Kit (Invitrogen). Reverse transcription and subsequent RT-qPCR was carried out in a single reaction with the Luna Universal One-Step RT-qPCR Kit (New England Biolabs) according to the manufacturer's instructions. For the quantification of eYFP mRNA levels, sequence-specific primers (F: 5′-GGCACAAGCTGGAGTACAAC-3′; R: 5′-AGTTCACCTTGATGCCGTTC-3′) that were designed with the GenScript Real-time PCR Primer Design online software were used. As an internal reference gene, the insect 28S rRNA [38] was applied (F: 5′-GCTTACAGAGACGAGGTTA-3′; R: 5′-TCACTTCTGGAATGGGTAG-3′). RT-qPCR was performed in 20 µL reactions consisting of 10 µL of Luna Universal One-Step Reaction Mix (2×), 1 µL of Luna WarmStart RT Enzyme Mix (20×), 0.8 µL of forward primer (10 µM), 0.8 µL of reverse primer (10 µM), 5 ng of DNA-free total RNA template, and nuclease-free water (fill up to 20 µL). The experiments were conducted on a BioRad C1000 Thermal Cycler in combination with a CFX96 Real-Time PCR Detection System (Hercules, CA, USA) using the following program: reverse transcription at 55 °C for 10 min, initial denaturation at 95 °C for 1 min, 40 cycles of denaturation at 95 °C for 10 s, and extension at 60 °C for 30 s (with plate read). Specific amplification was confirmed through melting curve analysis. Each co-infection experiment was repeated three times, and the data were analyzed using the $2^{-\Delta\Delta Cq}$ method [36]. For the evaluation of the statistical significance, the Student´s *t*-test was applied ($p < 0.05$).

4. Conclusions

In the framework of this study, a novel inducible knockdown system was established and evaluated in *Sf*9 cells. *Ac*MNPV-miR-1 pri-miRNA transcript mimics [20] harboring an artificial miRNA (targeting eYFP) were designed and assessed with regard to their silencing efficiency. According to plasmid-based screening experiments, the most potent construct was selected for the subsequent

evaluation on a viral basis. The inducibility of the viral system lies in the fact that the T7 promoter is inactive in the absence of the prokaryotic T7 RNAP. Thus, separate viruses were created either carrying the polymerase under control of a baculoviral promoter (ie1) or encoding the pri-miRNA transcript mimic accommodating an amiRNA regulated by the T7 promoter. The presence of mature amiRNAs was verified in *Sf*9 cultures co-infected with these viruses. Flow cytometry measurements revealed a reduction of approximately 30–40% in the target eYFP's overall fluorescence intensity in case the RNAP virus was applied in 5–10-fold excess as compared to the virus carrying the amiRNA. RT-qPCR measurements revealed a decrease in the mRNA level of eYFP, confirming the silencing effect and the functionality of the inducible system. The main advantage of the system is that even genes that are essential for baculovirus propagation can be downregulated. As soon as the two viruses are combined, any desired silencing effect can be triggered. Furthermore, since this system is based on the heterologous T7 expression system, the transcription of functional amiRNA sequences becomes independent of cell-specific PolIII promoters and thus becomes a versatile tool for all animal cells.

Author Contributions: Conceptualization, K.K., W.E., and R.G.; Methodology, K.K., W.E., D.P., M.K., L.N., and R.G.; Supervision, W.E. and R.G.; Visualization, K.K., W.E., D.P., and R.G.; Writing—original draft, K.K.; Writing—review & editing, W.E., D.P., M.K., L.N., and R.G.

Funding: This work has been supported by the Federal Ministry of Science, Research and Economy (BMWFW), the Federal Ministry of Traffic, Innovation and Technology (bmvit), the Styrian Business Promotion Agency SFG, the Standortagentur Tirol, the Government of Lower Austria, and Business Agency Vienna through the COMET-Funding Program managed by the Austrian Research Promotion Agency FFG. This work was also funded by the PhD programme "BioTop—Biomolecular Technology of Proteins" (Austrian Science Funds, Project number FWF W1224).

Conflicts of Interest: The authors declare no conflict of interest. The funders had no role in the design of the study; in the collection, analyses, or interpretation of data; in the writing of the manuscript; or in the decision to publish the results.

Abbreviations

*Ac*MNPV-pre-miR-1	precursor hairpin of *Ac*MNPV-miR-1
*Ac*MNPV-pri-miR-1	pri-miRNA transcript of *Autographa californica* nucleopolyhedrovirus miR-1
amiRNA	artificial microRNA
BEVS	baculovirus-insect cell expression system
dsRNA	double-stranded RNA
eGFP	enhanced green fluorescent protein
eYFP	enhanced yellow fluorescent protein
FC	fold change
MCS	multi cloning site
miRNAs	microRNAs
MOI	multiplicity of infection
mRNAs	messenger RNAs
NC	negative control
NTC	no-template control
PC	positive control
polh	polyhedrin
pri-miRNA	primary miRNA
RISC	RNAi-induced silencing complex
RNAi	RNA interference
RT-qPCR	real-time quantitative PCR
shRNAs	short hairpin RNAs
siRNAs	small-interfering RNAs
T7 RNAP	T7 RNA polymerase

Appendix A

Expression and Activity Assay of the Bacteriophage T7 RNA Polymerase

The T7 RNAP is a 100 kDa prokaryotic enzyme known for its tight promoter specificity and high catalytic activity [39]. The fact that the T7 promoter does not occur in insect cells and is inactive in the absence of the T7 polymerase served as a basis for a two-vector-based inducible system. In order to test the functionality of the bacteriophage T7 RNAP in the insect cell system, we created the baculovirus *Ac*-ie1T7RNAP expressing the bacteriophage T7 RNAP with an additional nuclear location signal of the SV40 T antigen [23,24]. *Sf*9 cells were infected with the *Ac*-ie1T7RNAP baculovirus, and samples (cell pellets) were then collected two days post-infection. First, the cell pellets were used to confirm the expression of the T7 polymerase by Western blot analysis. Second, to assess the activity of the enzyme, an in vitro transcription assay [23] was carried out using a short DNA sequence downstream of the T7 promoter as a template.

For the detection of T7 RNAP by Western blot analysis and the subsequent activity assay, *Sf*9 cells cultivated in a 20 mL suspension culture were infected with the *Ac*-ie1T7RNAP recombinant baculovirus at an initial cell density of 1×10^6 cells/mL with MOI 5. Samples of 1×10^6 cells taken at two days post-infection were used for subsequent SDS-PAGE and Western blot analysis, according to standard protocols [40,41]. Briefly, for the protein separation by SDS-PAGE, a NovexTM 4–12% Tris-Glycine Mini Protein Gel (Invitrogen) was applied, followed by electroblotting onto a PVDF transfer membrane (GE Healthcare Life Sciences, Vienna, Austria). Immunodetection was carried out using a primary anti-T7 RNA polymerase mouse monoclonal antibody (US170566-3, Merck, Kenilworth, NJ, USA) in combination with a secondary anti-mouse IgG alkaline phosphatase labeled goat antibody (A5153-1ML, Merck, Kenilworth, NJ, USA). Subsequently, the results were evaluated by visual estimation after the development of the PVDF transfer membrane using BCIP/NBT (Promega). The immunoblot presented in Figure A1 proved the presence of the 100 kDa T7 RNAP upon infection of insect cells with the *Ac*-ie1T7RNAP virus.

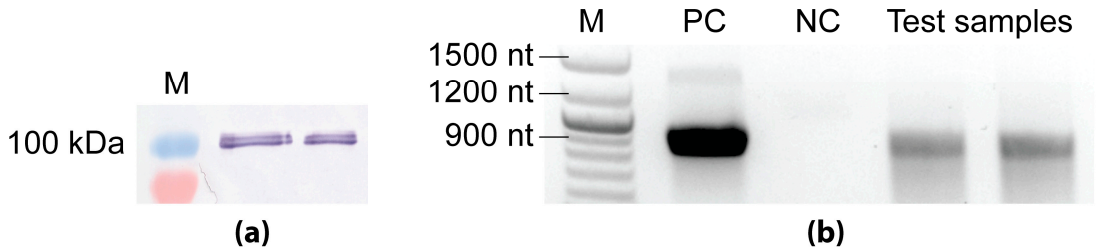

Figure A1. Analysis of recombinant T7 RNAP with immunoblotting (**a**) and in vitro transcription assay (**b**). (**a**) Antibodies binding specifically the T7 RNAP confirmed the expression of the 100 kDa protein upon the infection of *Sf*9 cells with the *Ac*-ie1T7RNAP virus in in the pellet of two different viral clones that were tested. (**b**) Agarose gel image of the transcript products from the in vitro transcription assay. The positive control (PC) reaction contained purified, concentrated T7 RNAP. The negative control (NC) reaction was set up with the cell lysate of *Sf*9 cells. The test reaction containing homogenized cell pellet of *Ac*-ie1T7RNAP infected *Sf*9 cells was set up in duplicate. (M) marker.

To confirm the functionality of the recombinant T7 RNAP, in vitro RNA transcription reactions were set up [23] using the components of the HiScribe T7 Quick High Yield RNA Synthesis Kit (New England Biolabs). In all three different reaction mixtures that were applied, a PCR fragment of 900 nt downstream of the T7 promoter was used as a template. The 20 µL positive control (PC) reaction contained 2 µL of nuclease-free water, 10 µL of NTP buffer mix, 1 µL of the template fragment (500 ng DNA), 5 µL (200 U) of a Murine RNase inhibitor (New England Biolabs), and 2 µL of a T7 RNA polymerase mix. The negative control (NC) and test reaction mixtures were composed of 10 µL of NTP buffer mix, 1 µL of the template fragment (500 ng DNA), and 5 µL (200 U) Murine RNase

inhibitor (New England Biolabs). Additionally, the T7 RNA polymerase mix was exchanged to 4 µL of resuspended cell pellets. The cell lysates were prepared as follows: samples of 2×10^6 cells originating from an uninfected and the *Ac*-ie1T7RNAP infected *Sf*9 cultures (see above) were centrifuged at 500× *g* for 10 min (Eppendorf microcentrifuge 5415R, Hamburg, Germany) to separate the cells from the supernatants. The pellets were then resuspended and homogenized in 20 µL of PBS. For the negative control and test transcription reactions, 4 µL of the non-infected or *Ac*-ie1T7RNAP-infected resuspended and homogenized cell pellets were used, respectively. After the transcription (2 h at 37 °C) and DNA-removal step (15 min at 37 °C), the final RNA products were visualized on a 1% agarose gel (Figure A1) containing 1% *v*/*v* sodium hypochlorite for the inactivation of RNAses [42]. Notwithstanding that the concentrated enzyme solution (PC) clearly produced higher amounts of template transcripts, the test reactions also contained the same size of transcripts, indicating that the T7 RNAP produced in *Sf*9 cells was active. In contrast, no transcripts were detected in the negative control reaction. The faint band of ~1400 nt in the PC reaction is most likely due to unspecific amplification by the concentrated enzyme mix.

Detection of Mature amiRNAs

The functionality of the T7 RNAP on the RNA level was verified with regard to the transcription of pri-miRNA mimics, of which the processing would subsequently lead to mature amiRNA production and the degradation of eYFP mRNAs. Thus, co-infected *Sf*9 samples of the inducible viral system, originating from the cultures used for the flow cytometry experiments (see Section 3.5) were analyzed for the presence of mature amiRNAs. As negative control (NC) for amiR-1C and amiR-1Cs, *Sf*9 cells were seeded into T25 flasks at a cell density of 2.5×10^6 cells/flask and were infected only with either the *Ac*-T7amiR-1C_ ie1eYFP or the *Ac*-T7amiR-1Cs_ ie1eYFP virus at MOI 5, respectively. In the absence of T7 RNAP, the T7 promoter is inactive and these cultures should not contain processed amiRNAs.

Total RNA was extracted from 1×10^6 infected cells at 48 h p.i. using TRIzol Reagent (Invitrogen) according to the manufacturer´s instructions. Genomic DNA was removed with the TURBO DNA-free Kit (Invitrogen). Five hundred nanograms of total RNA were reverse-transcribed using specific stem-loop primers [43] with the ProtoScript II First Strand cDNA Synthesis Kit (New England Biolabs, Ipswich, MA, USA). The 25 µL end-point PCR reaction mixtures contained 1 µL of cDNA as template, 5 µL of OneTaq Standard Reaction Buffer (5×), 0.5 µL of 10 mM dNTPs, 0.5 µL of 10 µM forward primer, 0.5 µL of 10 µM reverse primer, 0.125 µL of OneTaq DNA Polymerase, and 17.375 µL of nuclease-free water. The PCR was run on a Piko 24 PCR machine (Thermo Fisher Scientific, Waltham, MA, USA) according to the standard protocol recommended by the manufacturer for the OneTaq DNA Polymerase (New England Biolabs). No-template control (NTC) reactions were also included in the reverse transcription and end-point PCR steps. The PCR products visualized on a 3% agarose gel presented in Figure A2 provide a clear proof of the inducible system´s functionality. Bands representing the mature amiR-1C and amiR-1Cs RNA sequences were only observed in samples of *Sf*9 cells co-infected with both the *Ac*-ie1T7RNAP and *Ac*-T7amiR-1C_ ie1eYFP or *Ac*-T7amiR-1Cs_ ie1eYFP viruses, respectively. In contrast, no bands were visible in the NTC or NC lanes, as expected. These results demonstrate the suitability of the T7 inducible system for the production of mature miRNAs on a viral basis.

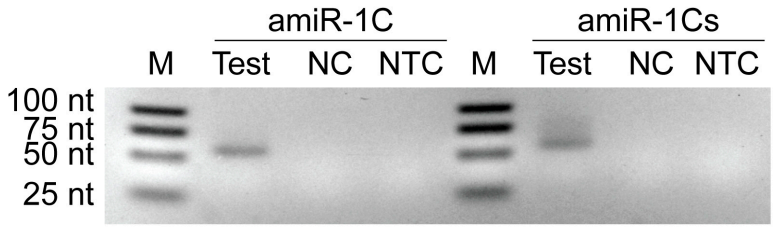

Figure A2. Agarose gel image of PCR amplified amiRNA products originating from the in vitro transcription assay. *Sf*9 cells were infected with *Ac*-ie1T7RNAP virus in combination with *Ac*-T7amiR-1C_ ie1eYFP (amiR-1C) or *Ac*-T7amiR-1Cs_ ie1eYFP (amiR-1Cs) virus. Cell pellets were harvested 48 h p.i. and total RNA was extracted for a subsequent reverse transcription reaction using specific stem-loop primers for mature amir-1C and its scrambled control, amiR-1Cs. The cDNA was used for end-point PCR to detect the production of mature amiRNAs (amiR-1C Test and amiR-1Cs Test). The negative control reactions contained cDNA originating from *Sf*9 cultures infected with *Ac*-T7amiR-1C_ ie1eYFP (amiR-1C NC) or *Ac*-T7amiR-1Cs_ ie1eYFP (amiR-1Cs NC) only. The no-template control (NTC) reverse transcription reactions contained no cDNA. Mature amiRNAs are produced exclusively upon the simultaneous presence of the *Ac*-ie1T7RNAP virus together with either the *Ac*-T7amiR-1C_ ie1eYFP or *Ac*-T7amiR-1Cs_ ie1eYFP virus proving the functionality of the recombinant polymerase and the inducibility of the system. Note that the 21 nt mature amiRNAs appeared as 62 nt products after the reverse transcription with the stem-loop primers.

References

1. Mena, J.A.; Kamen, A.A. Insect cell technology is a versatile and robust vaccine manufacturing platform. *Expert Rev. Vaccines* **2011**, *10*, 1063–1081. [CrossRef] [PubMed]
2. Nika, L.; Wallner, J.; Palmberger, D.; Koczka, K.; Vorauer-Uhl, K.; Grabherr, R. Expression of full-length her2 protein in sf9 insect cells and its presentation on the surface of budded virus-like particles. *Protein Expr. Purif.* **2017**, *136*, 27–38. [CrossRef] [PubMed]
3. Cecchini, S.; Negrete, A.; Kotin, R.M. Toward exascale production of recombinant adeno-associated virus for gene transfer applications. *Gene Therapy* **2008**, *15*, 823. [CrossRef] [PubMed]
4. Chen, C.Y.; Lin, C.Y.; Chen, G.Y.; Hu, Y.C. Baculovirus as a gene delivery vector: Recent understandings of molecular alterations in transduced cells and latest applications. *Biotechnol. Adv.* **2011**, *29*, 618–631. [CrossRef] [PubMed]
5. Thompson, C.M.; Petiot, E.; Mullick, A.; Aucoin, M.G.; Henry, O.; Kamen, A.A. Critical assessment of influenza vlp production in sf9 and hek293 expression systems. *BMC Biotechnol.* **2015**, *15*, 31. [CrossRef] [PubMed]
6. Van Oers, M.M.; Pijlman, G.P.; Vlak, J.M. Thirty years of baculovirus-insect cell protein expression: From dark horse to mainstream technology. *J. Gen. Virol.* **2015**, *96*, 6–23. [CrossRef] [PubMed]
7. Hannon, G.J. Rna interference. *Nature* **2002**, *418*, 244. [CrossRef] [PubMed]
8. Dana, H.; Chalbatani, G.M.; Mahmoodzadeh, H.; Karimloo, R.; Rezaiean, O.; Moradzadeh, A.; Mehmandoost, N.; Moazzen, F.; Mazraeh, A.; Marmari, V.; et al. Molecular mechanisms and biological functions of sirna. *Int. J. Biomed. Sci.* **2017**, *13*, 48–57.
9. Bhaskaran, M.; Mohan, M. Micrornas: History, biogenesis, and their evolving role in animal development and disease. *Vet. Pathol.* **2014**, *51*, 759–774. [CrossRef] [PubMed]
10. Huang, Y.; Deng, F.; Hu, Z.; Vlak, J.M.; Wang, H. Baculovirus-mediated gene silencing in insect cells using intracellularly produced long double-stranded rna. *J. Biotechnol.* **2007**, *128*, 226–236. [CrossRef]
11. Haley, B.; Hendrix, D.; Trang, V.; Levine, M. A simplified mirna-based gene silencing method for drosophila melanogaster. *Dev. Biol.* **2008**, *321*, 482–490. [CrossRef] [PubMed]
12. Kim, N.Y.; Baek, J.Y.; Choi, H.S.; Chung, I.S.; Shin, S.; Lee, J.I.; Choi, J.Y.; Yang, J.M. Short-hairpin rna-mediated gene expression interference in trichoplusia ni cells. *J. Microbiol. Biotechnol.* **2012**, *22*, 190–198. [CrossRef] [PubMed]

13. Zhang, X.; Xu, K.; Ou, Y.; Xu, X.; Chen, H. Development of a baculovirus vector carrying a small hairpin rna for suppression of sf-caspase-1 expression and improvement of recombinant protein production. *BMC Biotechnol.* **2018**, *18*, 24. [CrossRef] [PubMed]
14. Bofill-De Ros, X.; Gu, S. Guidelines for the optimal design of mirna-based shrnas. *Methods* **2016**, *103*, 157–166. [CrossRef] [PubMed]
15. Davidson, B.L.; McCray, P.B., Jr. Current prospects for rna interference-based therapies. *Nat. Rev. Gen.* **2011**, *12*, 329. [CrossRef] [PubMed]
16. Denli, A.M.; Tops, B.B.J.; Plasterk, R.H.A.; Ketting, R.F.; Hannon, G.J. Processing of primary micrornas by the microprocessor complex. *Nature* **2004**, *432*, 231. [CrossRef] [PubMed]
17. Winter, J.; Jung, S.; Keller, S.; Gregory, R.I.; Diederichs, S. Many roads to maturity: Microrna biogenesis pathways and their regulation. *Nat. Cell Biol.* **2009**, *11*, 228. [CrossRef] [PubMed]
18. Liu, J.; Carmell, M.A.; Rivas, F.V.; Marsden, C.G.; Thomson, J.M.; Song, J.-J.; Hammond, S.M.; Joshua-Tor, L.; Hannon, G.J. Argonaute2 is the catalytic engine of mammalian rnai. *Science* **2004**, *305*, 1437–1441. [CrossRef]
19. Zhang, J.; He, Q.; Zhang, C.D.; Chen, X.Y.; Chen, X.M.; Dong, Z.Q.; Li, N.; Kuang, X.X.; Cao, M.Y.; Lu, C.; et al. Inhibition of bmnpv replication in silkworm cells using inducible and regulated artificial microrna precursors targeting the essential viral gene lef-11. *Antiviral Res.* **2014**, *104*, 143–152. [CrossRef]
20. Zhu, M.; Wang, J.; Deng, R.; Xiong, P.; Liang, H.; Wang, X. A microrna encoded by autographa californica nucleopolyhedrovirus regulates expression of viral gene odv-e25. *J. Virol.* **2013**, *87*, 13029–13034. [CrossRef]
21. Chamberlin, M.; McGrath, J.; Waskell, L. New rna polymerase from escherichia coli infected with bacteriophage t7. *Nature* **1970**, *228*, 227. [CrossRef] [PubMed]
22. Lieber, A.; Kiessling, U.; Strauss, M. High level gene expression in mammalian cells by a nuclear t7-phase rna polymerase. *Nucleic Acids Res.* **1989**, *17*, 8485–8493. [CrossRef] [PubMed]
23. Van Poelwijk, F.; Broer, R.; Belsham, G.J.; Oudshoorn, P.; Vlak, J.M.; Goldbach, R.W. A hybrid baculovirus-bacteriophage t7 transient expression system. *Biotechnology* **1995**, *13*, 261–264. [CrossRef] [PubMed]
24. Polkinghorne, I.; Roy, P. Transient expression in insect cells using a recombinant baculovirus synthesising bacteriophage t7 rna polymerase. *Nucleic Acids Res.* **1995**, *23*, 188–191. [CrossRef] [PubMed]
25. Nguyen, H.T.; Leelavathi, S.; Reddy, V.S. Bacteriophage t7 rna polymerase-directed, inducible and tissue-specific over-expression of foreign genes in transgenic plants. *Plant Biotechnol. J.* **2004**, *2*, 301–310. [CrossRef] [PubMed]
26. Rao, D.D.; Vorhies, J.S.; Senzer, N.; Nemunaitis, J. Sirna vs. Shrna: Similarities and differences. *Advanced Drug. Deliv. Rev.* **2009**, *61*, 746–759. [CrossRef] [PubMed]
27. Koczka, K.; Peters, P.; Ernst, W.; Himmelbauer, H.; Nika, L.; Grabherr, R. Comparative transcriptome analysis of a trichoplusia ni cell line reveals distinct host responses to intracellular and secreted protein products expressed by recombinant baculoviruses. *J. Biotechnol.* **2018**, *270*, 61–69. [CrossRef] [PubMed]
28. Zhu, M.; Wang, J.; Deng, R.; Wang, X. Functional regulation of an autographa californica nucleopolyhedrovirus-encoded microrna, acmnpv-mir-1, in baculovirus replication. *J. Virol.* **2016**, *90*, 6526–6537. [CrossRef]
29. Ui-Tei, K.; Naito, Y.; Takahashi, F.; Haraguchi, T.; Ohki-Hamazaki, H.; Juni, A.; Ueda, R.; Saigo, K. Guidelines for the selection of highly effective sirna sequences for mammalian and chick rna interference. *Nucleic Acids Res.* **2004**, *32*, 936–948. [CrossRef]
30. De, N.; Young, L.; Lau, P.-W.; Meisner, N.-C.; Morrissey, D.V.; MacRae, I.J. Highly complementary target rnas promote release of guide rnas from human argonaute2. *Mol. Cell* **2013**, *50*, 344–355. [CrossRef]
31. Chang, K.; Elledge, S.J.; Hannon, G.J. Lessons from nature: Microrna-based shrna libraries. *Nat. Methods* **2006**, *3*, 707–714. [CrossRef] [PubMed]
32. Ma, H.; Wu, Y.; Choi, J.-G.; Wu, H. Lower and upper stem–single-stranded rna junctions together determine the drosha cleavage site. *Proce. Natl. Acad. Sci. USA* **2013**, *110*, 20687–20692. [CrossRef] [PubMed]
33. Han, J.; Lee, Y.; Yeom, K.-H.; Nam, J.-W.; Heo, I.; Rhee, J.-K.; Sohn, S.Y.; Cho, Y.; Zhang, B.-T.; Kim, V.N. Molecular basis for the recognition of primary micrornas by the drosha-dgcr8 complex. *Cell* **2006**, *125*, 887–901. [CrossRef] [PubMed]
34. Nguyen, T.A.; Jo, M.H.; Choi, Y.-G.; Park, J.; Kwon, S.C.; Hohng, S.; Kim, V.N.; Woo, J.-S. Functional anatomy of the human microprocessor. *Cell* **2015**, *161*, 1374–1387. [CrossRef] [PubMed]

35. Ando, H.; Hirose, M.; Kurosawa, G.; Impey, S.; Mikoshiba, K. Time-lapse imaging of microrna activity reveals the kinetics of microrna activation in single living cells. *Sci. Rep.* **2017**, *7*, 12642. [CrossRef] [PubMed]
36. Schmittgen, T.D.; Livak, K.J. Analyzing real-time pcr data by the comparative ct method. *Nat. Protocols* **2008**, *3*, 1101. [CrossRef] [PubMed]
37. Dunn, J.J.; Krippl, B.; Bernstein, K.E.; Westphal, H.; Studier, F.W. Targeting bacteriophage t7 rna polymerase to the mammalian cell nucleus. *Gene* **1988**, *68*, 259–266. [CrossRef]
38. Chen, Z.-S.; Han, N.-N.; Li, J.-H.; Wan, H.; Huang, G.-H. Selection and validation of reference genes for rt-qpcr analysis in sf9 cell line infected by heliothis virescens ascovirus 3h (hvav-3h). *J. Asia-Pac. Entomol.* **2017**, *20*, 463–468. [CrossRef]
39. Studier, F.W.; Moffatt, B.A. Use of bacteriophage t7 rna polymerase to direct selective high-level expression of cloned genes. *J. Mol. Biol.* **1986**, *189*, 113–130. [CrossRef]
40. Gallagher, S.R. One-dimensional sds gel electrophoresis of proteins. *Curr. Protocols Mol. Biol.* **2006**, *75*, 10.2.1–10.2A.37.
41. Duojiao, N.; Peng, X.; Sean, G. Immunoblotting and immunodetection. *Curr. Protocols Immunol.* **2016**, *114*, 8.10.1–8.10.36.
42. Aranda, P.S.; LaJoie, D.M.; Jorcyk, C.L. Bleach gel: A simple agarose gel for analyzing rna quality. *Electrophoresis* **2012**, *33*, 366–369.
43. Chen, C.; Ridzon, D.A.; Broomer, A.J.; Zhou, Z.; Lee, D.H.; Nguyen, J.T.; Barbisin, M.; Xu, N.L.; Mahuvakar, V.R.; Andersen, M.R.; et al. Real-time quantification of microrna by stem-loop rt-pcr. *Nucleic Acids Res.* **2005**, *33*, e179. [CrossRef] [PubMed]

4 CONCLUSIONS

The baculovirus-insect cell expression system is an integral component of recombinant protein production technologies. The widespread application of this binary system can be attributed to its advantageous properties, such as high product titers and the extensive eukaryotic post-translational modifications offered by the insect host. However, the large scale manufacturing of various, often complex, glycosylated recombinant products with insect cells is unconventional, as it is linked to a baculovirus infection leading to a complete viral control over the host cell machinery. Although, this phenomenon strongly affects the quality and quantity of the recombinant product, so far no systematic studies have been conducted in baculovirus-infected producer insect cells to elucidate the influencing parameters on the transcriptome level.

Our hypothesis suggested that the overexpression of a heterologous protein – especially a secreted one – has an effect on the production host and its stress response during an infection coupled production process. Certain studies report limited success in improving protein solubility and secreted product tires upon the co-expression of chaperones during a production process (Teng et al., 2013; Yokoyama et al., 2000). Based on literature data, we also selected several chaperones and tested the effect of their overexpression in combination with the secreted version of Influenza A virus hemagglutinin (unpublished data). However, the results showed that none of these proteins had any apparent positive influence on the recombinant product yield, suggesting that the so far uncharacterized interdependence and synergistic effects of processing enzymes and UPR proteins in infected insect cells need to be taken into account when designing such experiments.

Therefore, to support the better exploitation of insect cells as an expression system, one part of the thesis focused on the characterization of transcriptional regulatory and secretory bottlenecks during recombinant protein production. A comparative transcriptome analysis was conducted with the alphanodavirus-free *Tnms*42 cell line comparing the transcriptional host responses to recombinant *Ac*MNPVs inducing the formation of an intracellular or an extracellular model protein. Monitoring of the recombinant protein production throughout the experiment revealed that a large proportion of the secreted model product remained in the cells, most probably at different stages of its processing, in the form of unfolded or

misfolded and not properly glycosylated intermediates. Additionally, various chaperones and heat shock proteins were identified among the most highly upregulated unigenes in the producer cultures. A special set of 319 genes, specifically regulated in response to the formation of a secreted recombinant model protein (as compared to the intracellular product) was identified and subjected to Gene ontology (GO) enrichment analysis. Among the most highly enriched terms, UPR and protein folding-related categories were found. According to the KEGG pathway analysis, the second most prominent process these unigenes engage in is protein folding in the ER, with typical upregulated UPR genes such as BiP and PERK. Based on this transcriptomic data, the viral infection coupled recombinant protein production inflicts stress in the producer cells; thus as a specific response, genes involved in protein processing, glycosylation and UPR are upregulated. These key genes might serve as targets for future cell line engineering attempts; however, these experiments also proved that the complexity of the system does not allow us the overexpression of just a single factor in order to overcome the limitations of the secretory pathway.

The second major objective of the thesis was to develop an inducible system in the baculovirus-insect cell expression system for the effective downregulation of host or viral genes. The main motive behind this was the need to downregulate the contaminating baculovirus particle formation during an infection-coupled production process and thus, to facilitate the downstream processing of recombinant products. Several publications demonstrate that a feasible strategy for this would be to delete or downregulate genes that are essential for baculovirus budding. However, setups that involve the complete deletion of a gene necessitate the generation of stable cell lines to trans-complement the missing protein for inoculum production (Chaves et al., 2018; Marek et al., 2011). It is known that stable cell line generation is cumbersome, not to mention the reduced effectivity when it comes to inoculum generation. Thus, instead of a complete deletion, another strategy utilizing the natural RNAi process in combination with the prokaryotic T7 transcription machinery was developed to be able to downregulate any viral or host genes in a timely defined manner during an infection process. As a proof of concept, the system was first tested for the effectiveness using a model protein sequence. Further experiments are currently being conducted using mimics that target the *vp80* and *gp64* essential baculoviral genes.

Four custom-made versions of the *A. californica* pri-miR1 transcript were designed to harbor a synthetic siRNA sequence against the target sequence of eYFP (enhanced yellow fluorescent protein). The mimics were evaluated with regard to their silencing efficiency and the most promising structure was selected for the setup of the dual viral vector-based, inducible system. Recombinant baculoviruses were created carrying separately the artificial precursor mimic under the transcriptional control of the T7 promoter or solely the T7 RNA polymerase under a baculoviral promoter. Co-infections with various ratios of the two viruses provided proof for the functionality of the system, as they resulted in the effective downregulation of the model protein (shown on both the protein and the mRNA level). The main advantage of the developed system is that inoculums can be raised separately in conventional infection processes, since the mimic transcripts and the mature siRNAs are only created upon the co-infection of insect cells with both of the viruses. Additionally, with the heterologous T7 expression machinery, the use of cell specific PolIII promoters can be circumvented, resulting in an adaptable tool for various animal cells. A patent application encompassing this part of the work was recently submitted to the European Patent Office (application number: EP18194719.3).

5 REFERENCES

Abe, T., Matsuura, Y., (2010) Host innate immune responses induced by baculovirus in mammals. Curr Gene Ther 10, 226-231.

Altmann, F., (2007) The role of protein glycosylation in allergy. Int Arch Allergy Immunol 142, 99-115.

Au, S., Wu, W., Panté, N., (2013) Baculovirus Nuclear Import: Open, Nuclear Pore Complex (NPC) Sesame. Viruses 5, 1885-1900.

Aucoin, M.G., Jacob, D., Chahal, P.S., Meghrous, J., Bernier, A., Kamen, A.A., (2007) Virus-like particle and viral vector production using the baculovirus expression vector system/insect cell system: adeno-associated virus-based products. Methods Mol Biol 388, 281-296.

Aucoin, M.G., Mena, J.A., Kamen, A.A., (2010) Bioprocessing of baculovirus vectors: a review. Curr Gene Ther 10, 174-186.

Ayres, M.D., Howard, S.C., Kuzio, J., Lopez-Ferber, M., Possee, R.D., (1994) The complete DNA sequence of Autographa californica nuclear polyhedrosis virus. Virology 202, 586-605.

Bedard, C., Kamen, A., Tom, R., Massie, B., (1994) Maximization of recombinant protein yield in the insect cell/baculovirus system by one-time addition of nutrients to high-density batch cultures. Cytotechnology 15, 129-138.

Bofill-De Ros, X., Gu, S., (2016) Guidelines for the optimal design of miRNA-based shRNAs. Methods 103, 157-166.

Breitbach, K., Jarvis, D.L., (2001) Improved glycosylation of a foreign protein by Tn-5B1-4 cells engineered to express mammalian glycosyltransferases. Biotechnol Bioeng 74, 230-239.

Caron, A.W., Tom, R.L., Kamen, A.A., Massie, B., (1994) Baculovirus expression system scaleup by perfusion of high-density Sf-9 cell cultures. Biotechnol Bioeng 43, 881-891.

Chaves, L.C.S., Ribeiro, B.M., Blissard, G.W., (2018) Production of GP64-free virus-like particles from baculovirus-infected insect cells. J Gen Virol 99, 265-274.

Chen, Y.R., Zhong, S., Fei, Z., Gao, S., Zhang, S., Li, Z., Wang, P., Blissard, G.W., (2014) Transcriptome Responses of the Host Trichoplusia ni to Infection by the Baculovirus Autographa californica Multiple Nucleopolyhedrovirus. J Virol 88, 13781-13797.

Cheshenko, N., Krougliak, N., Eisensmith, R.C., Krougliak, V.A., (2001) A novel system for the production of fully deleted adenovirus vectors that does not require helper adenovirus. Gene Therapy 8, 846.

Clem, R.J., Passarelli, A.L., (2013) Baculoviruses: Sophisticated Pathogens of Insects. PLoS Pathog 9.

Contreras-Gomez, A., Sanchez-Miron, A., Garcia-Camacho, F., Molina-Grima, E., Chisti, Y., (2014) Protein production using the baculovirus-insect cell expression system. Biotechnol Prog 30, 1-18.

Cruz, P.E., Peixoto, C.C., Moreira, J.L., Carrondo, M.J.T., (1998) Production and quality analysis of Pr55gag particles produced in baculovirus-infected insect cells. Journal of Chemical Technology & Biotechnology 72, 149-158.

Doolan, P., Melville, M., Gammell, P., Sinacore, M., Meleady, P., McCarthy, K., Francullo, L., Leonard, M., Charlebois, T., Clynes, M., (2008) Transcriptional Profiling of Gene Expression Changes in a PACE-Transfected CHO DUKX Cell Line Secreting High Levels of rhBMP-2. Mol Biotechnol 39, 187-199.

Drugmand, J.C., Schneider, Y.J., Agathos, S.N., (2012) Insect cells as factories for biomanufacturing. Biotechnol Adv 30, 1140-1157.

Elias, C.B., Zeiser, A., Bedard, C., Kamen, A.A., (2000) Enhanced growth of Sf-9 cells to a maximum density of 5.2 x 10(7) cells per mL and production of beta-galactosidase at high cell density by fed batch culture. Biotechnol Bioeng 68, 381-388.

Fernandes, F., Teixeira, A.P., Carinhas, N., Carrondo, M.J., Alves, P.M., (2013) Insect cells as a production platform of complex virus-like particles. Expert Rev Vaccines 12, 225-236.

Fire, A., Xu, S., Montgomery, M.K., Kostas, S.A., Driver, S.E., Mello, C.C., (1998) Potent and specific genetic interference by double-stranded RNA in Caenorhabditis elegans. Nature 391, 806-811.

Gordon, K.H.J., Waterhouse, P.M., (2007) RNAi for insect-proof plants. Nat Biotechnol 25, 1231.

Grace, T.D., (1962) Establishment of four strains of cells from insect tissues grown in vitro. Nature 195, 788-789.

Grace, T.D., (1967) Establishment of a line of cells from the silkworm Bombyx mori. Nature 216, 613.

Granados, R., Blissard, G., Debbie, P., (2016) Cell lines that are free of viral infection and methods for their production. Google Patents.

Gronowski, A.M., Hilbert, D.M., Sheehan, K.C.F., Garotta, G., Schreiber, R.D., (1999) Baculovirus Stimulates Antiviral Effects in Mammalian Cells. J Virol 73, 9944-9951.

Gupta, P., Lee, K.H., (2007) Genomics and proteomics in process development: opportunities and challenges. Trends in Biotechnology 25, 324-330.

Haley, B., Hendrix, D., Trang, V., Levine, M., (2008) A simplified miRNA-based gene silencing method for Drosophila melanogaster. Dev Biol 321, 482-490.

Harper, D.M., (2008) Impact of vaccination with Cervarix (trade mark) on subsequent HPV-16/18 infection and cervical disease in women 15-25 years of age. Gynecol Oncol 110, S11-17.

Harrison, R.L., Jarvis, D.L., (2006) Protein N-glycosylation in the baculovirus-insect cell expression system and engineering of insect cells to produce "mammalianized" recombinant glycoproteins. Adv Virus Res 68, 159-191.

Harrison, R.L., Jarvis, D.L., (2007) Transforming lepidopteran insect cells for improved protein processing. Methods Mol Biol 388, 341-356.

Hetz, C., (2012) The unfolded protein response: controlling cell fate decisions under ER stress and beyond. Nature Reviews Molecular Cell Biology 13, 89.

Hickerson, R.P., Vlassov, A.V., Wang, Q., Leake, D., Ilves, H., Gonzalez-Gonzalez, E., Contag, C.H., Johnston, B.H., Kaspar, R.L., (2008) Stability Study of Unmodified siRNA and Relevance to Clinical Use. Oligonucleotides 18, 345-354.

Hink, W.F., (1970) Established insect cell line from the cabbage looper, Trichoplusia ni. Nature 226, 466-467.

Hollister, J.R., Shaper, J.H., Jarvis, D.L., (1998) Stable expression of mammalian beta 1,4-galactosyltransferase extends the N-glycosylation pathway in insect cells. Glycobiology 8, 473-480.

Huang, Y., Deng, F., Hu, Z., Vlak, J.M., Wang, H., (2007) Baculovirus-mediated gene silencing in insect cells using intracellularly produced long double-stranded RNA. J Biotechnol 128, 226-236.

Imai, S., Kusakabe, T., Xu, J., Li, Z., Shirai, S., Mon, H., Morokuma, D., Lee, J.M., (2015) Roles of silkworm endoplasmic reticulum chaperones in the secretion of recombinant proteins expressed by baculovirus system. Mol Cell Biochem 409, 255-262.

Imperiali, B., O'Connor, S.E., (1999) Effect of N-linked glycosylation on glycopeptide and glycoprotein structure. Curr Opin Chem Biol 3, 643-649.

Jarvis, D.L., (2009) Baculovirus-insect cell expression systems. Methods Enzymol 463, 191-222.

Jarvis, D.L., Finn, E.E., (1996) Modifying the insect cell N-glycosylation pathway with immediate early baculovirus expression vectors. Nat Biotechnol 14, 1288-1292.

Kantoff, P.W., Higano, C.S., Shore, N.D., Berger, E.R., Small, E.J., Penson, D.F., Redfern, C.H., Ferrari, A.C., Dreicer, R., Sims, R.B., Xu, Y., Frohlich, M.W., Schellhammer, P.F., (2010) Sipuleucel-T immunotherapy for castration-resistant prostate cancer. N Engl J Med 363, 411-422.

Kenoutis, C., Efrose, R.C., Swevers, L., Lavdas, A.A., Gaitanou, M., Matsas, R., Iatrou, K., (2006) Baculovirus-mediated gene delivery into Mammalian cells does not alter their transcriptional and differentiating potential but is accompanied by early viral gene expression. J Virol 80, 4135-4146.

Kim, N.Y., Baek, J.Y., Choi, H.S., Chung, I.S., Shin, S., Lee, J.I., Choi, J.Y., Yang, J.M., (2012) Short-hairpin RNA-mediated gene expression interference in Trichoplusia ni cells. J Microbiol Biotechnol 22, 190-198.

Kioukia, N., Nienow, A.W., Emery, A.N., al-Rubeai, M., (1995) Physiological and environmental factors affecting the growth of insect cells and infection with baculovirus. J Biotechnol 38, 243-251.

Kitajima, M., Takaku, H., (2008) Induction of antitumor acquired immunity by baculovirus Autographa californica multiple nuclear polyhedrosis virus infection in mice. Clin Vaccine Immunol 15, 376-378.

Kost, T.A., Condreay, J.P., Jarvis, D.L., (2005) Baculovirus as versatile vectors for protein expression in insect and mammalian cells. Nat Biotechnol 23, 567-575.

Kozutsumi, Y., Segal, M., Normington, K., Gething, M.J., Sambrook, J., (1988) The presence of malfolded proteins in the endoplasmic reticulum signals the induction of glucose-regulated proteins. Nature 332, 462-464.

Kuystermans, D., Krampe, B., Swiderek, H., Al-Rubeai, M., (2007) Using cell engineering and omic tools for the improvement of cell culture processes. Cytotechnology 53, 3-22.

Lam, J.K.W., Chow, M.Y.T., Zhang, Y., Leung, S.W.S., (2015) siRNA Versus miRNA as Therapeutics for Gene Silencing. Molecular Therapy - Nucleic Acids 4, e252.

Lee, H.S., Lee, H.Y., Kim, Y.-J., Jung, H.-D., Choi, K.J., Yang, J.M., Kim, S.S., Kim, K., (2015) Small interfering (Si) RNA mediated baculovirus replication reduction without affecting target gene expression. Virus Research 199, 68-76.

Li, T.C., Scotti, P.D., Miyamura, T., Takeda, N., (2007) Latent infection of a new alphanodavirus in an insect cell line. J Virol 81, 10890-10896.

Lis, H., Sharon, N., (1993) Protein glycosylation. Structural and functional aspects. Eur J Biochem 218, 1-27.

Lynn, D.E., (2001) Novel techniques to establish new insect cell lines. In Vitro Cell Dev Biol Anim 37, 319-321.

Lynn, D.E., (2002) Methods for Maintaining Insect Cell Cultures. J Insect Sci 2.

Ma, H., Galvin, T.A., Glasner, D.R., Shaheduzzaman, S., Khan, A.S., (2014) Identification of a novel rhabdovirus in Spodoptera frugiperda cell lines. J Virol 88, 6576-6585.

Mabashi-Asazuma, H., Jarvis, D.L., (2017) CRISPR-Cas9 vectors for genome editing and host engineering in the baculovirus–insect cell system. Proc Natl Acad Sci U S A 114, 9068-9073.

Mabashi-Asazuma, H., Shi, X., Geisler, C., Kuo, C.W., Khoo, K.H., Jarvis, D.L., (2013) Impact of a human CMP-sialic acid transporter on recombinant glycoprotein sialylation in glycoengineered insect cells. Glycobiology 23, 199-210.

Marek, M., van Oers, M.M., Devaraj, F.F., Vlak, J.M., Merten, O.W., (2011) Engineering of baculovirus vectors for the manufacture of virion-free biopharmaceuticals. Biotechnol Bioeng 108, 1056-1067.

Marques, J.T., Williams, B.R.G., (2005) Activation of the mammalian immune system by siRNAs. Nat Biotechnol 23, 1399.

Meghrous, J., Aucoin, M.G., Jacob, D., Chahal, P.S., Arcand, N., Kamen, A.A., (2005) Production of recombinant adeno-associated viral vectors using a baculovirus/insect cell suspension culture system: from shake flasks to a 20-L bioreactor. Biotechnol Prog 21, 154-160.

Mena, J.A., Kamen, A.A., (2011) Insect cell technology is a versatile and robust vaccine manufacturing platform. Expert Rev Vaccines 10, 1063-1081.

Miller, L.K., (1988) Baculoviruses as gene expression vectors. Annu Rev Microbiol 42, 177-199.

Morais, V.A., Serpa, J., Palma, A.S., Costa, T., Maranga, L., Costa, J., (2001) Expression and characterization of recombinant human alpha-3/4-fucosyltransferase III from Spodoptera frugiperda (Sf9) and Trichoplusia ni (Tn) cells using the baculovirus expression system. Biochem J 353, 719-725.

Murges, D., Kremer, A., Knebel-Morsdorf, D., (1997) Baculovirus transactivator IE1 is functional in mammalian cells. J Gen Virol 78 (Pt 6), 1507-1510.

Nissom, P.M., Sanny, A., Kok, Y.J., Hiang, Y.T., Chuah, S.H., Shing, T.K., Lee, Y.Y., Wong, T.K., Hu, W.-s., Sim, M.Y.G., Philp, R., (2006) Transcriptome and proteome profiling to understanding the biology of high productivity CHO cells. Mol Biotechnol 34, 125-140.

Okada, T., Ihara, H., Ito, R., Nakano, M., Matsumoto, K., Yamaguchi, Y., Taniguchi, N., Ikeda, Y., (2010) N-Glycosylation engineering of lepidopteran insect cells by the introduction of the beta1,4-N-acetylglucosaminyltransferase III gene. Glycobiology 20, 1147-1159.

Paddison, P.J., Caudy, A.A., Hannon, G.J., (2002) Stable suppression of gene expression by RNAi in mammalian cells. Proceedings of the National Academy of Sciences 99, 1443-1448.

Palmberger, D., Wilson, I.B., Berger, I., Grabherr, R., Rendic, D., (2012) SweetBac: a new approach for the production of mammalianised glycoproteins in insect cells. PLoS One 7, e34226.

Pennock, G.D., Shoemaker, C., Miller, L.K., (1984) Strong and regulated expression of Escherichia coli beta-galactosidase in insect cells with a baculovirus vector. Mol Cell Biol 4, 399-406.

Saarinen, M.A., Troutner, K.A., Gladden, S.G., Mitchell-Logean, C.M., Murhammer, D.W., (1999) Recombinant protein synthesis in Trichoplusia ni BTI-Tn-5B1-4 insect cell aggregates. Biotechnol Bioeng 63, 612-617.

Sequeira, D.P., Correia, R., Carrondo, M.J.T., Roldao, A., Teixeira, A.P., Alves, P.M., (2018) Combining stable insect cell lines with baculovirus-mediated expression for multi-HA influenza VLP production. Vaccine 36, 3112-3123.

Sharan, S.K., Thomason, L.C., Kuznetsov, S.G., Court, D.L., (2009) Recombineering: a homologous recombination-based method of genetic engineering. Nat Protoc 4, 206-223.

Sharp, P.A., (1999) RNAi and double-strand RNA. Genes Dev 13, 139-141.

Slack, J., Arif, B.M., (2006) The Baculoviruses Occlusion-Derived Virus: Virion Structure and Function. Adv Virus Res. Academic Press, pp. 99-165.

Smith, G.E., Summers, M.D., Fraser, M.J., (1983) Production of human beta interferon in insect cells infected with a baculovirus expression vector. Mol Cell Biol 3, 2156-2165.

Sokolenko, S., George, S., Wagner, A., Tuladhar, A., Andrich, J.M., Aucoin, M.G., (2012) Co-expression vs. co-infection using baculovirus expression vectors in insect cell culture: Benefits and drawbacks. Biotechnol Adv 30, 766-781.

Summers, M.D., (2006) Milestones leading to the genetic engineering of baculoviruses as expression vector systems and viral pesticides. Adv Virus Res 68, 3-73.

Teng, C.Y., Chang, S.L., van Oers, M.M., Wu, T.Y., (2013) Enhanced protein secretion from insect cells by co-expression of the chaperone calreticulin and translation initiation factor eIF4E. Mol Biotechnol 54, 68-78.

Thompson, C.M., Petiot, E., Mullick, A., Aucoin, M.G., Henry, O., Kamen, A.A., (2015) Critical assessment of influenza VLP production in Sf9 and HEK293 expression systems. BMC Biotechnol 15, 31.

Treanor, J.J., El Sahly, H., King, J., Graham, I., Izikson, R., Kohberger, R., Patriarca, P., Cox, M., (2011) Protective efficacy of a trivalent recombinant hemagglutinin protein vaccine (FluBlok(R)) against influenza in healthy adults: a randomized, placebo-controlled trial. Vaccine 29, 7733-7739.

Trummer, E., Ernst, W., Hesse, F., Schriebl, K., Lattenmayer, C., Kunert, R., Vorauer-Uhl, K., Katinger, H., Müller, D., (2008) Transcriptional profiling of phenotypically different Epo-Fc expressing CHO clones by cross-species microarray analysis. Biotechnology Journal 3, 924-937.

Valdes, V.J., Sampieri, A., Sepulveda, J., Vaca, L., (2003) Using double-stranded RNA to prevent in vitro and in vivo viral infections by recombinant baculovirus. J Biol Chem 278, 19317-19324.

van Lier, F.L., van den End, E.J., de Gooijer, C.D., Vlak, J.M., Tramper, J., (1990) Continuous production of baculovirus in a cascade of insect-cell reactors. Appl Microbiol Biotechnol 33, 43-47.

van Oers, M.M., (2011) Opportunities and challenges for the baculovirus expression system. J Invertebr Pathol 107 Suppl, S3-15.

van Oers, M.M., Pijlman, G.P., Vlak, J.M., (2015) Thirty years of baculovirus-insect cell protein expression: from dark horse to mainstream technology. J Gen Virol 96, 6-23.

Vaughn, J.L., Goodwin, R.H., Tompkins, G.J., McCawley, P., (1977) The establishment of two cell lines from the insect Spodoptera frugiperda (Lepidoptera; Noctuidae). In Vitro 13, 213-217.

Volkman, L.E., Summers, M.D., (1977) Autographa californica nuclear polyhedrosis virus: comparative infectivity of the occluded, alkali-liberated, and nonoccluded forms. J Invertebr Pathol 30, 102-103.

Wang, M., Kaufman, R.J., (2014) The impact of the endoplasmic reticulum protein-folding environment on cancer development. Nature Reviews Cancer 14, 581.

Wang, P., Granados, R.R., Shuler, M.L., (1992) Studies on serum-free culture of insect cells for virus propagation and recombinant protein production. J Invertebr Pathol 59, 46-53.

Wang, W., Wang, W.-H., Azadzoi, K.M., Su, N., Dai, P., Sun, J., Wang, Q., Liang, P., Zhang, W., Lei, X., Yan, Z., Yang, J.-H., (2016) Activation of innate antiviral immune response via double-stranded RNA-dependent RLR receptor-mediated necroptosis. Scientific Reports 6, 22550.

Wilde, M., Klausberger, M., Palmberger, D., Ernst, W., Grabherr, R., (2014) Tnao38, high five and Sf9--evaluation of host-virus interactions in three different insect cell lines: baculovirus production and recombinant protein expression. Biotechnol Lett 36, 743-749.

Yokoyama, N., Hirata, M., Ohtsuka, K., Nishiyama, Y., Fujii, K., Fujita, M., Kuzushima, K., Kiyono, T., Tsurumi, T., (2000) Co-expression of human chaperone Hsp70 and Hsdj or Hsp40 co-factor increases solubility of overexpressed target proteins in insect cells. Biochim Biophys Acta 1493, 119-124.

Yu, N., Christiaens, O., Liu, J., Niu, J., Cappelle, K., Caccia, S., Huvenne, H., Smagghe, G., (2013) Delivery of dsRNA for RNAi in insects: an overview and future directions. Insect Science 20, 4-14.

Zhang, J., He, Q., Zhang, C.D., Chen, X.Y., Chen, X.M., Dong, Z.Q., Li, N., Kuang, X.X., Cao, M.Y., Lu, C., Pan, M.H., (2014) Inhibition of BmNPV replication in silkworm cells using inducible and regulated artificial microRNA precursors targeting the essential viral gene lef-11. Antiviral Res 104, 143-152.

Zhang, X., Xu, K., Ou, Y., Xu, X., Chen, H., (2018) Development of a baculovirus vector carrying a small hairpin RNA for suppression of sf-caspase-1 expression and improvement of recombinant protein production. BMC Biotechnol 18, 24.

6 CURRICULUM VITAE

Address:	Rüdigergasse 6/14 1050 Vienna, Austria
Telephone:	+43 660 7100 883
E-mail:	krisztina.koczka@boku.ac.at
Date of birth:	14 April 1990
Place of birth:	Budapest, Hungary

PROFESSIONAL EXPERIENCE

02/2015 – Present	Junior researcher/PhD student at Austrian Centre of Industrial Biotechnology
09/2014 – 01/2015	Internship at Vienna University of Technology
09/2013 – 04/2014	MSc thesis student at Gedeon Richter Plc. (Hungary)
06/2013	Internship at Gedeon Richter Plc. (Hungary)
06/2010 – 08/2010	Internship at GlaxoSmithKline Biologicals (Hungary)

EDUCATION

06/2015 – Present	Doctoral studies at University of Natural Resources and Life Sciences, Vienna
06/2017 – 12/2017	Graduate research trainee at McGill University (Canada)
01/2012 – 06/2014	MSc at Budapest University of Technology and Economics (Hungary)
01/2012 – 05/2012	Erasmus student at Lund University (Sweden)
09/2008 – 01/2012	BSc at Budapest University of Technology and Economics (Hungary)
09/2002 – 06/2008	Eötvös Loránd University – Trefort Ágoston High School (Hungary)

LANGUAGE SKILLS

Hungarian	**Mother Language**
English	**Near native/fluent** ▪ Cambridge Certificate in Advanced English ▪ C2 level certificate, 2012
German	**Proficient user** ▪ Österreichisches Sprachdiplom Deutsch ▪ C1 level certificate, 2018
French	**Basic user** ▪ Budapest University of Technology and Economics ▪ C1 level certificate, 2010

SCIENTIFIC PUBLICATIONS

Koczka K, Ernst W, Palmberger D, Klausberger M, Nika L, Grabherr R. 2019. Development of a dual-vector system utilizing microRNA mimics of the *Autographa californica* miR-1 for an inducible knockdown in insect cells. *International Journal of Molecular Sciences* 20(3):533.

Nika L, Cuadrado-Castano S, Arunkumar G, Grünwald-Gruber C, McMahon M, **Koczka K**, Garcia-Sastre A, Krammer F, Grabherr R. 2019. A HER2-displaying virus-like particle vaccine protects from challenge with mammary carcinoma cells in a mouse model. Manuscript submitted to *npj Vaccines*.

Venereo-Sánchez A, Fulton K, **Koczka K**, Twine S, Ansorge S, Gilbert R, Henry O, Kamen A. 2018. Characterization of Influenza H1N1 Gag virus-like particles and extracellular vesicles co-produced in HEK-293SF. Manuscript submitted to *Vaccine*.

Koczka K, Peters P, Ernst W, Himmelbauer H, Nika L, Grabherr R. 2018. Comparative transcriptome analysis of a *Trichoplusia ni* cell line reveals distinct host responses to intracellular and secreted protein products expressed by recombinant baculoviruses. *Journal of Biotechnology* 270:61–69.

Nika L, Wallner J, Palmberger D, **Koczka K**, Vorauer-Uhl K, Grabherr R. 2017. Expression of full-length HER2 protein in *Sf*9 insect cells and its presentation on the surface of budded virus-like particles. *Protein Expression and Purification* 136:27-38.

Zalai D, **Koczka K**, Parta L, Wechselberger P, Klein T, Herwig C. 2015. Combining mechanistic and data-driven approaches to gain process knowledge on the control of the metabolic shift to lactate uptake in a fed-batch CHO process. *Biotechnology Progress* 31(6):1657-1668.

CONFERENCE PARTICIPATION

Koczka K, Peters P, Ernst W, Himmelbauer H, Grabherr R. 2018. Comparative transcriptome analysis of a Trichoplusia ni cell line in response to recombinant baculoviral infections (Poster) [7th Vaccine Technology Conference, Mont Tremblant, Canada, June 17 - 22, 2018]

Koczka K, Strobl F, Schneider T, Ernst W, Grabherr R, Striedner G, Jungbauer A. 2016. Continuous integrated biomanufacturing of complex bionanoparticles, viruses and virus-like particles (Poster) [European Summit of Industrial Biotechnology, Graz, Austria, November 14-16, 2016]

Koczka K, Schneider T, Ernst W, Blissard G, Grabherr R. 2016. Viral engineering for better secretion of hemagglutinin virus like particles in insect cells (Poster) [Virus-Like Particle & Nano-Particle Vaccines Conference, Leiden, The Netherlands, June 22-24, 2016]

Koczka K, Wilde M, Palmberger D, Ernst W, Grabherr R. 2015. Viral engineering for better secretion of hemagglutinin virus like particles in insect cells (Poster) [12th Protein Expression in Animal Cells Conference, San Diego, California, USA, September 20-24, 2015]

PATENTS

Grabherr R, Ernst W, **Koczka K**, Klausberger M. 2018. Dual vector system for improved production of proteins in animal cells. Application number: 18194719.3-1120.

7 APPENDIX

7.1 PUBLICATION C

Expression of full-length HER2 protein in *Sf*9 insect cells and its presentation on the surface of budded virus-like particles

Lisa Nika, Jakob Wallner, Dieter Palmberger, **Krisztina Koczka**, Karola Vorauer-Uhl, Reingard Grabherr

Published in Protein Expression and Purification

Protein Expression and Purification 136:27-38 (2017)

doi: 10.1016/j.pep.2017.06.005

Protein Expression and Purification 136 (2017) 27–38

Contents lists available at ScienceDirect

Protein Expression and Purification

journal homepage: www.elsevier.com/locate/yprep

Expression of full-length HER2 protein in *Sf*9 insect cells and its presentation on the surface of budded virus-like particles

Lisa Nika [a], Jakob Wallner [a], Dieter Palmberger [a, b], Krisztina Koczka [a, b], Karola Vorauer-Uhl [a], Reingard Grabherr [a, *]

[a] Department of Biotechnology, University of Natural Resources and Life Sciences, Muthgasse 18, 1190 Vienna, Austria
[b] ACIB - Austrian Centre of Industrial Biotechnology, Muthgasse 11, 1190 Vienna, Austria

ARTICLE INFO

Article history:
Received 27 February 2017
Received in revised form
19 May 2017
Accepted 11 June 2017
Available online 12 June 2017

Keywords:
Baculovirus-insect cell expression system
*Sf*9 insect cells
Virus-like particles
Surface display
Human epidermal growth factor receptor 2
Biolayer interferometry

ABSTRACT

Biomarkers of cancer are often glycosylated membrane receptor proteins present on the cellular surface. In order to develop new antibodies for cancer diagnostics or treatment, it is a main pre-requisite that these target proteins are available in a native conformation. However, membrane receptor proteins are notoriously difficult to produce due to their hydrophobic nature and complex architecture. Here, we used the baculovirus-insect cell expression system to produce budded virus-like particles (VLPs) as the scaffold for the presentation of complex membrane proteins. Since the human epidermal growth factor receptor 2 (HER2) is known to be overexpressed in a number of cancers it was chosen as model for a tumor antigen. VLPs displaying full-length HER2 on the surface were produced in *Spodoptera frugiperda* 9 (*Sf*9) insect cells and purified by sucrose gradient ultracentrifugation. The number of secreted particles was quantified by nanoparticle tracking analysis. To confirm the presence of HER2 protein on the surface, VLPs were labeled with gold-conjugated antibodies and analyzed by transmission electron microscopy. Functionality of displayed HER2 was investigated by ELISA and a newly established biolayer interferometry based technique. Detection was accomplished using the specific monoclonal antibody Herceptin and filamentous phages displaying a single-chain variable fragment of an anti-HER2 antibody. Significant stronger binding of Herceptin and anti-HER2 phages to HER2-displaying VLPs as compared to control VLPs was demonstrated. Thus, we suggest that *Sf*9 insect cells are highly feasible for the fast and easy production of various budded VLPs that serve as a platform for full-length membrane receptor presentation.

1. Introduction

Recombinant production of therapeutically active proteins is the main pre-requisite and a tremendous challenge for the development of cancer specific antibodies, cancer vaccines and diagnostics [1]. The specific antigen has to be available in an authentically folded manner with posttranslational modifications similar to its native counterpart. Tumor antigens are often complex and glycosylated membrane proteins and their production is technically challenging due to their membrane crossing or membrane attached configuration. To date, mammalian cells such as Chinese hamster ovary (*CHO*) or human embryonic kidney (*HEK*) cells are the most commonly used systems to produce these recombinant proteins since they are able to generate human like posttranslational modifications and grow to high cell densities in suspension cultures in bioreactors [2]. Yet, full-length expression is hardly achieved and mostly truncated versions of membrane proteins are produced and purified. Hence, there exists an urgent need to develop alternative approaches for the expression of native antigens to serve as a basis for the development of highly specific antibodies and vaccines.

The human epidermal growth factor receptor 2 (HER2) is one of the most prominent surface tumor antigens of breast cancer cells, and as such, a valuable target for antibody based therapies [3,4]. Like many other tumor antigens, HER2 is a complex membrane protein. Recent findings demonstrated, that the HER2 extracellular domain could be expressed in *Drosophila melanogaster* Schneider2

* Corresponding author.
E-mail addresses: lisa.nika@boku.ac.at (L. Nika), jakob.wallner@boku.ac.at (J. Wallner), dieter.palmberger@boku.ac.at (D. Palmberger), krisztina.koczka@boku.ac.at (K. Koczka), karola.vorauer-uhl@boku.ac.at (K. Vorauer-Uhl), reingard.grabherr@boku.ac.at (R. Grabherr).

http://dx.doi.org/10.1016/j.pep.2017.06.005
1046-5928/

cells in a native state [5]. Based on these findings, we aimed to express full-length HER2 on the surface of *Spodoptera frugiperda* 9 (*Sf*9)-derived virus-like particles (VLPs) in order to evaluate whether this approach is feasible for expression and display of functional HER2, suitable for biomedical applications. VLPs are self-assembled nanostructures that constitute an attractive scaffold for the display of various epitopes as well as glycosylated and complex proteins [6–9]. VLPs consist of viral matrix proteins that, when overexpressed and transported to the cellular surface, spontaneously self-assemble into particles [10]. They are safe since they resemble the natural virus shells but lack the nucleic acid and are therefore not infectious, they are easy to be produced on a large scale [11]. Moreover, VLPs are highly potent of stimulating humoral and cellular immune responses [9,12]. They can induce strong B cell responses due to a high avidity of epitopes on the VLP surface [13] and can also be internalized by antigen presenting cells that activate $CD4^+$ and $CD8^+$ T cells to elicit specific cytotoxic T lymphocyte responses [14–16]. Previous studies have shown, that VLPs are an ideal bait for the selection of monoclonal antibodies (mAbs) against membrane proteins like the G-protein coupled glucagon receptor [17] or viral envelope proteins like the chikungunya virus envelope glycoproteins E2 and E1 [18] out of surface display libraries. Depending on the chosen matrix protein, VLPs are produced as intracellular entities or as budded particles. In our approach, we used the Gag matrix protein of the human immunodeficiency virus (HIV), which covers the inner surface of the viral membrane and is crucial for the formation of budded VLPs. During the budding process, naked capsids acquire the host-derived membrane. In a natural HIV life cycle, the cell membrane is enriched in viral envelope proteins that are essential for attachment to the host cells. In our experimental set-up, no corresponding viral envelope proteins were present. Instead, we overexpressed the complete HER2 with the purpose to generate particles that, by budding through the cell membrane, would result in displaying the full-length membrane receptor on their surface.

Antibodies against HER2 have been used as successful therapeutics and are highly important for diagnostic purposes [4,19]. With the development of next generation scaffold proteins such as nanobodies [20] and minimalist antibodies [21], additional therapeutic HER2 binding molecules are expected to be designed. Therefore, and for the development of HER2 vaccines, there is a demand for authentic presentation of this cancer antigen in many medical research approaches. Using our strategy, we can provide HER2 in the authentic form and as complete molecule. We chose the baculovirus-insect cell expression system (BES) for the production of VLPs, since the BES has proven to be well-suited for the expression of eukaryotic proteins and the production of versatile VLPs including those from influenza virus [22], human immunodeficiency virus [9], bluetongue virus [23] and Ebola virus [24,25]. In the past few years different baculovirus-insect cell-derived proteins have entered clinical application including GlaxoSmithKline's and Merck's VLP-based human papillomavirus vaccines Cervarix® and Gardasil® respectively or the immune-therapeutic against advanced prostate tumors PROVENGE® (sipuleucel-T). From a bioprocessing point of view, insect cells have shown significantly higher production levels of influenza VLPs as compared to *HEK*-293 cells [26], rendering insect cells the more applicable system for particle production.

Binding studies of surface displayed proteins are often done by flow cytometry, which is mainly feasible for whole cells. Due to their small size, VLPs are mostly analyzed by ELISA, Western Blot analysis and biosensor based techniques instead. The most commonly applied biosensor based techniques are Surface Plasmon Resonance (SPR) and Biolayer interferometry (BLI). BLI is an optical analytical method [27] that was previously shown to be a valuable tool for diagnostics and pharmacokinetics [28,29]. In contrast to micro-fluidic SPR, which commonly delivers samples to a stationary sensor chip, BLI technology is established in an open shaking micro-well plate format without any micro-fluidics [30]. Thus, there is no risk for clogging effects as described for SPR, the samples can be recovered and used in other assays and the association phase and dissociation phase are only restricted by evaporation of the sample. Therefore, we evaluated a biosensor based analytical approach for detection of HER2 binding in the context of VLPs.

Overall, we present a study on full-length HER2 presentation on the surface of *Sf*9-derived VLPs and claim a newly established BLI based technique to be a fast and simple method to detect specific binding to functional membrane cancer targets. We suggest our approach as a valuable contribution for cancer diagnostics, vaccine production or as bait for antibody libraries.

2. Materials and methods

All DNA manipulations were carried out as summarized by Sambrook et al. [31]. DNA polymerase, restriction enzymes, T4 DNA ligase and Calf Intestinal Alkaline Phosphatase were purchased from New England Biolabs (Ipswich, USA). All enzymes were used according to manufacturer's recommendation. All primers and oligos were synthesized by IDT - Integrated DNA Technology (Leuven, Belgium). All chemicals and reagents used were of analytical grade. Tween20, bovine serum albumin (BSA), Kolliphor P 188, 3,3'-diaminobenzidine (DAB), Heparin, HEPES, polyethylene glycol (PEG), glutaraldehyde 25% and uranyl acetate-dihydrate >98% were purchased from Sigma-Aldrich (St. Louis, Missouri, USA). Sodium azide (NaN_3) was acquired from Merck (Darmstadt, Germany). Sulfuric acid 25% (H_2SO_4) was purchased from Roth (Karlsruhe, Germany). The biotinylated PEG-Cholesterol linker was obtained from Nanocs (Innovative Life Science Products, New York, USA).

2.1. Cells

Spodoptera frugiperda 9 (*Sf*9) (ATCC CRL-1711) [32] cells were maintained using HyClone SFM4 Insect cell medium (GE Healthcare, Little Chalfont, UK) supplemented with 0,1% Kolliphor P188 (Sigma-Aldrich, St. Louis, Missouri, USA) at 27 °C. Adherent cultures were grown in T-flasks and suspension cultures were grown in 500-ml shaker flasks at a cell density between 5E+5 and 3E+6 cells/ml at 100 rpm.

2.2. Recombinant baculovirus generation

Recombinant baculoviruses encoding full-length HER2 and the HIV-1 Gag matrix protein were generated as follows. The sequence coding for the transmembrane domain (TMD) and the intracellular domain (ICD) of HER2 was PCR amplified using a plasmid containing full-length human HER2 (GenBank accession no. X03363.1) as a template. The resulting fragment was ligated into the MultiBac acceptor vector pACEBac-1 (EMBL, Grenoble, France) resulting in pACEBac-1-HER2-TMD-ICD. The sequence of the HER2 ectodomain (ECD) and the signal peptide (SP) were chemically synthesized by IDT - Integrated DNA Technology (Leuven, Belgium), equipped with flanking *PvuII* and *SalI* restriction sites. After PCR amplification, pACEBac-1-HER2-TMD-ICD and Her2-ECD-SP were digested with *PvuII* and *SalI* restriction endonucleases according to manufacturer's instructions and ligated, resulting in pACEBac-1-HER2.

The HIV-1 Gag gene was acquired from the complete human immunodeficiency virus type 1 (HXB2) genome (GenBank accession no. K03455.1), chemically synthesized by IDT (Leuven, Belgium) and PCR amplified using primers containing *BamHI* and *XbaI* restriction sites. The digested and purified HIV-1 Gag fragment

was ligated into a *BamHI* and *XbaI* digested pIDC donor vector (EMBL, Grenoble, France) resulting in pIDC-HIV-1 Gag.

Acceptor-donor fusions were generated by Cre-LoxP recombination. The HIV-1 Gag-HER2 fusion construct was inserted into the MultiBac genome via Tn7 transposition using DH10MultiBacY cells (EMBL, Grenoble, France) according to Fitzgerald et al. [33]. In addition, DH10MultiBacY cells encode yellow fluorescent protein (YFP) which gets expressed intracellularly once insect cells are infected and was therefore used as infection marker in the present experiments. Recombinant baculoviruses were generated by transfecting *Sf*9 cells with the bacmid HIV-1 Gag-HER2_YFP using FuGENE HD transfection reagent (Promega, Madison, Wisconsin, USA) according to manufacturer's instructions. Four days post infection the viral seed stock was harvested by centrifugation for 10 min at 3000×*g* (HERAEUS Megafuge16, Thermo Scientific, Waltham, Massachusetts, USA). The virus was amplified and viral titers were determined using plaque assay.

2.3. Flow cytometry

To evaluate whether HER2 is expressed on the cell surface, *Sf*9 cells were infected with the recombinant baculovirus encoding HER2 or the recombinant virus solely carrying the HIV-1 Gag matrix protein (negative control) at a multiplicity of infection (MOI) of 10 and a cell density of 1E+5 cells/ml. 48 h post infection cells were harvested and were investigated by flow cytometry. Therefore, 2E+6 cells were stained with 200 µl of Herceptin at a dilution of 1:100 (40 µg), followed by an anti-kappa biotin-labeled antibody (ABIN375958, antibodies online, Atlanta, Georgia, USA) and streptavidin-labeled Alexa Flour647 (S21374, Life Technologies, Carlsbad, California, USA) at a dilution of 1:100 and analyzed using a Gallios Flow Cytometer (Beckman Coulter, Vienna, Austria). Raw data were evaluated using the Kaluza1.2 software (Beckman Coulter, Vienna, Austria).

2.4. VLP production and purification

*Sf*9 cells were infected with the recombinant baculovirus expressing HER2 and HIV-1 Gag matrix protein at a MOI of 10 and a cell density of 1E+6 cells/ml in shaker flasks. Cells were harvested 72 h post infection by low speed centrifugation for 10 min at 3000×*g* (HERAEUS Megafuge16, Thermo Scientific, Waltham, Massachusetts, USA) at room temperature and for sample clarification a second, higher speed centrifugation step for 15 min at 15 000×*g*. Pelleted cells and supernatants were investigated by SDS-PAGE and Western Blot analysis. VLPs were harvested by ultracentrifugation using a SW-38Ti rotor (Beckmann Coulter, Vienna, Austria) at 30 000 rpm, at 4 °C for 100 min. Pellets were resuspended in phosphate-buffered saline (PBS) over night at 4 °C. VLPs were further purified by discontinuous sucrose density gradient centrifugation (20-30-40-50-60%) at 38 000 rpm at 4 °C for 16 h using a SW-41Ti rotor (Beckmann Coulter, Vienna, Austria). Gradients were harvested in 1 ml fractions and analyzed by SDS-PAGE and Western Blot. Fractions containing most VLP protein were diluted in PBS, were pooled and pelleted by ultracentrifugation at 4 °C, 30 000 rpm for 100 min (SW-41Ti rotor, Beckmann Coulter, Vienna, Austria). Pellets were resuspended in 20 mM HEPES (Sigma-Aldrich, St. Louis, Missouri, USA) over night at 4 °C and were analyzed for VLP content by nanoparticle tracking analysis (NTA).

2.5. SDS-PAGE and western blot analysis

Infected *Sf*9 cells, supernatants and sucrose gradient fractions were examined by SDS-PAGE and Western blotting according to Laemmli [34]. Samples were mixed with 4x NuPage LDS sample buffer (Invitrogen, Carlsbad, USA) containing lithium dodecyl sulfate, pH 8.4. Proteins were separated by SDS-PAGE and electroblotted onto a PVDF transfer membrane (GE Healthcare Life Sciences, Vienna, Austria). Detection of the matrix protein HIV-1 Gag was performed using an anti-human HIV-1 Gag rabbit antibody (E63H00201, Enogene, Atlanta, Georgia, USA) and a secondary anti-rabbit IgG alkaline phosphatase-labeled goat antibody (A9919, Sigma-Aldrich, St. Louis, Missouri, USA). Detection of human HER2 was accomplished using Herceptin (anti-human HER2 antibody) and a secondary anti-human IgG alkaline phosphatase-labeled goat antibody (A3187, Sigma-Aldrich, St. Louis, Missouri, USA). Membranes were developed applying BCIP/NBT (Promega, Madison, Wisconsin, USA).

2.6. Nanoparticle tracking analysis (NTA)

To determine the VLP concentration NTA measurements were performed using a NanoSight LM-10 (Malvern Instruments Ltd., Worcestershire, UK) equipped with a blue laser (405 nm). The NTA technology utilizes the properties of light scattering and Brownian motion in order to obtain the size distribution and concentration of particles in liquid suspension. A laser beam is passed through the sample chamber, and particles in the path of this beam scatter light in a manner that they can easily be visualized via a 20× magnification microscope. For the measurement, sucrose gradient purified VLP samples were serially diluted in particle-free water to obtain a suitable particle concentration (60–100 particles per video frame) for analysis. Videos of three dilution steps for each sample were captured for 60 s and were analyzed and evaluated by NTA 3.2 software. All steps were carried out at room temperature. The camera level and analysis parameters were adjusted manually and were kept constant during all measurements. The particle number was evaluated for particles with a diameter between 100 and 200 nm [35].

2.7. Transmission electron microscopy (TEM)

*Sf*9-derived VLPs were pelleted and used for electron microscopy. HER2-displaying VLPs as well as control VLPs were absorbed for 5 min on copper grids, fixed for 15 min using 2,5% glutaraldehyde, washed twice with PBS and stained for 1 h with 2 µg/ml monoclonal anti-human HER2 (3B5) antibody (MA5-13675, Thermo Scientific, Rockford, Illinios, USA). Samples were washed three times with PBS containing 2% BSA and incubated with 30 µg/ml secondary anti-mouse IgG 10 nm gold-labeled antibody (G7652, Sigma-Aldrich, Saint Louis, Missouri, USA) for 1 h. Negative staining was performed using uranyl acetate. Samples were examined using a transmission electron microscope (FEI Tecnai G^2 200 kV, FEI, Hillsboro, Oregon, USA) at various magnifications.

2.8. Scanning electron microscopy (SEM)

Sucrose gradient purified VLPs were immobilized to biosensors (see “Biolayer inerferometry”, Materials and Methods section) using the Octet QK, sensors were collected and their surface was imaged using the in-lens detector of a Zeiss Supra 55 VP scanning electron microscope (Zeiss, Jena, Germany). The detector operated at 2 kV. Samples were coated with a gold-palladium layer before transferring them into the chamber of the electron microscope.

2.9. Phages

Anti-HER2 phages (C6.5: human single-chain variable fragment (scFv) isolated from a non-immune phage library binding the tumor antigen c-erbB-2) [36] were kindly provided by G. Wozniak-Knopp (BOKU, Vienna). Phages were maintained by infecting

500 μl of mid-log *E. coli* tg1 cells with 1 μl of commercial anti-HER2 phage. Cells were incubated for 15 min at 37 °C to allow the phage particles to infect the cells. Infected cells were plated on LB agar (Sigma-Aldrich, St. Louis, Missouri, USA) containing 10 μg/ml tetracycline and were incubated at 37 °C overnight. The next day a single colony was picked and was grown in LB 2x media in the presence of 10 μg/ml tetracycline at 37 °C and 180 rpm shaking. The volume of the bacterial cell suspension was increased step by step from 5 ml to 1 L using tetracycline as selection pressure. Amplifications were centrifuged at 13 000×*g* (Avanti JXN-26 Centrifuge, Beckman Coulter, Vienna, Austria) for 15 min at 4 °C to remove cells. Supernatants were centrifuged using the same conditions. 0,15 vol of PEG/NaCl were added and mixed. Phages were allowed to precipitate for at least 2 h at 4 °C and pelleted by centrifugation at 13 000×*g* (Avanti JXN-26 Centrifuge, Beckman Coulter, Vienna, Austria) for 90 min at 4 °C. Phage pellets were resuspended in PBS, clarified by centrifugation at 14 500×*g* (HERAEUS Megafuge16, Thermo Scientific, Waltham, Massachusetts, USA) for 10 min at 4 °C and NaN_3 was added at a final concentration of 0,02%.

Phage titers were determined by infecting *E. coli* tg1 cells with the produced phages as described before, plating the cells, incubating over night at 37 °C and counting the colonies. The titer was determined to be 2,88E+11 cfu/ml.

2.10. Enzyme-linked immunosorbent assay (ELISA)

To evaluate efficient presentation of functional HER2 on the VLP surface, binding of Herceptin and HER2-specific phages to displayed target protein was examined by ELISA.

VLP - antibody ELISA: Wells of a 96 well Maxisorp ELISA plate (Nunc Thermo Scientific, Waltham, Massachusetts, USA) were coated with different concentrations of HER2-VLPs and control VLPs (0-1E+10 particles/well) in PBS over night at 4 °C. The concentration of VLPs/well was assessed based on NTA results. Wells were blocked using PBS +0,1% Tween20 + 0,3% BSA at room temperature for 1 h. After washing three times with 300 μl PBS +0,1% Tween20 per well, Herceptin (4 μg/ml) was applied in PBS for 1 h at room temperature while gentle agitation. Plates were washed six times with PBS and anti-human IgG-HRP-conjugated antibody (628420, Invitrogen, Carslbad, California, USA) diluted 1:2000 in blocking buffer was added and incubated at RT for 1 h. After washing six times with 300 μl PBS, 50 μl of HRP substrate, 3,3′,5′-tetramethylbenzidine (TMB Stabilized chromogen, Invitrogen, Carlsbad, California, USA) were added to each well. The reaction was stopped with 2 N H_2SO_4 and optical density was measured at 450 nm using an Infinite M1000 plate reader (Tecan Group, Männedorf, Switzerland). Raw data were evaluated using Excel spreadsheets (Version 2003, Microsoft, USA).

VLP - phage ELISA: For the phage ELISA, 96 well Maxisorp ELISA plates were coated with 50 μl of the target HER2-VLPs and control VLPs at a previously determined optimal VLP concentration of 5E+9 particles/well in PBS over night at 4 °C. Wells were blocked using PBS +0,1% Tween20 + 0,3% skim milk powder at room temperature for 1 h. After washing three times with 300 μl PBS +0,1% Tween20 each well, different concentrations of anti-HER2 phages (0–2,88E+11 cfu/ml) were added in PBS for 1 h at room temperature while gentle agitation. Plates were washed six times with PBS and anti-M13 antibody HRP-conjugated (GE Healthcare 27942101, UK) diluted 1:2500 in blocking buffer was applied at RT for 1 h. Development and evaluation were carried out the same way as described for the antibody ELISA.

2.11. Biolayer interferometry (BLI)

BLI sensing is an optical analytical technique based on the measurement of the interference pattern of white light reflected from a reference surface and a biofunctionalized sensor surface. Any change in the molecule number bound to the biosensor surface causes a shift in the interference pattern which is a real-time measure of the change in the thickness of the immobilized biolayer [37]. In this study an Octet QK instrument (ForteBio, PALL Life Sciences, Menlo Park, California, USA) equipped with 8 parallel biosensors was used to analyze biomolecular interactions between VLP-displayed HER2 and anti-HER2 phages.

HER2-displaying VLPs and control VLPs were immobilized to a streptavidin biosensor (PALL Life Sciences, Menlo Park, California, USA) via a biotinylated PEG-Cholesterol linker (Nanocs, Innovative Life Science Products, New York, USA). The biotin binds to streptavidin on the biosensor and PEG-Cholesterol inserts into the hydrophobic portion of the VLP membrane with sufficient strength to immobilize the VLPs [38]. The binding of the phages was detected by 3,3'-diaminobenzidine (DAB) signal enhancement [39]. Thereby a secondary anti-M13-HRP-labeled antibody (27942101, GE Healthcare, Little Chalfont, UK) is applied. The antibody recognizes the phage and the HRP tag oxidizes the substrate DAB, which precipitates on the sensor surface and causes an enhanced BLI signal. All steps were carried out in the same buffers as used for the phage ELISA. In detail, the assay was performed as follows (Fig. 1): (1) the baseline was recorded in PBS for 60 s, (2) the biotinylated PEG-Cholesterol linker (7 μM in HQ-H_2O) was loaded for 300 s, (3) the sensors were washed in PBS for 60 s, (4) HER2-VLPs or control VLPs were immobilized on the sensors for 900 s, (5) the sensors were washed in PBS for 180 s, (6) sensors were blocked in PBST (0,1% Tween20) + 0,3% skimmed milk powder for 600 s, (7) sensors were placed into different dilutions of phage samples for 600 s, (8) sensors were washed in PBST (0,1% Tween20) for 180 s, (9) sensors were placed into anti-M13 IgG labeled with HRP (1:800 in PBST + 0,3% skimmed milk powder) to detect the anti-HER2 phages that were bound to the HER2-VLPs, (10) sensors were washed in PBST for 180 s, (11) DAB enhancement was performed by dipping sensors into 0,05% DAB-0,015% H_2O_2 in PBS for 1800 s, (12) sensors were washed in PBST for 600 s. The stirring speed in measurement phases before adding VLPs was 1000 rpm, and was reduced to 500 rpm after addition of VLPs. Black, flat-bottom 96 well plates (Thermo Scientific, Slangerup, Denmark) were used as measurement plates. The temperature during the BLI measurements was set at 30 °C. Raw data were obtained with the Octet analysis software version 6.4 (ForteBio, PALL Life Sciences, Menlo Park, California, USA) and were exported to Excel spreadsheets (Version 2003, Microsoft, USA). Raw data of the individual steps were aligned to the corresponding association step and were determined as response at a defined time. Individual signal responses at each concentration were calculated as average of three independent measurements. For the determination of the limit of quantitation (LOQ) and the evaluation of the significance of the measurements, the baseline signal was measured by equilibrating the streptavidin biosensor tip with PBS. LOQ is defined as the lowest concentration at which the analyte can not only be reliably detected but at which some predefined goals for bias and precision are met and it's assumed to be a signal-to-noise ratio of 10:1 [40]. The baseline noise of the initial 60 s PBS equilibration step was 0,09 nm (n = 8). Thus, the LOQ was calculated as 0,9 nm.

3. Results

3.1. Flow cytometry studies of Sf9 insect cells

To prove the presentation of HER2 protein on the cellular surface, both, uninfected *Sf*9 cells and *Sf*9 cells infected with either HER2 expressing baculovirus or HIV-1 Gag expressing virus were

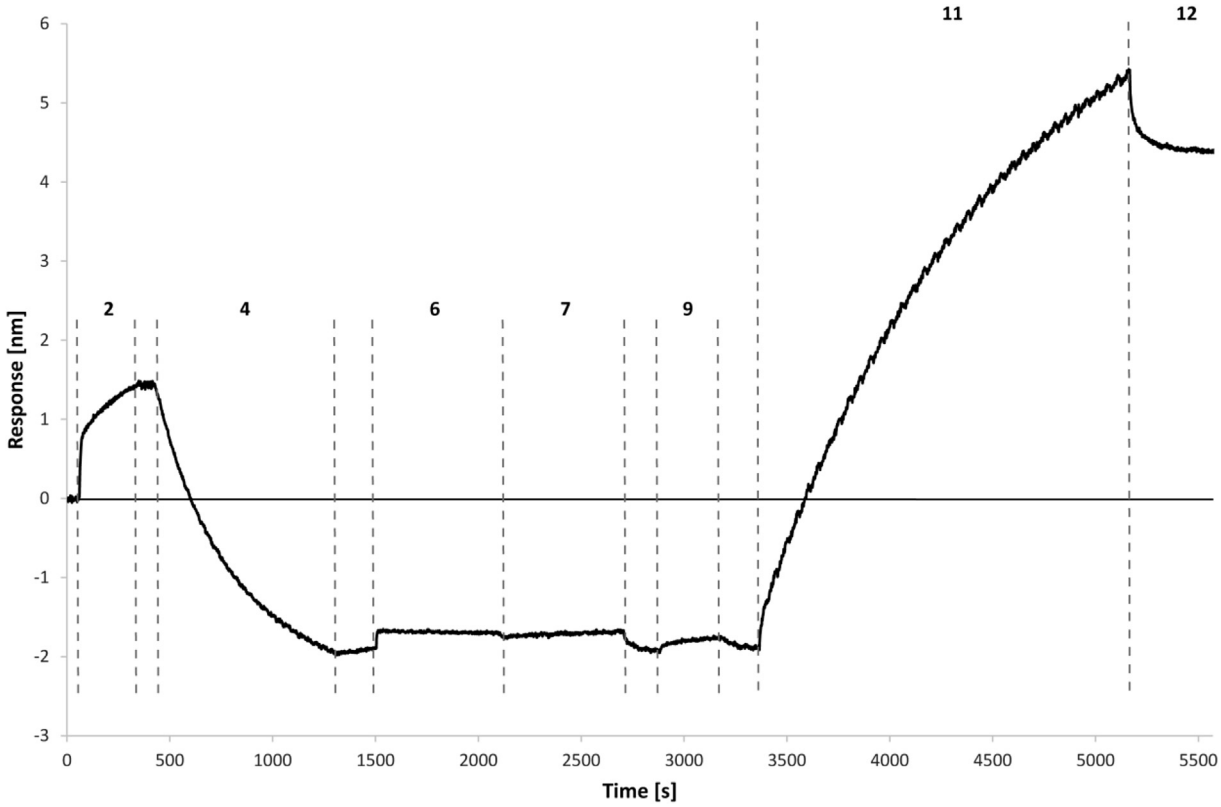

Fig. 1. Complete representative sensogram of the BLI based method. Step 2 indicates loading of the biotinylated PEG-Cholesterol linker, step 4 exhibits the immobilization of HER2-displaying VLPs, in step 6 blocking with PBST (0,1% Tween20) + 0,3% skimmed milk powder is shown, in step 7 anti-HER2 scFv phages are loaded, step 9 shows loading of the secondary anti-phage-HRP-labeled antibody and in step 11 (signal enhancement) DAB is applied which leads to a tremendous signal increase by the formation of a metal precipitate on the sensor surface. Finally, in step 12 the dissociation of the metal complex is indicated. After every loading step, a buffer step was applied.

stained with Herceptin, an anti-kappa biotin-labeled antibody and Alexa Flour647-tagged streptavidin and were analyzed by flow cytometry. Efficient baculovirus infection was confirmed by measuring the level of the intracellular marker protein yellow fluorescent protein (YFP) co-expressed along with HER2 and VLPs. 99% of cells infected with either the HIV-1 Gag virus or the HER2 encoding virus expressed YFP (Fig. 2A). Flow cytometry results of the HER2 expression studies indicate efficient presentation of HER2 protein on the surface of *Sf*9 cells since 86% of cells infected with HER2 expressing virus gave clearly detectable AF647 signals as compared to cells solely infected with the HIV-1 Gag matrix protein where no signal was obtained (Fig. 2B).

3.2. Generation and purification of VLPs

VLPs were generated by infection of *Sf*9 cells with recombinant baculovirus encoding HIV-1 Gag and full-length human HER2. As a control cells were infected with a baculovirus, solely expressing HIV-1 Gag matrix protein, resulting in VLPs lacking HER2 on the surface. VLPs were harvested from supernatants of infected cells by ultracentrifugation. The cell pellet of infected cells, the infection supernatants and the ultracentrifugation pellet were analyzed by Western Blotting. HER2 was detected as a protein of approximately 140 kDa in the cell pellet and supernatant of infected cells (Fig. 3), which concurs with the calculated molecular protein mass of 138 kDa. Control cells and control infections did not show any signal. An additional specific band was visible at a size of approximately 65 kDa (Fig. 3). Since Herceptin recognizes the most membrane proximal domain of HER2 (domain IV), it seems that HER2 is prone to proteolytic cleavage resulting in a mix of the full-length receptor and a 65 kDa truncated membrane-bound fragment.

VLPs were further purified by sucrose density gradient ultracentrifugation and separated fractions were analyzed by Western Blotting. HER2 was detected as a protein of about 140 kDa, again showing an additional band at 65 kDa (Fig. 4A). HIV-1 Gag was detected as a protein of 55 kDa (Fig. 4A, B), matching the theoretical molecular protein mass. Both proteins were present in sucrose density gradient fractions 3–12 and in the pellet. Fractions 8–11 were considered to contain the most VLP material and were therefore pooled and examined for their VLP concentration by NanoSight measurements. The concentration of particles with a diameter between 100 and 200 nm ranged from 1,6E+11 to 8,1E+11 particles/ml for control VLPs and from 5E+10 to 5,6E+11 particles/ml for HER2-displaying VLPs.

3.3. Transmission electron microscopy studies

To confirm the presence of budded VLPs and to investigate their morphology, transmission electron microscopy was performed. Both, HER2-displaying VLPs (Fig. 5B) and control VLPs (Fig. 5A) appeared spherical and ranged in a diameter size between 100 and 200 nm. For the visualization of HER2 displayed on the VLP surface, HER2-VLPs as well as control VLPs were stained with 10 nm gold-labeled anti-mouse IgG antibodies directed against a monoclonal anti-HER2 antibody and examined by electron microscopy (Fig. 6). Gold particles were detected exclusively on the surface of HER2-displaying VLPs (Fig. 6B) but not on control VLPs (Fig. 6A),

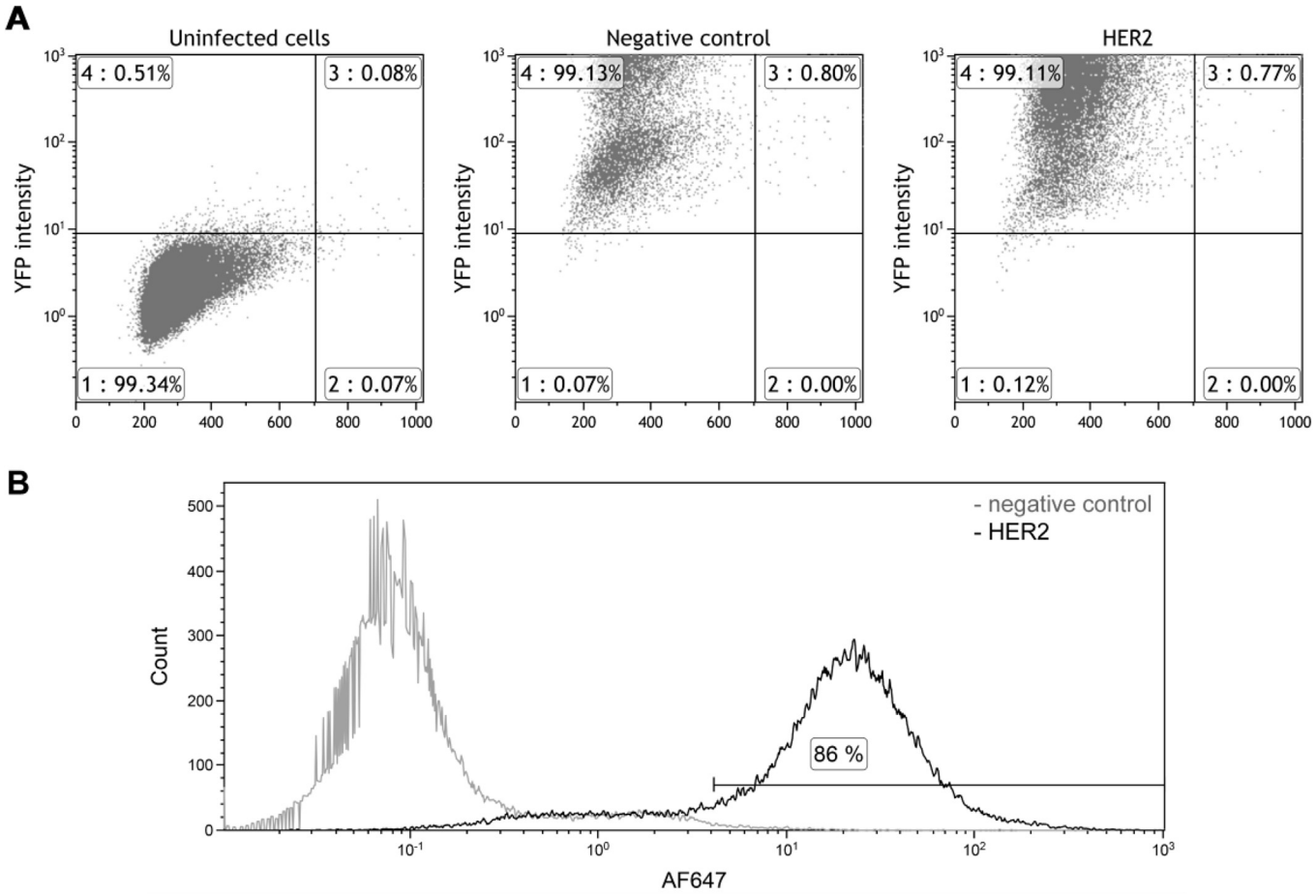

Fig. 2. Flow cytometry analysis of HER2 expressing *Sf*9 cells. Non-infected insect cells or cells infected with recombinant baculovirus encoding full-length HER2 or solely encoding the matrix protein HIV-1 Gag (negative control) were stained with Herceptin, followed by an anti-kappa biotin-labeled antibody and streptavidin-labeled Alexa Flour647. In **(A)** the infection efficiency is shown by the intensity of co-expressed intracellular yellow fluorescent protein (YFP) and is given as percentage of total cells. In **(B)** measured AF647-positive cells are indicated and are given as percentage of cells gated according to the YFP marker.

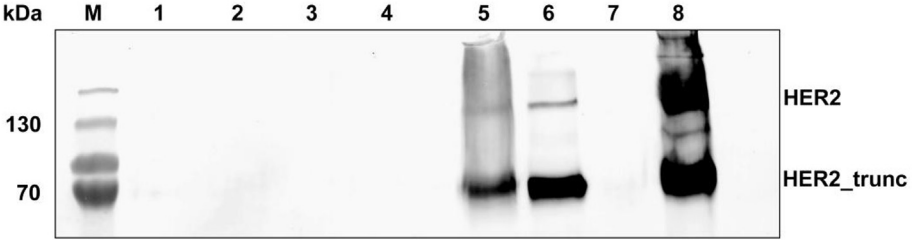

Fig. 3. Detection of HER2 protein in uninfected and infected *Sf*9 cells using Western Blot analysis. Lane 1 indicates the cell pellet and lane 2 the supernatant of uninfected *Sf*9 cells, lane 3 indicates the cell pellet and lane 4 the supernatant of *Sf*9 cells infected with the recombinant baculovirus carrying the HIV-1 Gag matrix protein gene, lane 5 shows the cell pellet and lane 6 the supernatant of *Sf*9 cells infected with viruses encoding HIV-1 Gag and HER2, lane 7 and 8 present the ultracentrifuged supernatants of *Sf*9 cells infected with the HIV-1 Gag carrying virus and the HER2 carrying virus, respectively. Full-length HER2 protein (140 kDa) and truncated HER2 protein (65 kDa) are indicated and were exclusively detected in samples infected with the HER2 expressing baculovirus.

indicating presence of HER2 on the surface of VLPs.

3.4. ELISA studies applying HER2-displaying VLPs

Efficient display of functional HER2 on the VLP surface was confirmed by ELISA using Herceptin as detection antibody. Fig. 7A shows specific binding of Herceptin to HER2-displaying VLPs. No binding of antibodies to control VLPs was observed. Moreover, binding of Herceptin was concentration dependent and accomplished saturation at a concentration of 5E+9 VLPs/well. In Fig. 7B the difference in binding of Herceptin to positive and negative VLPs is depicted at the point of inceptive saturation. 12-fold higher signal intensity of Herceptin binding to HER2-displaying VLPs compared to control VLPs alludes efficient display of structurally intact HER2 on the VLP surface.

As phage display is one of the most commonly used technologies for mAb discovery and has already been successfully applied in combination with antigen-displaying VLPs [17,18], we had a stake in the applicability of insect cell-derived VLPs as detection platform for phages displaying single chain variable antibody fragments

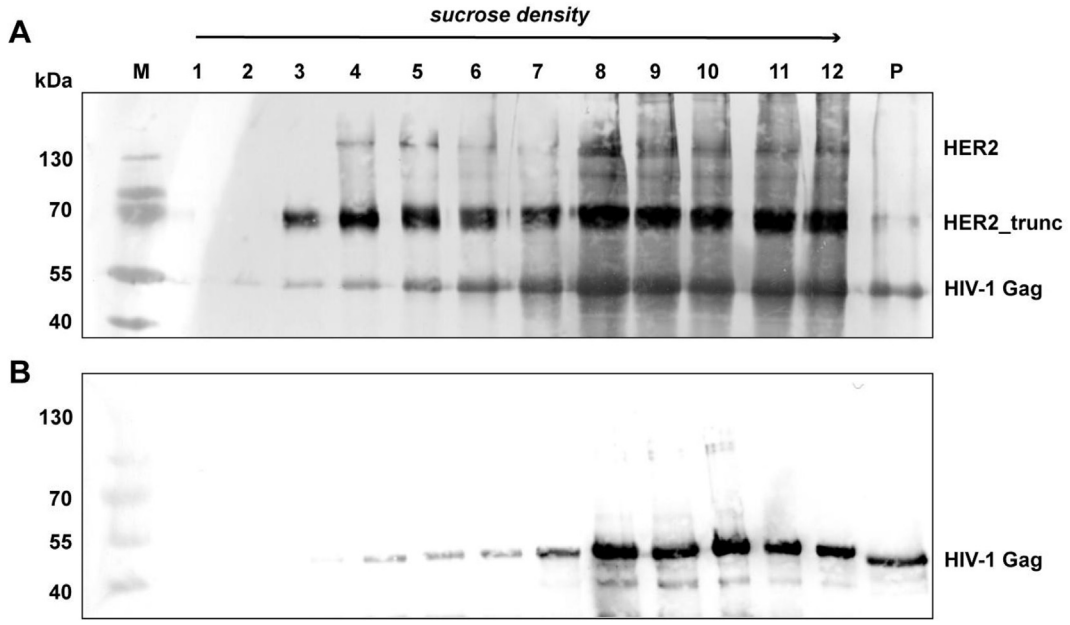

Fig. 4. Western blot analysis of (A) HER2-displaying VLP fractions and (B) control VLP fractions derived from sucrose gradient (20–60%) ultracentrifugation. HER2 was detected using Herceptin and a monoclonal anti-human IgG alkaline phosphatase-conjugated antibody. Detection of the HIV-1 Gag matrix protein was accomplished applying an HIV-1 Gag specific antibody and an anti-rabbit alkaline phosphatase-conjugated IgG antibody. Sucrose concentration increases from lane 1 to 12, P indicates the pellet. (A) Full-length HER2 and truncated HER2 were detected as proteins of about 140 kDa and 65 kDa respectively in fraction 3–12 and the pellet. (A, B) HIV-1 Gag was detected as a protein of approximately 55 kDa and was also present in fraction 3–12 and the pellet.

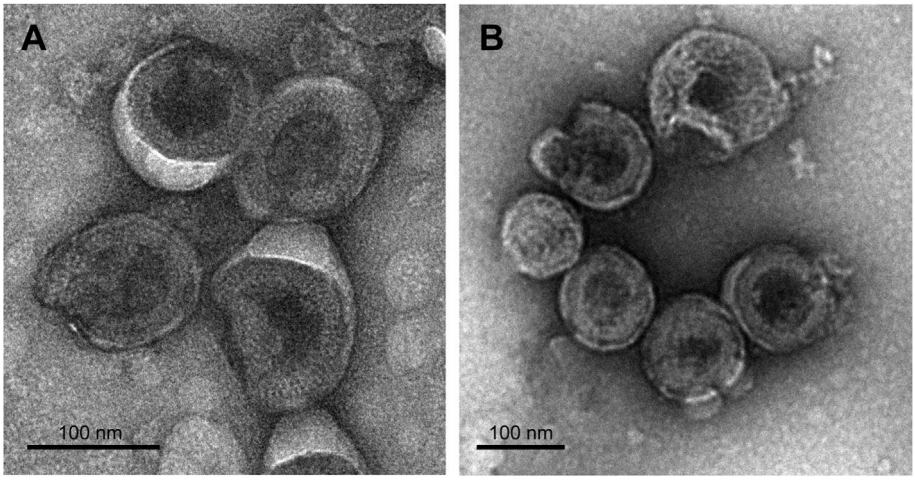

Fig. 5. Representative transmission electron micrographs of (A) control VLPs and (B) HER2-displaying VLPs. Sucrose density purified VLPs were negative stained and investigated using a transmission electron microscope (FEI Tecnai G^2 200 kV, FEI, Hillsboro, Oregon, USA). Both types of VLPs appeared spherical and ranged in a diameter size between 100 and 200 nm.

(scFv). For that purpose, a 96 well plate was coated with the previously determined VLP concentration at inceptive saturation (5E+9 particles/well). Detection was accomplished by applying target specific phages. In Fig. 7C unique and concentration dependent binding of anti-HER2 phages to HER2-displaying VLPs is shown. Only low background binding to control VLPs was obtained. At the highest phage concentration (2,88E+11 cfu/ml) around 6-fold higher signal intensity of anti-HER2 phages binding to HER2-displaying VLPs compared to control VLPs was attained (Fig. 7D).

3.5. BLI studies applying HER2-displaying VLPs

Fast and reliable detection of target specific binding to VLPs was approved by a newly established BLI based technique (Fig. 8). Therefore, HER2-displaying VLPs were immobilized to a streptavidin biosensor via a biotinylated PEG-Cholesterol anchor [38]. Immobilization of the VLPs induced a negative BLI signal in the resulting sensogram (Fig. 1), occurring when large molecules bind to the sensor surface [27]. Stable immobilization and consistent distribution of VLPs on the BLI tip were confirmed by SEM (Fig. 9). After immobilizing both, HER2-displaying VLPs and control VLPs, HER2-specific phages were applied. HER2-displaying VLPs gave clearly detectable and concentration dependent signals indicating specific binding of phages to displayed HER2 (Fig. 10A). In Fig. 10B the specific responses at the time t = 1800 s are shown. According to the LOQ-based principle for reliable measurement (see “Biolayer interferometry”, Materials and Methods section), the mean response of triplicates of DAB precipitation towards the control

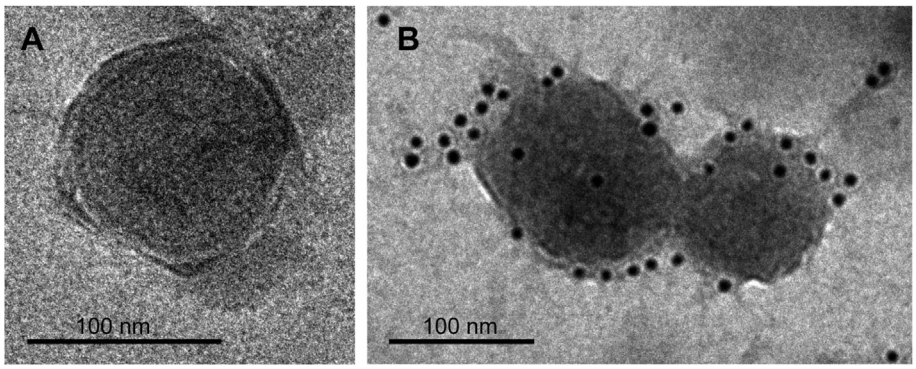

Fig. 6. Representative transmission electron micrographs of immunogold-labeled (A) control VLPs and (B) HER2-displaying VLPs. Anti-HER2 antibodies exclusively detected the membrane receptor HER2 on HER2-displaying VLPs, binding to control VLPs could not be observed.

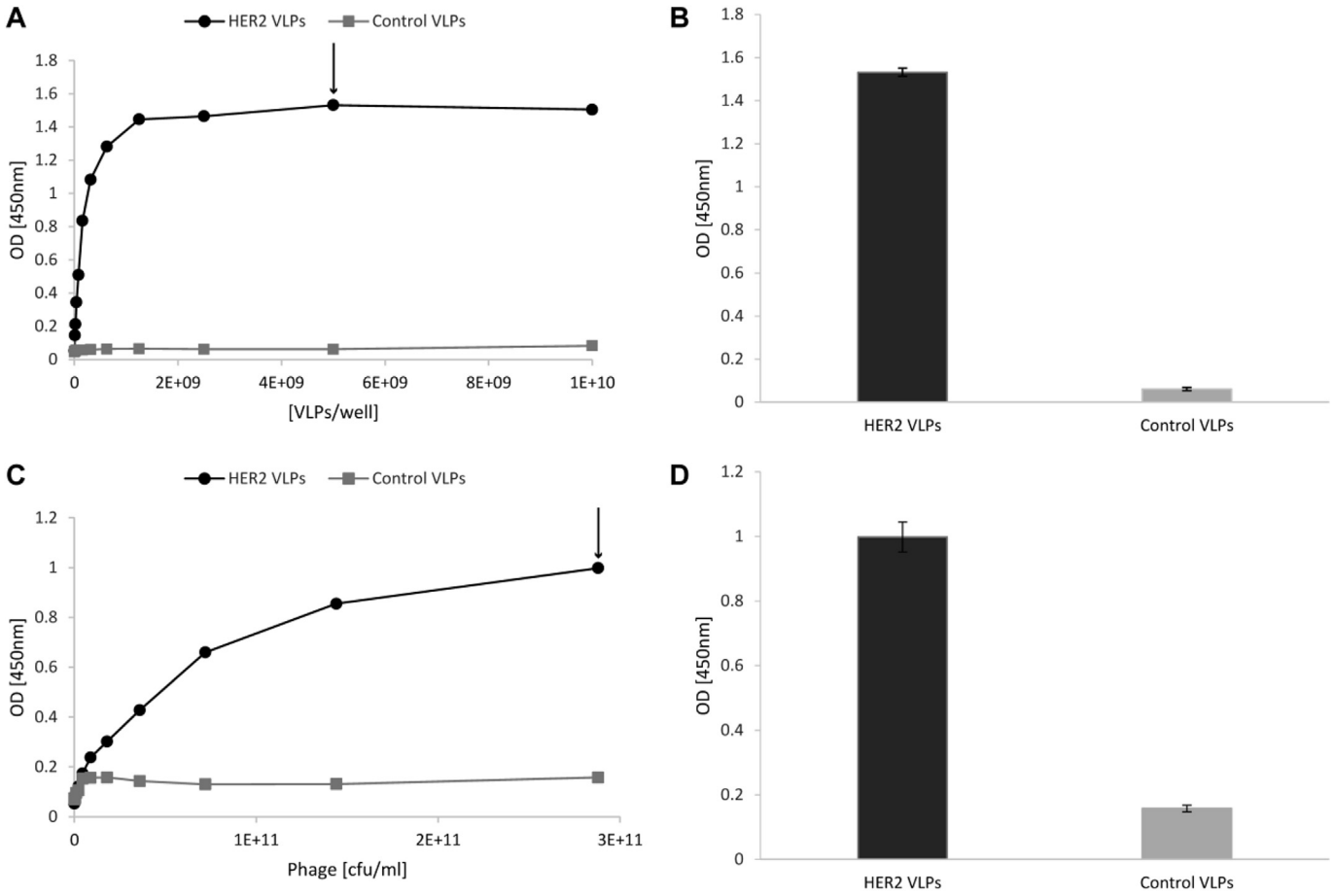

Fig. 7. Binding of Herceptin (A, B) and HER2 specific phages (C, D) to HER2-displaying VLPs and control VLPs using ELISA. (A) A 96 well plate was coated with different concentrations of HER2-VLPs and control VLPs. Detection of HER2 was accomplished using Herceptin. In (**B**) the difference in binding of Herceptin to HER2-VLPs and control VLPs at a concentration of 5E+9 VLPs/well is shown. (**C**) A 96-well plate was coated with 5E+9 VLPs/well. Detection was carried out applying HER2 specific phages. In (**D**) the difference in binding of anti-HER2 phages to HER2-VLPs and control VLPs using a phage concentration of 2,88E+11 cfu/ml is depicted. Both, Herceptin and HER2 specific phages exclusively bound to HER2-displaying VLPs in a concentration dependent manner. Results are shown as average of two independent measurements. Arrows signify data points which are indicated in the bar diagram.

VLPs was significantly below the calculated threshold value of 0,9 nm (data not shown).

4. Discussion

Only a few regulatory-approved serum cancer biomarkers are currently available, including HER2/neu, CA27-29, and CA15-3 for breast cancer; CA125 for ovarian cancer; CEA for colon cancer, CA19-9 for pancreatic cancer, and PSA for prostate cancer. Out of these, PSA is the only serological biomarker used to screen asymptomatic patients, which is still controversial due to inadequate sensitivity and low specificity (90% and 21%, respectively) [41]. Cancer biomarkers are often glycosylated membrane receptor proteins present on the cellular surface. In order to develop highly

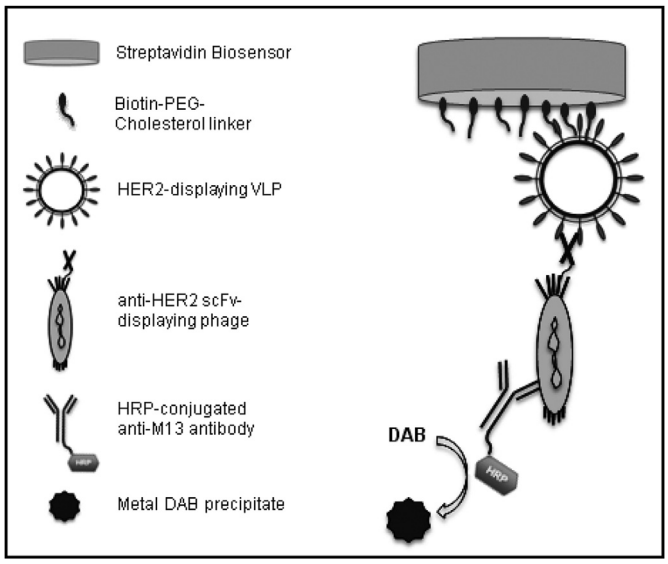

Fig. 8. Biosensor based assay format for the detection of HER2 displayed on the VLP surface. HER2-displaying VLPs were immobilized to a streptavidin biosensor using a biotin-PEG-Cholesterol linker. Phages, displaying a single chain variable fragment (scFv) of an anti-HER2 antibody were applied and detected via an anti-M13 (p8) IgG HRP-conjugated secondary antibody. The signal was enhanced with 3,3'-diaminobenzidine (DAB), which is oxidized by HRP and forms a metal precipitate on the sensor surface.

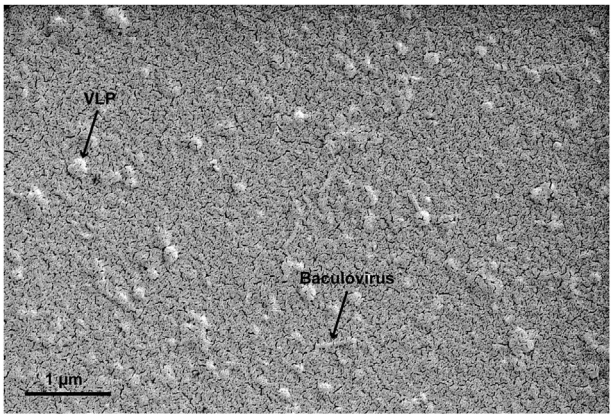

Fig. 9. Representative scanning electron micrograph of a VLP functionalized biosensor. Sucrose gradient purified VLPs were immobilized to a streptavidin biosensor and investigated using a scanning electron microscope (Zeiss Supra 55 VP, Zeiss, Jena, Germany). Arrows indicate a spherical VLP and a rod-shaped baculovirus.

specific and sensitive screening methods for early cancer detection or to select new antibodies for cancer diagnostics or treatment, it is a pre-requisite that the target proteins are available in an authentic form in terms of structure and glycosylation. However, membrane receptor proteins are notoriously difficult to produce due to their hydrophobic nature and complex structures. The human epidermal growth factor receptor 2 (HER2) is known to be overexpressed in a number of tumors including breast cancer, lung cancer, gastric cancer and glioblastoma multiform [3,42] and was therefore, chosen as the model for a tumor antigen in our studies. Here we used the baculovirus-insect cell expression system (BES) to evaluate the feasibility of *Sf*9 insect cells to express functional HER2 and budded virus-like particles (VLPs) serving as a scaffold for the presentation of complex membrane proteins. We are aware of the fact that glycosylation patterns of insect cell derived proteins differ from human glycosylation patterns. However, glycoengineering in insect cells [43] as well as on baculoviruses [44] has successfully allowed for the production of human-like glycan structures in *Sf*9 and High5 cells.

We showed that HER2 was efficiently expressed and displayed on the surface of *Sf*9 cells by flow cytometry. Cells were gated according to the infection marker YFP (yellow fluorescent protein) and were then investigated for their HER2 expression. Since 86% of all infected cells displayed HER2 on the surface (Fig. 2B), we confirmed the transport of the target protein to the cell membrane. Next, recombinant baculoviruses coding for both, the HER2 and the HIV-1 Gag matrix protein were generated and used to infect *Sf*9 insect cells. Since it was expected that VLPs would be released from the cells, a Western Blot experiment was performed to provide first evidence of VLP presence in the supernatant of infected cells. Cell pellets were analyzed as well. Results showed HER2 expression in both, the cell pellet and the supernatant of infected cells (Fig. 3), suggesting the presence of budded VLPs. Moreover, we found that Herceptin bound to two fragments where one represents the full-length HER2 (138 kDa) and the other represents a truncated membrane-bound portion of HER2 (65 kDa). Apparently the receptor is prone to proteolytic cleavage resulting in a mix of full-length protein and the truncated membrane-bound fragment. Interestingly, the observed HER2 shredding effect seems to be native as both, the HER2 ectodomain and the truncated membrane-bound domain were previously detected in HER2-overexpressing breast cancer cells [45] and also in serum of breast cancer patients [46]. Also in this study, presentation of full-length HER2 on the surface of VLPs was accompanied by the presentation of a truncated membrane-bound version.

Since there is always co-production of recombinant baculovirus in *Sf*9 cells [47], resulting VLPs were purified by sucrose density gradient ultracentrifugation to reduce viral impurities. Size and surface properties of baculoviruses and VLPs are similar. Several methods such as filtration and size exclusion chromatography have been tested, however, in our hands sucrose gradient centrifugation usually worked best and gave the highest yield of VLPs. After purification only a few rod-shaped baculovirus particles could be detected using SEM (Fig. 9). The VLP concentration was measured by nanoparticle tracking analysis using a NanoSight LM-10. This method was evaluated as a suitable and accurate characterization method for nanoparticle analysis giving an approximate particle concentration and size information [48]. Electron microscopy of purified VLPs showed the typical size and shape of HIV-1 Gag nanoparticles which is comparable to results of previous studies with *Sf*21-derived HIV-1 Gag VLPs [49] and studies based on *HEK*-293-derived Gag VLPs [26]. In addition, the presentation of the membrane receptor HER2 on the surface of the VLPs was confirmed by immunogold staining (Fig. 6).

Since VLPs can be easily coated onto ELISA plates [18] we used purified HER2-displaying VLPs as target in an ELISA assay to assess efficient presentation and functionality of displayed HER2. For the detection, we applied Herceptin, which binds to HER2 at its C-terminal portion of domain IV [50]. The antigen-antibody interaction is mediated by three regions of HER2 [50], indicating that only proper folded HER2 enables antibody binding. Results showed specific binding of Herceptin to HER2-displaying VLPs (Fig. 7A, B). Also filamentous phages that displayed a HER2 specific single chain antibody bound to the VLPs and were suitable for detection in an ELISA format. Only low background binding to the control VLPs was visible (Fig. 7C, D). This could be due to the sticky nature of the phages and the fact, that VLPs are membrane-derived and therefore, not only contain the target protein but also other cell surface proteins.

Biolayer interferometry (BLI) is a standard tool for monitoring almost all biomolecular interactions in a label-free, real-time and

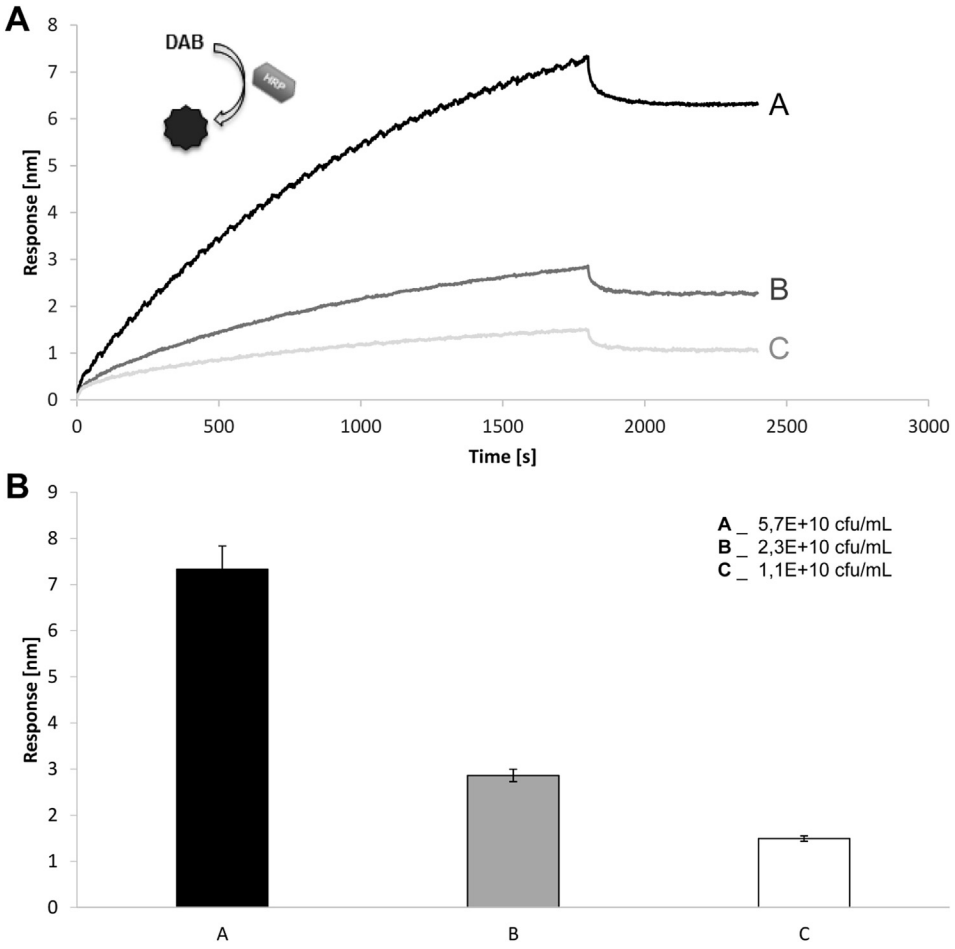

Fig. 10. Detection of interaction between HER2-displaying VLPs and target specific phages using biolayer interferometry. In (**A**) the BLI responses of different phage concentrations (A = 5,7E+10 cfu/ml, B = 2,3E+10 cfu/ml, C = 1,1E+10 cfu/ml) binding to HER2-VLP functionalized sensors are shown. In (**B**) the visualization of the interaction at t = 1800 s is indicated. Specific and concentration dependent binding of anti-HER2 phages to HER2-displaying VLPs can be observed. Curves, bars and error bars represent the average of three independent measurements. The mean response of the association (DAB precipitation) towards the control VLPs was significantly below the calculated threshold values of 0.9 nm (data not shown).

high-throughput manner [27]. In our study, we wanted to evaluate the feasibility of BLI to detect target specific binding to VLPs. Since our particles were enveloped by a lipid bilayer, we used biotinylated PEG-Cholesterol as anchor, which allowed us to immobilize HER2-displaying VLPs as well as control VLPs to the surface of a streptavidin biosensor. Through the possibility of immobilizing control VLPs we provide a valuable blank that could be beneficial when working on the selection of target specific molecules. Moreover, our strategy can not only be used for budded VLPs, but could also be applicable for all other enveloped particles, produced either in insect cells or mammalian cells. For screening and selection of tumor specific antibodies, it is highly important to display the cancer antigen in an authentically folded manner, to provide accessibility to the pool of binding molecules, and in the case of phage display libraries, to be able to recover specifically bound phages in an infectious state. In our study we incubated the VLP-functionalized sensor with a phage, displaying a HER2 specific single chain antibody. Results showed specific and concentration dependent binding to HER2 present on the surface of immobilized VLPs (Fig. 10A, B). Binding to control VLPs was below the calculated LOQ and therefore negligible. Hence, we were not only able to confirm findings observed in the ELISA studies, but also demonstrated that *Sf*9-derived VLPs can be used in a highly sensitive biosensor based assay for the detection of target protein specific phages. When compared to ELISA, in our hands, BLI was the more convenient method for detection of target molecules as it was much faster, required less target protein and sample volume, was easy to handle and furthermore bears the advantages of real-time measurements [37]. Therefore, BLI, utilizing VLP-functionalized biosensors, is considered as preferred method for the detection of target specific phages. But not only for detection, also for library screening purposes this method bears great potential since we managed to recover phages, previously selected by a VLP-functionalized sensor surface, which retained their infectivity (data not shown).

5. Conclusions

In conclusion, it was shown that the baculovirus-insect cell expression system (BES) is a feasible system for the expression of complex full-length membrane proteins such as the cancer target HER2. In addition the BES was highly efficient in producing self-assembled budded nanoparticles based on viral matrix proteins. Such budded VLPs, solely consisting of the HIV-1 Gag matrix protein and the *Sf*9-derived membrane, were also feasible for the display of the target protein. In several binding studies including a newly established biosensor based technique, successful presentation of functional HER2 on the surface of the infected *Sf*9 cells as

well as on purified VLPs was shown. To the best of our knowledge, this is the first work showing that *Sf*9-derived VLPs, immobilized to a biosensor via a PEG-Cholesterol linker, can be utilized to detect target specific phages in a real-time biosensor based assay, alluding the potential of this method to be used for antibody screenings. Besides our model protein HER2, many other membrane proteins including cancer antigens, various immune cell markers and immune receptors could be expressed in high avidity, in a pure manner and in sufficient amounts. As such, VLP surface display may contribute markedly to antibody selection and engineering as well as cancer vaccine design and diagnostics.

Authors' contributions

Conceived and designed the experiments: LN, DP, JW, KV-U, KK, RG. Performed the experiments: LN, JW. Analyzed the data: LN, JW, DP. Contributed to the manuscript: LN, RG, JW, KV-U, DP, KK.

Conflicts of interest

Authors confirm that they have no conflicts of interest.

Acknowledgements

The authors would like to thank Gordana Wozniak-Knopp (University of Natural Resources and Life Sciences, Department for Chemistry, Vienna) for kindly providing the scFv phage, Tobias Schneider (Austrian Centre of Industrial Biotechnology, Vienna) for performing the Nanosight analysis, Eva Berger (Austrian Centre of Industrial Biotechnology, Vienna) for her TEM expertise and the TEM performance and Stephan Puchegger (University of Vienna, Faculty of Physics) for his technical support with the SEM. This work was funded by the PhD programme "BioTop – Biomolecular Technology of Proteins" (Austrian Science Funds, Project number FWF W1224).

References

[1] T. Dingermann, Recombinant therapeutic proteins: production platforms and challenges, Biotechnol. J. 3 (2008) 90–97.
[2] Y. Genzel, I. Behrendt, J. Rodig, E. Rapp, C. Kueppers, S. Kochanek, G. Schiedner, U. Reichl, CAP, a new human suspension cell line for influenza virus production, Appl. Microbiol. Biotechnol. 97 (2013) 111–122.
[3] C.T. Kuan, C.J. Wikstrand, D.D. Bigner, EGF mutant receptor vIII as a molecular target in cancer therapy, Endocr. Relat. Cancer 8 (2001) 83–96.
[4] S. Loibl, L. Gianni, HER2-positive Breast Cancer, Lancet, 2016.
[5] S. Kanthala, C.P. Mill, D.J. Riese 2nd, M. Jaiswal, S. Jois, Expression and purification of HER2 extracellular domain proteins in Schneider2 insect cells, Protein Expr. Purif. 125 (2016) 26–33.
[6] G. Amexis, N.H. Hematology Branch, Lung, and Blood Institute, National Institutes of Health, Bethesda, Maryland, N.S. Young, N.H. Hematology Branch, Lung, and Blood Institute, National Institutes of Health, Bethesda, Maryland, Parvovirus B19 Empty Capsids as Antigen Carriers for Presentation of Antigenic Determinants of Dengue 2 Virus. The Journal of Infectious Diseases 194 (2017) 790–794.
[7] C.J. Dale, X.S. Liu, R. De Rose, D.F. Purcell, J. Anderson, Y. Xu, G.R. Leggatt, I.H. Frazer, S.J. Kent, Chimeric human papilloma virus-simian/human immunodeficiency virus virus-like-particle vaccines: immunogenicity and protective efficacy in macaques, Virology 301 (2002) 176–187.
[8] B. Chackerian, M. Rangel, Z. Hunter, D.S. Peabody, Virus and virus-like particle-based immunogens for Alzheimer's disease induce antibody responses against amyloid-beta without concomitant T cell responses, Vaccine 24 (2006) 6321–6331.
[9] L. Deml, C. Speth, M.P. Dierich, H. Wolf, R. Wagner, Recombinant HIV-1 Pr55gag virus-like particles: potent stimulators of innate and acquired immune responses, Mol. Immunol. 42 (2005) 259–277.
[10] A. Zeltins, Construction and characterization of virus-like particles: a review, Mol. Biotechnol. 53 (2013) 92–107.
[11] D. Sari, K. Gupta, D.B. Thimiri Govinda Raj, A. Aubert, P. Drncova, F. Garzoni, D. Fitzgerald, I. Berger, The MultiBac baculovirus/insect cell expression vector system for producing complex protein biologics, Adv. Exp. Med. Biol. 896 (2016) 199–215.
[12] J. Liu, S. Dai, M. Wang, Z. Hu, H. Wang, F. Deng, Virus like particle-based vaccines against emerging infectious disease viruses, Virol. Sin. 31 (2016) 279–287.
[13] A. Roldao, M.C. Mellado, L.R. Castilho, M.J. Carrondo, P.M. Alves, Virus-like particles in vaccine development, Expert Rev. Vaccines 9 (2010) 1149–1176.
[14] R. Wagner, L. Deml, R. Schirmbeck, J. Reimann, H. Wolf, Induction of a MHC class I-restricted, CD8 positive cytolytic T-cell response by chimeric HIV-1 virus-like particles in vivo: implications on HIV vaccine development, Behring Inst. Mitt (1994) 23–34.
[15] B. Chackerian, P. Lenz, D.R. Lowy, J.T. Schiller, Determinants of Autoantibody Induction by Conjugated Papillomavirus Virus-like Particles, 2002.
[16] R.G. Cox, J.J. Erickson, A.K. Hastings, J.C. Becker, M. Johnson, R.E. Craven, S.J. Tollefson, K.L. Boyd, J.V. Williams, Human metapneumovirus virus-like particles induce protective B and T cell responses in a mouse model, J. Virol. 88 (2014) 6368–6379.
[17] B. van der Woning, G. De Boeck, C. Blanchetot, V. Bobkov, A. Klarenbeek, M. Saunders, M. Waelbroeck, T. Laeremans, J. Steyaert, A. Hultberg, H. De Haard, DNA immunization combined with scFv phage display identifies antagonistic GCGR specific antibodies and reveals new epitopes on the small extracellular loops, MAbs 8 (2016) 1126–1135.
[18] R.H. Fong, S.S.R. Banik, K. Mattia, T. Barnes, D. Tucker, N. Liss, K. Lu, S. Selvarajah, S. Srinivasan, M. Mabila, A. Miller, M.O. Muench, A. Michault, J.B. Rucker, C. Paes, G. Simmons, K.M. Kahle, B.J. Doranz, Exposure of epitope residues on the outer face of the chikungunya virus envelope trimer determines antibody neutralizing efficacy, J. Virol. (2014) 14364–14379.
[19] G.D. Lewis Phillips, G. Li, D.L. Dugger, L.M. Crocker, K.L. Parsons, E. Mai, W.A. Blattler, J.M. Lambert, R.V. Chari, R.J. Lutz, W.L. Wong, F.S. Jacobson, H. Koeppen, R.H. Schwall, S.R. Kenkare-Mitra, S.D. Spencer, M.X. Sliwkowski, Targeting HER2-positive breast cancer with trastuzumab-DM1, an antibody-cytotoxic drug conjugate, Cancer Res. 68 (2008) 9280–9290.
[20] G. Van Heeke, K. Allosery, V. De Brabandere, T. De Smedt, L. Detalle, A. de Fougerolles, Nanobodies(R) as inhaled biotherapeutics for lung diseases, Pharmacol. Ther. 169 (2017) 47–56.
[21] V.J. Bruce, A.N. Ta, B.R. McNaughton, Minimalist antibodies and mimetics: An update and recent applications, Chembiochem 17 (2016) 1892–1899.
[22] F. Krammer, T. Schinko, D. Palmberger, C. Tauer, P. Messner, R. Grabherr, Trichoplusia ni cells (High Five) are highly efficient for the production of influenza A virus-like particles: a comparison of two insect cell lines as production platforms for influenza vaccines, Mol. Biotechnol. 45 (2010) 226–234.
[23] T.J. French, J.J. Marshall, P. Roy, Assembly of double-shelled, viruslike particles of bluetongue virus by the simultaneous expression of four structural proteins, J. Virol. 64 (1990) 5695–5700.
[24] Y. Sun, R. Carrion Jr., L. Ye, Z. Wen, Y.T. Ro, K. Brasky, A.E. Ticer, E.E. Schwegler, J.L. Patterson, R.W. Compans, C. Yang, Protection against lethal challenge by Ebola virus-like particles produced in insect cells, Virology 383 (2009) 12–21.
[25] T. Vicente, A. Roldao, C. Peixoto, M.J. Carrondo, P.M. Alves, Large-scale production and purification of VLP-based vaccines, J. Invertebr. Pathol. 107 (Suppl) (2011) S42–S48.
[26] A. Venereo-Sanchez, R. Gilbert, M. Simoneau, A. Caron, P. Chahal, W. Chen, S. Ansorge, X. Li, O. Henry, A. Kamen, Hemagglutinin and neuraminidase containing virus-like particles produced in HEK-293 suspension culture: an effective influenza vaccine candidate, Vaccine 34 (2016) 3371–3380.
[27] D. Verzijl, T. Riedl, P.W. Parren, A.F. Gerritsen, A novel label-free cell-based assay technology using biolayer interferometry, Biosens. Bioelectron. 87 (2017) 388–395.
[28] V. Donzella, F. Crea, Optical biosensors to analyze novel biomarkers in oncology, J. Biophot. 4 (2011) 442–452.
[29] M. Dysinger, L.E. King, Practical quantitative and kinetic applications of biolayer interferometry for toxicokinetic analysis of a monoclonal antibody therapeutic, J. Immunol. Methods 379 (2012) 30–41.
[30] J. Wallner, G. Lhota, M. Schosserer, K. Vorauer-Uhl, An approach for liposome immobilization using sterically stabilized micelles (SSMs) as a precursor for bio-layer interferometry-based interaction studies, Colloids Surf. B Biointer. 154 (2017) 186–194.
[31] J. Sambrook, Molecular cloning: a laboratory manual. Second edition. Volumes 1, 2, and 3. Current protocols in molecular biology. Volumes 1 and 2, Cell 61 (1990) 17–18.
[32] J.L. Vaughn, R.H. Goodwin, G.J. Tompkins, P. McCawley, The establishment of two cell lines from the insect Spodoptera frugiperda (Lepidoptera; Noctuidae), In Vitro 13 (1977) 213–217.
[33] D.J. Fitzgerald, P. Berger, C. Schaffitzel, K. Yamada, T.J. Richmond, I. Berger, Protein complex expression by using multigene baculoviral vectors, Nat. Methods 3 (2006) 1021–1032.
[34] U.K. Laemmli, Cleavage of structural proteins during the assembly of the head of bacteriophage T4, Nature 227 (1970) 680–685.
[35] P. Steppert, D. Burgstaller, M. Klausberger, E. Berger, P.P. Aguilar, T.A. Schneider, P. Kramberger, A. Tover, K. Nobauer, E. Razzazi-Fazeli, A. Jungbauer, Purification of HIV-1 gag virus-like particles and separation of other extracellular particles, J. Chromatogr. A 1455 (2016) 93–101.
[36] R. Schier, A. McCall, G.P. Adams, K.W. Marshall, H. Merritt, M. Yim, R.S. Crawford, L.M. Weiner, C. Marks, J.D. Marks, Isolation of picomolar affinity anti-c-erbB-2 single-chain Fv by molecular evolution of the complementarity determining regions in the center of the antibody binding site, J. Mol. Biol. 263 (1996) 551–567.
[37] J. Wallner, G. Lhota, D. Jeschek, A. Mader, K. Vorauer-Uhl, Application of Bio-Layer Interferometry for the analysis of protein/liposome interactions,

J. Pharm. Biomed. Anal. 72 (2013) 150–154.
[38] P. Kuhn, K. Eyer, T. Robinson, F.I. Schmidt, J. Mercer, P.S. Dittrich, A facile protocol for the immobilisation of vesicles, virus particles, bacteria, and yeast cells, Integr. Biol. (Camb) 4 (2012) 1550–1555.
[39] S. Auer, T. Koho, H. Uusi-Kerttula, T. Vesikari, V. Blazevic, V.P. Hytönen, Rapid and sensitive detection of norovirus antibodies in human serum with a biolayer interferometry biosensor, Sensors Actuators B Chem. 221 (2017) 507–514.
[40] D.A. Armbruster, T. Pry, Limit of blank, limit of detection and limit of quantitation, Clin. Biochem. Rev. 29 (Suppl 1) (2008) S49–S52.
[41] A.M. Wolf, R.C. Wender, R.B. Etzioni, I.M. Thompson, A.V. D'Amico, R.J. Volk, D.D. Brooks, C. Dash, I. Guessous, K. Andrews, C. DeSantis, R.A. Smith, A.C.S.P.C.A. Committee, American Cancer Society guideline for the early detection of prostate cancer: update 2010, CA Cancer J. Clin. 60 (2010) 70–98.
[42] E.C. Smyth, D. Cunningham, Targeted therapy for gastric cancer, Curr. Treat. Options Oncol. 13 (2012) 377–389.
[43] C. Geisler, H. Mabashi-Asazuma, D.L. Jarvis, An overview and history of glycoengineering in insect expression systems, Methods Mol. Biol. 1321 (2015) 131–152.
[44] D. Palmberger, I.B. Wilson, I. Berger, R. Grabherr, D. Rendic, SweetBac: a new approach for the production of mammalianised glycoproteins in insect cells, PLoS One 7 (2012) e34226.
[45] M.A. Molina, J. Codony-Servat, J. Albanell, F. Rojo, J. Arribas, J. Baselga, Trastuzumab (herceptin), a humanized anti-Her2 receptor monoclonal antibody, inhibits basal and activated Her2 ectodomain cleavage in breast cancer cells, Cancer Res. 61 (2001) 4744–4749.
[46] T.A. Christianson, J.K. Doherty, Y.J. Lin, E.E. Ramsey, R. Holmes, E.J. Keenan, G.M. Clinton, NH2-terminally truncated HER-2/neu protein: relationship with shedding of the extracellular domain and with prognostic factors in breast cancer, Cancer Res. 58 (1998) 5123–5129.
[47] C.M. Thompson, E. Petiot, A. Mullick, M.G. Aucoin, O. Henry, A.A. Kamen, Critical assessment of influenza VLP production in Sf9 and HEK293 expression systems, BMC Biotechnol. 15 (2015) 31.
[48] V. Filipe, A. Hawe, W. Jiskoot, Critical evaluation of Nanoparticle Tracking Analysis (NTA) by NanoSight for the measurement of nanoparticles and protein aggregates, Pharm. Res. 27 (2010) 796–810.
[49] Z. Valley-Omar, A.E. Meyers, E.G. Shephard, A.L. Williamson, E.P. Rybicki, Abrogation of contaminating RNA activity in HIV-1 Gag VLPs, Virol. J. 8 (2011) 462.
[50] H.S. Cho, K. Mason, K.X. Ramyar, A.M. Stanley, S.B. Gabelli, D.W. Denney Jr., D.J. Leahy, Structure of the extracellular region of HER2 alone and in complex with the Herceptin Fab, Nature 421 (2003) 756–760.